UNIVERSITY OF RIJEKA
FACULTY OF MEDICINE

Sanja Mikašinović

IMMUNOLOGICAL MECHANISMS OF LOWERING BLOOD GLUCOSE CONCENTRATION IN VIRAL INFECTION AND ITS IMPACT ON VIRAL CONTROL

Doctoral thesis

Rijeka, 2025

UNIVERSITY OF RIJEKA
FACULTY OF MEDICINE

Sanja Mikašinović

IMMUNOLOGICAL MECHANISMS OF LOWERING BLOOD GLUCOSE CONCENTRATION IN VIRAL INFECTION AND ITS IMPACT ON VIRAL CONTROL

Doctoral thesis

Mentor: Prof. dr. sc. Bojan Polić

Rijeka, 2025

SVEUČILIŠTE U RIJECI
MEDICINSKI FAKULTET

Sanja Mikašinović

IMUNOLOŠKI MEHANIZMI SNIŽAVANJA KONCENTRACIJE GLUKOZE U KRVI U VIRUSNOJ INFEKCIJI TE NJEZIN UČINAK NA KONTROLU VIRUSNE REPLIKACIJE

Doktorski rad

Rijeka, 2025

Mentor rada: prof. dr. sc. Bojan Polić

Doktorski rad obranjen je dana _____ godine na Medicinskom fakultetu, Sveučilišta u Rijeci, pred povjerenstvom u sastavu:

1. izv. prof. dr. sc. Vanda Juranić Lisnić, dipl. ing. bioteh.
2. doc. dr. sc. Maja Baretić, dr. med.
3. prof. dr. sc. Natalia Kučić, dr. med.

Rad ima 111 stranica, 21 sliku, 4 tablice i 126 literaturna navoda.

UDK:

Doktorski rad izrađen je na Zavodu za histologiju i embriologiju te u Centru za proteomiku Medicinskog fakulteta Sveučilišta u Rijeci pod vodstvom prof. dr. sc. Bojana Polića te prof. dr. sc. Felixa Wensveena, a u sklopu Doktorske škole iz područja „Biomedicina i zdravstvo“ na Medicinskom fakultetu Sveučilišta u Rijeci. Znanstveno istraživanje je provedeno u sklopu projekata prof. dr. sc. Bojana Polića: „Imunosni mehanizmi u razvoju upale i metaboličkog sindroma u debljini“ Hrvatske zaklade za znanost (HRZZ) IP-2016-06-9306; hrvatsko-švicarskog bilateralnog projekta „Mehanizmi imunološkog prepoznavanja u jetri i njihova uloga u razvoju nealkoholnog steatohepatitisa“ IPCH-2020-10-8440; te „HRZZ projekta razvoja karijera mladih istraživača: izobrazba novih doktora znanosti“ pod brojem 3606. Osim navedenog, dio istraživanja je odrađeno u grupi za pedijatrijsku endokrinologiju i dijabetologiju u sklopu Sveučilišne dječje bolnice u Zürichu, Švicarska, pod vodstvom prof. dr. sc. Daniela Konrada. Boravak u stranoj instituciji ostvaren je uz podršku hrvatsko-švicarskog bilateralnog projekta „Mehanizmi imunološkog prepoznavanja u jetri i njihova uloga u razvoju nealkoholnog steatohepatitisa“ IPCH-2020-10-8440 te EFIS Short-term fellowship stipendije.

ZAHVALE

Zahvaljujem se mentoru prof. dr. sc. Bojanu Poliću te prof. dr. sc. Felixu Wensveenu na ukazanom povjerenju, stalnoj motivaciji, podršci i strpljenju. Zahvalna sam na svoj pruženoj pomoći, na stručnim i dragocjenim savjetima tijekom provedbe istraživanja kao i izrade doktorskog rada!

Hvala i svim kolegama i bivšim kolegama Zavoda za histologiju i embriologiju. Veliko hvala Marku – pokazao si mi kako strast za znanost izgleda i naučio me skoro svemu što znaš. Također, veliko hvala ide Maji, Ingi, Sali i Vedrani iz Laba 4/5, a posebno hvala ekipi iz knjižnice – bili ste tu i u dobrim i lošim trenucima, u labosu i van labosa, vječna pomoć i potpora, ali i društvo za kavu! Hvala i svim laborantima i ostalim profesorima i doktorandima - a svima vam zahvaljujem za svu pomoć te ugodno i prijateljsko raspoloženje tijekom svih ovih godina zajedničkog rada!

Zahvaljujem se i svim kolegama iz Centra za proteomiku, kao i ekipi iz LAMRI-ja. Hvala na svim savjetima, nesebičnoj pomoći i uvijek dobrodošloj ugodnoj čašici razgovora!

Zahvaljujem se i prof. dr. sc. Danielu Konradu, dr. sc. Stephanu Wueestu, Chiari, Fede i Carlosu na svoj pruženoj pomoći, savjetima i prijateljstvu tijekom mog boravaka u grupi za pedijatrijsku endokrinologiju i dijabetologiju u sklopu Sveučilišne dječje bolnice u Zürichu!

Posebno hvala ide svim mojim dragim ljudima koji su stalni dio moga života, i koji su me pratili i na ovom životnom putovanju. Bez obzira na udaljenost, manjak vremena i puno obaveza, uvijek ste imali razumijevanja, bili potpora i spremni za avanturu, kavu ili pelin. Bili ste uz mene od početka do kraja, i kada sam se žalila i prigovarala, ali i kada sam bila sretna i slavila. Hvala i jednom čupavcu koji me naučio da vjerujem u sebe. Hvala vam što ste mi u životu!

I naposljetku, beskrajno hvala mojim roditeljima na stalnoj potpori i strpljenju te bezuvjetnoj ljubavi i sigurnosti koju mi pružaju cijeli život. Bez vas ništa od ovoga ne bi bilo moguće, a ja ne bih bila osoba koja jesam!

SUMMARY

Objectives: The immune and endocrine systems are intricately intertwined. In response to viral infection, the immune system induces metabolic changes that contribute to “sickness behavior”, enhancing the body’s ability to combat the pathogen. As glucose serves as a vital source of energy not only for hosts but also for pathogens, its regulation is vitally important. Strong viral infections induce glucose restriction, but the purpose and underlying mechanism behind this phenomenon are still unclear. Moreover, endocrine hormones are significant players in shaping immune cell activity, ensuring their energy consumption aligns with systemic availability. However, many immunomodulatory effects of hormones remain unknown. We aimed to investigate the immunomodulatory effects of glucose and insulin-like growth factor 1 (IGF-1) hormone on antiviral response.

Materials and Methods: To investigate infection-mediated changes in blood glucose levels *in vivo*, mice were infected with varying doses of mCMV, mCMV-Δm157, LCMV, and influenza. To confirm that glucose restriction is beneficial, we prevented it by inducing hyperglycemia using glucose-spiked drinking water. Three days post-infection, fasting plasma glucose (FPG) was measured, and viral load was determined in tissues using plaque assay or qPCR. To examine the impact of different glucose concentrations on viral replication, we established an *in vitro* model. Primary and immortalized cell lines were infected with GFP-expressing mCMV, and infection was monitored using flow cytometry or confocal microscopy. To identify the cause of impaired viral replication, we supplemented the medium with various nutrients and inhibitors. Cellular metabolism was assessed using the Seahorse analyzer, while levels of biomarkers were determined using colorimetric assays and ELISA. To investigate the role of IGF-1 in CD8 T cells, we developed an *in vitro* model where effector and memory OT-1 T cells were stimulated with ovalbumin peptide (N4) and αCD28, in the presence or absence of varying IGF-1 concentrations. Proliferation, phenotype, and cytokine production were analyzed using flow cytometry. To validate *in vitro* findings *in vivo*, we transferred a mix of naïve WT OT-1 cells and OT-1 cells from mice genetically deficient for insulin and IGF-1 receptor into recipient mice, infected them with mCMV-N4, and subsequently reinfected them with LCMV-N4. At specific time points, donor cells were tracked in the blood and organs using flow cytometry, and viral titers were determined via plaque assay.

Results: Strong viral infection induced transient relative hypoglycemia, both in males and females, which benefited the antiviral immune response. Glucose restriction impaired viral replication *in vitro* and altered cellular metabolism by limiting lactate production, enhancing the production of type I IFNs. Infection-induced glucose restriction depended on increased insulin secretion and inhibited glycogenolysis. However, this mechanism was disrupted in the context of metabolic

disease, increasing susceptibility to pathogens. We also demonstrated that insulin does not influence the anti-viral CD8 response through the insulin receptor. However, the expression of the IGF1R, which can also bind insulin, is significantly upregulated at memory time points. Although IGF-1 stimulation did not affect the proliferation and phenotype of effector and memory CD8 T cells *in vitro*, it increased IFNγ production by memory CD8 T cells and promoted glycolytic metabolism. IGF-1 signalling plays a crucial role in the formation of both primary and secondary effector and memory cells.

Conclusion: We demonstrated an immune-endocrine circuit that reduces blood glucose to enhance the innate antiviral immune response. Furthermore, we showed that IGF-1 signalling promotes CD8 T cell memory formation. Together, these findings help explain why individuals with diabetes are more susceptible to viral infection and why their T cells are dysfunctional.

Keywords: Endocrine system; Glucose; IGF-1; Immune system; Insulin; Viral infections.

PROŠIRENI SAŽETAK

Cilj istraživanja: Imunološki i endokrini sustav usko su povezani. Tijekom infekcije imunološki sustav potiče metaboličke promjene koje rezultiraju ponašanju povezanim s bolešću (tzv. *sickness behavior*), kojim se povećava sposobnost organizma da se bori protiv patogena. Budući da je glukoza ključan izvor energije ne samo za domaćina, već i za patogene, vrlo je bitna njezina regulacija. Jake virusne infekcije uzrokuju smanjenje dostupnosti glukoze, no svrha i mehanizam ovog fenomena još uvijek nisu u potpunosti razjašnjeni. Također, endokrini hormoni imaju značajnu ulogu u oblikovanju aktivnosti imunoloških stanica, osiguravajući da njihova potrošnja energije bude usklađena sa sustavnom dostupnošću. Međutim, mnogi imunomodulacijski učinci hormona još uvijek nisu poznati. Poredloženo istraživanje ima za cilj istražiti imunomodulacijske učinke glukoze te inzulinu sličnog čimbenika rasta 1 (IGF-1) na antivirusni odgovor.

Materijali i metode: U svrhu istraživanja promjena u razini glukoze u krvi uzrokovanih infekcijom *in vivo*, miševi su bili inficirani različitim dozama virusa mCMV-a, mCMV-Δm157, LCMV-a i influence. Kako bi potvrdili da smanjenje glukoze pogoduje antivirusnom odgovoru, spriječili smo njezinu pojavu induciranjem hiperglikemije osiguravajući miševima vodu za piće koja je prethodno obogaćena glukozom. Tri dana nakon infekcije izmjerena je razina glukoze natašte (FPG), a virusno opterećenje u tkivima određeno je pomoću testa virusnih čistina ili qPCR-a. Za ispitivanje utjecaja različitih koncentracija glukoze na replikaciju virusa, uspostavili smo *in vitro* model. Primarne i immortalizirane stanične linije inficirali smo sa mCMV-om koji eksprimira GFP, a infekciju smo pratili protočnom citometrijom ili konfokalnom mikroskopijom. Radi identifikacije uzroka smanjene replikacije virusa, medij smo nadopunili različitim nutrijentima i inhibitorima. Pomoću Seahorse analizatora odredili smo stanični metabolizam, dok su razine biomarkera određene kolorimetrijskim testovima i ELISA-om. S ciljem istraživanja uloge IGF-1 u CD8 T stanicama, razvili smo *in vitro* model u kojem su efektorske i memorijske OT-1 T stanice stimulirane pomoću peptida N4 te αCD28 u prisutnosti ili nedostatku IGF-1. Proliferacija, fenotip i produkcija citokina analizirani su protočnom citometrijom. Kako bi potvrdili *in vitro* rezultate *in vivo*, transferirali smo mješavinu naivnih WT OT-1 i OT-1 stanice iz genetski deficijentnih miševa za inzulin i IGF-1 receptor u recipijentne WT miševe, inficirali ih s mCMV-N4 te ih naknadno reinficirali s LCMV-N4. Transferirane stanice praćene su u određenim vremenskim točkama u krvi i organima pomoću protočne citometrije, a virusni titar određen je pomoću testa virusnih čistina.

Rezultati: Jaka virusna infekcija dovodi do privremenog smanjenja razine glukozi u krvi koje pogoduje antivirusnom imunološkom odgovoru. Smanjenje glukoze dovodi do bolje kontrole virusa u *in vitro* uvjetima te mijenja stanični metabolizam smanjujući proizvodnju laktata i time pojačavajući peoizvodnju interferona α/β. Infekcijom izazvano smanjenje glukoze ovisi o pojačanom lučenju inzulina te inhibiciji glikogenolize. Ovaj mehanizam ne funkcionira u uvjetima povećane razine glukoze što dovodi do povećane osjetljivosti na virusne infekcije. Također smo

pokazali da inzulin ne utječe na antivirusni CD8 odgovor putem inzulinskog receptora. Međutim, ekspresija IGF1R, koji također može vezati inzulin, značajno je povećana u memorijskoj fazi. Iako stimulacija sa IGF-1 nije imala učinak na proliferaciju i fenotip efektorskih i memorijskih CD8 T stanica *in vitro*, dovela je do povećane proizvodnje IFNγ u memorijskim CD8 T stanicama te potaknula glikolitički metabolički potencijal. Signalizacija IGF-1 ima ključnu ulogu u formiranju primarnih i sekundarnih efektorskih i memorijskih stanica.

Zaključak: Ovaj rad otkriva imunološko-endokrini krug koji smanjuje razinu glukoze u krvi radi pojačavanja urođenog antivirusog imunog odgovora. Nadalje, pokazali smo da signalizacija IGF-1 potiče stvaranje memorijskih CD8 T stanica. Dobiveni rezultati pomažu objasniti povećanu osjetljivost na virusne infekcije te disfunkcionalnost T limfocita kod osoba s dijabetesom.

Ključne riječi: Endokrini sustav; Glukoza; IGF-1; Imuni sustav; Inzulin; Virusne infekcije.

TABLE OF CONTENTS

1. INTRODUCTION AND LITERATURE REVIEW 1

1.1. Immune response to viral infection 1

1.1.1. Innate immune response 1

1.1.2. Adaptive immune response 4

1.1.2.1. CD8 T cells 5

1.1.3. Glucose metabolism and cellular energy production 8

1.1.4. Viral infections and their impact on metabolism 10

1.2 Immune-endocrine interactions in viral infection 11

1.2.1. Regulation of blood glucose levels during infection 12

1.2.1.1. Mild viral infection 13

1.2.1.2. Severe viral infection 14

1.2.2. Regulation of endocrine hormone levels during infection 14

1.2.2.1. Insulin 15

1.2.2.2. Insulin-like growth factor 17

1.3 Diabetes and viral infections 18

2. RESEARCH GOALS 21

3. MATERIALS AND METHODS 23

3.1. Materials 23

3.1.1. Laboratoratory mice 23

3.1.2. Cell lines 24

3.1.3. Viruses 24

3.1.4. Cell culture media 25

3.1.5. Buffers 26

3.1.6. Antibodies, peptides, chemicals, and kits 28

3.2 Methods 32

3.2.1. Mouse genotyping 32

3.2.2. Immune cell isolation protocols 33

3.2.3. Cell counting 34

3.2.4. Flow cytometry 34

3.2.5. *In vitro* experiments 36

3.2.6. *In vivo* experiments 37

3.2.7. ELISA 39
3.2.8. L-lactate assay and inhibition of lactate production 39
3.2.9. Glucose uptake 39
3.2.10. Hyperinsulinemic-euglycemic clamping 40
3.2.11. Virus plaque assay 41
3.2.12. Quantitative RT-PCR 41
3.2.13. Extracellular flux assay 42
3.2.14. Quantification and statistical analysis 43
4. RESULTS 45
4.1. Strong viral infection induces transient relative hypoglycemia 45
4.2. Relative hypoglycemia is not a sex-dependent phenomenon 47
4.3. Relative hypoglycemia benefits the antiviral response 48
4.4. Low glucose concentrations impair viral replication *in vitro* 49
4.5. Metabolic deficiency is not the cause of an impaired viral infection 51
4.6. Glucose restriction affects viral replication through modification of cellular metabolism 53
4.7. Low glucose concentrations inhibit viral replication by limiting lactate production 55
4.8. Infection-induced glucose restriction is the result of increased insulin release from the pancreas 58
4.9. Relative hypoglycemia is the result of inhibited glycogenolysis in the liver 60
4.10. Hyperglycemia in the context of diabetes negatively impacts the ability of mice to control viral replication 62
4.11. Insulin does not impact the anti-viral CD8 T cell response through the insulin receptor 64
4.12. IGF-1 concentrations change during infection 66
4.13. IGF-1 stimulation has no impact on the proliferation of effector and memory CD8 T cells *in vitro* 67
4.14. IGF-1 stimulation has no impact on the phenotype of effector and memory CD8 T cells *in vitro* 68
4.15. IGF-1 stimulation increased IFNγ production by memory CD8 T cells *in vitro* 70
4.16. IGF-1 promotes glycolytic metabolism in memory CD8 T cells 72
4.17. IGF-1 signalling is important for the generation of CD8 memory T cells 74
4.18. The functionality of T cells lacking the IGF-1 receptor is not affected *in vivo* 76
4.19. IGF-1 receptor signalling is not required for memory CD8 T cell-mediated control of viral replication 77
4.20. IGF-1 receptor signalling is important for memory CD8 T cell-mediated control of melanoma cells 78

5. DISCUSSION.....81
6. CONCLUSIONS.....88
7. LITERATURE.....90
LIST OF FIGURES AND TABLES.....100
ABBREVIATIONS LIST.....103
CURRICULUM VITAE.....109

1. INTRODUCTION AND LITERATURE REVIEW

1. INTRODUCTION AND LITERATURE REVIEW

1.1. Immune response to viral infection

The immune system is a carefully controlled, complex system of specialized cells, humoral components, and organs collaborating to protect the body against harmful pathogens and tumours. The immune system can be divided into two lines of host defence: innate immunity and adaptive immunity. Although they have unique functions, these two subsystems work closely together to provide effective protection.

1.1.1. Innate immune response

The innate immune system, also known as natural immunity, provides a rapid, non-specific response to prevent infections from intruding pathogens. Once pathogens cross initial physical barriers, such as skin and mucosal surfaces, or chemical barriers such as saliva and stomach acid, they are detected by epithelial or patrolling immune cells. Innate immunity controls the infection until more specialized cells can take over. It is initiated within minutes or hours and forms no immunologic memory.

Innate cells express pattern recognition receptors (PRRs) that specifically identify pathogen-associated molecular patterns (PAMPs), small conserved molecular motifs characteristic of microorganisms, or damage-associated molecular patterns (DAMPs), endogenous molecules released from damaged or dying cells that induce potent inflammatory responses. PRRs can be categorized into five types based on protein domain homology: Toll-like receptors (TLRs), retinoic acid-inducible gene-I (RIG-I)-like receptors (RLRs), nucleotide oligomerization domain (NOD)-like receptors (NLRs), C-type lectin receptors (CLRs), and absent in melanoma-2 (AIM2)-like receptors (ALRs). DAMPs can arise from various sources and include proteoglycans, heat shock proteins, S100, histones, etc. Examples of PAMPs would be components building bacterial cell walls, such as lipopolysaccharides (LPS), flagellin, double-stranded deoxyribonucleic acid (DNA), or ribonucleic acid (RNA) produced in viral infection. Recognition of PAMPs enables a swift inflammatory response and production of different cytokines, chemokines, cell adhesion molecules, and immunoreceptors that rapidly recruit immune cells to sites of infection. These small proteins involved in cell recruitment and inflammation that are produced in downstream activities of PRR signalling, such as tumour necrosis factor (TNFα), interleukin 6 (IL-6), and type I interferons (IFNs), are critical for clearing many pathogens and proinflammatory activities (1). Although innate immune cells

play a central role, the recognition of PAMPs by peripheral cells such as epithelial, endothelial, and hematopoietic cells via TLRs is a crucial component of innate immune defence at infection sites. The innate immune system includes a plethora of cells, including macrophages, neutrophils, natural killer (NK) cells, dendritic cells (DCs), basophils, eosinophils, innate lymphoid cells (ILCs), and γδ T cells. Neutrophils and macrophages are phagocytes. While neutrophils are short-lived and have granules that aid in eliminating pathogens, macrophages are long-lived and play a role in phagocytosis and in presenting antigens to T cells. DCs are also phagocytes, but their main role is to serve as a key messenger between innate and adaptive immunity since they are the main antigen-presenting cells (APCs). Eosinophils play a significant role in destroying parasites too big for phagocytosis, and basophils are involved in acute inflammatory responses such as asthma or allergies. NK cells are crucial for destroying virus-infected and tumour cells. This is achieved by the release of perforins and granzymes from their granules. These cells are also a source of interferon-gamma (IFNγ). ILCs are important for their regulatory roles. ILC-1, ILC-2, and ILC-3 selectively produce cytokines IFN-γ, IL-4, and IL-17, respectively, directing the appropriate immune response to specific pathogens (2).

Among innate-like T cells, a distinct population representing a bridge between innate and adaptive immune responses are γδ T cells. γδ T cells are a small population of lymphocytes that have unique biological functions. Besides innate-like features, they also express a T-cell receptor (TCR) that recognizes certain antigens. These cells develop alongside αβ T cells in the thymus, however, after leaving the thymus, some of them home to the lymph nodes, but many localize to non-lymphoid peripheral tissues, such as the dermis, lungs, and intestine, where they serve as the first line of defence (3). γδ T cells produce immunomodulatory cytokines and are divided into IL-17 and IFNγ producers. Additionally, they are responsible for recruiting macrophages that boost innate response, modulating innate and adaptive immune effector cells through the production of immunosuppressive cytokines (transforming growth factor-β (TGFβ) and IL-10), and promoting tissue healing and epithelial cell regeneration (4).

All these cells can recognize a wide array of molecules, making them more effective at combating rapidly mutating pathogens. However, they struggle to combat pathogens that have developed mechanisms to shield or hide their PAMPs to evade detection. This is due to their inability to remember specific molecules. In response to the inflammatory environment

triggered by the innate immune response, adaptive immune cells (lymphocytes) are activated. They begin to proliferate and differentiate into various specialized cells rapidly, each tailored to address the specific immunological challenge (2).

IFNs are a diverse group of immunomodulatory molecules important for defence against the virus. IFNs can be divided into three families: (1) type I, (2) type II, and (3) type III IFNs. The type I IFN family includes IFN-α, which has 13 distinct subtypes in humans and 14 in mice, along with IFN-β, and several poorly characterized single-gene products IFN-δ, IFN-ε, IFN-κ, IFN-ω, and IFN-ζ. These cytokines are recognized for their ability to induce an anti-viral state in both virus-infected and uninfected bystander cells by disrupting multiple stages of the viral replication cycle. However, IFN-α/β also has a broad range of additional functions that shape both innate and adaptive immune responses, against viruses, bacteria, and other pathogens. IFN-α/β response during infection can lead to various outcomes that are highly context-dependent. IFN-α is produced by immune cells, among which the major producers are plasmacytoid dendritic cells (pDCs) (5), while almost all cells can produce IFN-β, usually as a response to the stimulation of PRRs by microbial products, in the earliest phase of the immune response. PRRs are located on the cell surface, cytosol, or endosomal compartments. Recognition of foreign molecules by TLRs and RIG-I induces type I IFNs via distinct signalling pathways. One of the molecular complexes involved in this signalling cascade is the RIG-mitochondrial antiviral-signalling protein (MAVS) complex. It comprises about 30 proteins and coordinates many cellular processes like energy metabolism, anti-inflammatory responses, and mitochondrial metabolism. Activation of the RIG-MAVS complex splits signalling pathways into interferon regulatory factor 3 (IRF3) / IRF7 and nuclear factor-κB (NF-κB), resulting in type I IFN secretion (IRF branch) and a pro-inflammatory response (NF-κB branch) (6). Lactate is a key negative regulator of MAVS aggregation, preventing full antiviral response activation (7). After secretion, type I IFNs bind and signal through to type I IFN receptor (IFNAR), triggering the canonical Janus kinase–signal transducer and activator of transcription (JAK/STAT) pathway, leading to the transcription of numerous interferon-stimulated genes (ISGs) involved in inflammation, IFN II production, protein synthesis inhibition, autophagy, and apoptosis. Type I IFN has been shown to directly stimulate NK cells, prompting them to release IFN-γ during lymphocytic choriomeningitis virus (LCMV) infections (8). Additionally, non-JAK/STAT pathways, such as mitogen-activated protein

kinase (MAPKs) and phosphoinositide 3-kinase (PI3K), can be activated downstream of IFNAR, resulting in varied cellular effects (6).

Type III IFNs are the most recent members to join the IFN family. Type III IFNs encompass IFN-λ1, IFN-λ2, and IFN-λ3, also known as IL-29, IL-28A, and IL-28B, along with the recently identified IFN-λ4 (6). Viral infection induces the production of type III IFNs in many cell types, especially dendritic cells. Although type III IFNs have similar functions as type I IFNs, they have restricted activity since IFN-λR1 is not expressed on leukocytes but on cells of epithelial origin such as epidermal, bronchial epithelial cells, and even hepatocytes (9). This unique feature makes them primary defenders of barrier integrity at mucosal sites.

1.1.2. Adaptive immune response

The adaptive immune system, also known as acquired immunity, is complementary to the innate immune system and is able to generate a stronger, but more specific response. The adaptive immune response requires amplification of pathogen-specific cells, which are initially present in low numbers. For this reason, it takes several days before an effective adaptive immune response is formed. The adaptive immune system involves two main types of lymphocytes - B and T cells. Naïve lymphocytes are unspecialized, not tailored to any specific response before activation. Each lymphocyte has a unique antigen receptor, which has only been negatively selected for self-recognition, but not positively for pathogen recognition. Naïve lymphocytes are multipotent, meaning they can differentiate into distinct effector cells based on additional signals received during activation (10).

B cells originate from hematopoietic stem cells in the bone marrow. Unlike T cells, they can directly recognize antigens through unique antigen-binding receptors on their surface. Their main function is to produce antibodies against foreign antigens, but they can also act as APCs since they constitutively express MHC I and II. Upon activation by binding to foreign antigens, B cells multiply and differentiate into antibody-secreting plasma cells, with the help of cytokines such as IL-6, or memory B cells. B cells are crucial for the humoral or antibody-mediated immune response, in contrast to the cell-mediated immune response governed by T cells.

T cells also originate from hematopoietic stem cells in the bone marrow but mature in the thymus. APCs like dendritic cells, macrophages, B cells, and epithelial cells are necessary for

T cells to recognize specific antigens. T cells eliminate infected cells by recognizing non-self peptides (antigens) presented by major histocompatibility complex (MHC) molecules through their unique TCRs. Each T cell has a single type of TCR and can rapidly proliferate and differentiate upon receiving the right signals. There are three distinct phases in a T cell response to acute infection: clonal expansion, contraction of T cells, and memory formation. The T cell compartment includes CD4 T cells and CD8 T cells. CD4 T cells, also known as helper T cells, mediate the immune response. CD4 cells are activated when their TCRs recognize antigens bound to class II MHC molecules. Once activated, cells release cytokines that influence the activity of various cell types. They promote the proliferation and differentiation of B cells, antibody isotype switch, promote the destruction of ingested microbes by macrophages, and play a crucial role in activating CD8 T cells.

IFN-γ is the only member of the type II interferon family and is produced by lymphocytes, both of the innate immune system such as NK cells, and by adaptive immune cells, including CD4 and CD8 T lymphocytes (6). IFN-γ is a distinct cytokine compared to type I IFNs since it was initially categorized within the IFN family due to its capacity to 'interfere' with viral infections, which aligns with the original definition of interferons. IFNγ serves as a link between the innate and adaptive immune responses and influences a wide range of cells that express the cell-surface IFNγ receptor (IFNγR). Unlike type I IFNs, which are secreted in the early phase of infection in response to the presence of pathogens, IFNγ is typically secreted in the later phase of infection. IFN II also causes the activation of the JAK/STAT signalling cascade, which results in the activation of numerous ISGs. These two signalling cascades are distinguished by different STAT molecules in these pathways and different adapters that cause the complexes to bind to different parts of the DNA. In the IFN I pathway, STAT complexes in the nucleus bind to the interferon-stimulated response element (ISRE). In contrast, in the IFN II pathway, they bind to the interferon gamma-activated site (GAS), thereby activating different sets of genes (11).

1.1.2.1. CD8 T cells

CD8 T cells are crucial for protecting the body from infections and re-infections with intracellular pathogens like viruses and tumours, by directly targeting and killing infected cells using a variety of cytotoxic molecules. The naïve CD8 T-cell pool consists of many different clones, each unique in its antigen receptor, and ability to bind antigens presented by MHC I

molecules. To conserve nutrients, each clone is present in low numbers. Upon encountering an antigen, CD8 T cells must be activated to proliferate and achieve their full cytotoxic potential, a process called priming. The priming of CD8 T cells starts after the interaction of TCR with antigen/MHC I complex presented by APCs, for example, mature DCs. During the expansion phase that takes place in the lymph node, CD8 T cells differentiate into cytotoxic T lymphocytes (CTLs). CTLs migrate to all tissues and kill infected cells, which they specifically recognize by TCR. After pathogen identification, CTLs release granzymes and perforin and secrete cytokines like IFNγ and TNFα. Following the clearance of the pathogen, most effector CD8 T cells die by apoptosis during a contraction phase. However, a small percentage (~5–10%), differentiated at priming into memory CD8 T cells, survive (12). This selection process is not entirely random, as some CD8 T cells are intrinsically better at persisting and forming the memory pool than others (13). Upon re-encountering an antigen, memory cells can respond much more quickly and effectively than naïve cells, preventing pathogen expansion before clinical symptoms appear. This provides the organism with long-lasting immunological memory (12).

CD8 T cell proliferation and differentiation are modulated by three major signals: (1) antigen recognized by TCR, (2) co-stimulation, and (3) inflammation via cytokines. The main sources of these three signals are DCs and CD4 T cells. As APCs, DCs play a central role in priming both primary and secondary CD8 T cell response, which was confirmed by selective depletion of DCs by diphtheria toxin (14). Mature DCs are activated by the type I IFNs, secreted by innate cells, or by co-stimulation through interaction with antigen-specific CD4 helper cells via CD40/CD40L (CD40 on DCs which binds CD40L on CD4 T helper cells). CD4+ T cells are important in licensing the ability of DCs to prime CTL responses. Also, they provide a unique signal required to promote long-lived CD8 memory T cell function. (15). During infections, key co-stimulatory receptors for CD8 T cells include 4-1BB (ligand on APC is 4-1BBL), CD27 (CD70), CD28 (CD80/CD86), CD40 (CD40L), and OX40 (OX40L). The CD28 costimulatory pathway is the most studied due to its crucial role in the expansion and survival of antigen-specific CD8 T cells following infections with pathogens like influenza (16). During CD8 T cell priming, signalling through CD28 increases IL-2 production. IL-2 acts as an autocrine growth factor, it is produced by and stimulates the effector CD8 T cells (17). Pro-inflammatory cytokines like type I IFNs, IFNγ, IL-2, IL-12, IL-27, and IL-33 enhance CTL proliferation, differentiation, and survival. These cytokines promote CTL survival by increasing the

expression of cytokine and co-stimulatory receptors (e.g., CD25, OX40, 4-1BB), and BCL-3, an NF-κB inhibitor (18).

Effector and memory cells represent two distinct phenotypic and functional outcomes of CD8 T cell activation following antigen encounter. Following activation, CD25 and CD69 are rapidly upregulated on T cells. CD69, an early activation marker, is transiently expressed on both effector and memory T cells during activation (19). Another activation marker is CD25, the alpha chain of the IL-2 receptor, which is present on the surface of both immune and non-immune cells. It is abundantly expressed on activated circulating T cells and regulatory T cells (20). CD44 is upregulated upon activation and distinguishes naïve from effector and memory T cells since it is a marker for antigen-experienced T cells (21). Memory CD8 T cells, on the other hand, are distinguished by their long-term persistence, and ability to respond rapidly upon re-exposure to antigens than naïve cells. Survival and homeostatic proliferation of memory cells largely depend on cytokines, particularly the common γ chain cytokines IL-7 and IL-15 (17). Memory CD8 T cells typically express high levels of CD127, the IL-7 receptor alpha chain, which is important for their survival and homeostasis. L-selectin (CD62L), a lymph node homing receptor, is downregulated on effector T cells but re-expressed on central memory T cells, allowing them to circulate through lymphoid tissues (22). Together, these markers help define the functional states and migratory patterns of effector and memory CD8 T cells, enabling them to effectively protect the body against infections and tumours.

To unravel the complexity of the adaptive immune system, studying T cells in vivo is essential. The OT-1 TCR transgenic T cell system is a widely used experimental mode and powerful tool for unravelling the mechanism of T cell immunity and exploring how cells recognize and respond to a specific antigen. It involves T cells that are genetically engineered to express an MHC-I-restricted TCR known as OT-1. These T cells recognize specifically a peptide called SIINFEKL derived from the protein ovalbumin (OVA) with high affinity. Besides specificity, this system provides versatility and can be used to investigate different aspects of CD8 T cell biology, including activation, proliferation, differentiation, and formation of the memory, both *in vivo* and *in vitro* (23). Despite decades of research and ample knowledge about the role of cytokines, how other factors impact CD8 T cell differentiation, memory formation, and functionality still needs to be investigated.

1.1.3. Glucose metabolism and cellular energy production

Glucose is a key nutrient in the body, which is used as a building block for the generation of molecules such as nucleotides and amino acids and as a source of fuel for catabolic metabolism. As a fuel, it is used to produce ATP to provide energy so cells can function normally. The classical division of glucose energy metabolism in the cell is into glycolysis, and the complex reactions of the tricarboxylic acid cycle (Krebs cycle), which fuels oxidative phosphorylation (OXPHOS). During these processes, the breakdown of glucose is mediated and energy is produced. Glucose is a large hydrophilic molecule that cannot pass the hydrophobic plasma membrane of cells by simple diffusion. Therefore, it is transported by glucose transporters (GLUTs), integral membrane proteins that facilitate the transport. GLUTs are present on the cellular plasma membrane and there are 14 GLUT members. The most characterized are members of Class I; GLUT-1 to GLUT-4. GLUT1 is widely expressed in various cell types, including erythrocytes, fibroblasts, and the brain, where it handles basal glucose uptake. GLUT2 is found in the liver, pancreatic β-cells, intestine, and kidney. GLUT3 is primarily in neurons and other cells like sperm, white blood cells, and carcinoma cell lines. GLUT4, an insulin-mediated transporter, is present in adipose tissue, skeletal muscle, and cardiac muscle. Increased glucose uptake is common in most cancers and virus-infected cells (24). GLUTs are important for maintaining glucose homeostasis and providing cells with an adequate supply of glucose for energy production. Once inside the cell, glucose undergoes glycolysis.

Glycolysis is an ancient pathway and represents the fundamental process of producing energy. Glycolysis generates energy without the use of oxygen and can therefore operate in cells that function under low-oxygen conditions or in cells lacking mitochondria, for example, red blood cells. Glycolysis is a series of 10 enzymatic reactions that convert one glucose molecule into two pyruvate molecules. Moreover, this process yields a net gain of two ATP molecules, all occurring in the cytosol. Under aerobic conditions, generated pyruvate enters mitochondria and the Krebs cycle. Under anaerobic conditions, pyruvate is catalyzed by lactate dehydrogenase (LDH) to lactate (25). Lactate was thought to be just a waste product, however accumulating evidence unraveled its role in M2-like tumour-associated macrophage polarization (26), inhibiting T cell motility and effector function (27), and inhibiting RLR signalling and production of type I interferons in viral infection (6). Moreover, lactate is also a source of energy – it can be oxidized to pyruvate which then enters into mitochondria and

goes into the TCA cycle. Also, lactate accumulation can activate gluconeogenesis in the liver, a process through which lactate is a substrate for glucose production (28).

The Krebs cycle, also known as the citric acid or three-carbonic acid (TCA) cycle, and oxidative phosphorylation are essential processes in cellular respiration. Taking place in the mitochondria, the Krebs cycle breaks down acetyl-CoA into carbon dioxide while transferring energy to nicotinamide adenine dinucleotide (NADH) and flavin adenine dinucleotide (FADH2). It is recognized as an amphibolic pathway because it serves dual roles in metabolism: it provides intermediates for the synthesis of macromolecules such as lipids (anabolism) and generates reducing equivalents like NADH and FADH2, crucial for producing ATP through oxidative phosphorylation (catabolism). These high-energy electron carriers then proceed to the electron transport chain, where oxidative phosphorylation occurs. During this process, electrons from NADH and FADH2 pass through a series of protein complexes, ultimately reducing reactive oxygen to water. This electron transfer creates a proton gradient across the inner mitochondrial membrane, driving the production of ATP, the cell's primary energy currency. Oxidative phosphorylation synthesizes 32 molecules of ATP through the stepwise transfer of electrons to oxygen (25).

Although oxidative phosphorylation yields more ATP molecules from glucose breakdown than anaerobic glycolysis, many proliferating cells prefer glycolysis even when oxygen is available and the mitochondrial metabolism is functional (40). This phenomenon, known as the Warburg effect, was first observed by Otto Heinrich Warburg in the 1920s while studying tumour cell metabolism. He noted that tumour cells rely on aerobic glycolysis, converting glucose to lactate instead of channelling it through the Krebs cycle. Similar behaviour is seen in activated immune cells, such as neutrophils, eosinophils, basophils, dendritic cells (29), and T cells (30). For example, after the activation of TLRs, immune cells increase the expression of glucose transporters on their surface, allowing greater glucose uptake and promoting glycolysis (31). Generally, short-lived effector cells that require rapid proliferation and biomolecule synthesis switch to aerobic glycolysis, while long-lived regulatory cells prefer fatty acid oxidation and oxidative phosphorylation. Metabolic plasticity is a feature of the naïve CD8 T cells. Upon activation, CD8 T cells undergo major metabolic changes and switch towards glycolysis. Glycolytic metabolism is necessary to support rapid cell growth, proliferation, and differentiation (32). Costimulatory molecules CD28 and IL-2 enhance this metabolic phenotype and support the activation and expansion (33). Memory CD8 T cells,

compared to effector CD8 T cells, have a higher reliance on OXPHOS than on glycolysis. These cells exhibit a greater ability to consume oxygen and generate energy within the mitochondria. Moreover, they burn fatty acids through fatty acid oxidation to provide a substrate for the TCA cycle, acetyl-CoA (34). The shift to glycolysis, despite being less energy-efficient, offers several advantages for rapidly growing or highly active cells, including rapid growth under hypoxic conditions, faster and simpler energy generation, and the production of various small molecules that serve as intermediates in biosynthetic processes during periods of accelerated growth or activity (35). It enables increased utilization of the pentose phosphate pathway, which is essential for maintaining redox balance within the cell and metabolizing hexoses and pentoses. Pentoses are important for the synthesis of nucleotides and nucleic acids, which are necessary for rapidly dividing cells. This shift allows the cell to use glucose primarily as a carbon source rather than an energy source (36).

1.1.4. Viral infections and their impact on metabolism

Viral infections are among the most common diseases that remain a major challenge in modern medicine. Viruses are infectious particles containing genetic material, however, lacking self-sustaining or autoreplicative cellular machinery. Consequently, they can only replicate within living cells, known as host cells (37). When a virus enters a host cell, it alters crucial cellular metabolic pathways to facilitate its replication and spread. Although many viruses increase the consumption of essential nutrients such as glucose and glutamine and utilize similar anabolic metabolic pathways, these alterations are specific to each virus. These changes can vary even within the same virus family and depend on the type of host cell that is infected (38).

The genetic material of all viruses, which can be negative, or positive-sense, single-stranded, or double-stranded DNA or RNA, is surrounded by a protein coat known as a capsid. Some viruses also have an envelope, a lipid bilayer. For example, human cytomegalovirus (hCMV) is an enveloped, double-stranded DNA virus, while LCMV and influenza A are single-stranded RNA viruses (37). To meet their biosynthetic and energetic needs, DNA and RNA viruses have been demonstrated to extensively remodel host carbon metabolism. This includes enhancing glycolysis, increasing pentose phosphate pathway activity to support DNA and RNA replication, and promoting amino acid and lipid production (38). In essence, the cell metabolic rate increases as a consequence of increased demand for building blocks to sustain

virus particle formation. Many viruses such as hCMV and influenza A upregulate cellular glucose transporters to increase glucose uptake and glycolysis to meet the energy demands for viral replication. On the other hand, herpes simplex virus-1 (HSV-1), and Zika virus have been shown to increase oxidative phosphorylation to optimize adenosine triphosphate (ATP) production. In addition to glucose, which will be discussed in detail in the next subsection, viruses such as vaccinia virus (39), HSV-1, and adenoviruses (40) utilize glutamine for energy production (38).

Viruses hijack and alter the metabolism of individual cells, which can lead to metabolic changes in specific organs and, ultimately, systemic effects. Currently, it is still unknown whether and how our body uses glucose restriction as an antiviral defence mechanism.

1.2 Immune-endocrine interactions in viral infection

Recent findings highlight that the interaction between the immune and endocrine systems is crucial for maintaining metabolic homeostasis and protecting tissues during infections. The immune system plays a vital role in defending our bodies from pathogens, such as bacteria and viruses, utilizing cytokines and immune receptors as its weapons. On the other hand, the endocrine system uses hormones to maintain appropriate metabolic function in peripheral organs by regulating systemic homeostasis. Immune and endocrine cells often coexist within the same tissues, influencing each other's functions. In addition to its primary role in detecting and eliminating threats, the immune system is highly responsive to signals from the endocrine system due to the presence of hormone receptors on numerous immune cells. Conversely, the endocrine system is also highly reactive to immune mediators, such as cytokines. For example, macrophages are present in the pancreas and have a proliferative effect on β-cells (41). Moreover, in models of type 1 diabetes, upon the death of β-cells, islet macrophages produce insulin-like growth factor 1 (IGF-1) and shift to a reparative state (42). Pro-inflammatory cytokines, such as TNF, IFNγ, and IL-1β, typically produced during viral infections, directly influence insulin signalling and can promote the development of insulin resistance (IR) (43). N. V. Fedorova et al. showed that insulin, glucagon, and 17β-estradiol (E2) modulate human neutrophil activation and promote their adherence to blood vessels, particularly in the context of metabolic disorders (44). Even when located in different parts of the body, these cells can send and receive signals to and from each other. This

immuno-endocrine interaction plays a key role in various metabolically active organs and is important for regulating metabolic balance and the development of many metabolic diseases, such as diabetes. For example, for CD8 T cell functionality metabolic state is crucial. We showed that memory CD8 T cells have reduced functionality in response to viral infection in obese mice fed with a high-fat diet, a model for type 2 diabetes. Our findings showed that the functionality of CD8 T cells is independent of insulin signalling, but hyperglycemia impaired their anti-viral capacity (45). However, it is still necessary to investigate whether and which other hormones are responsible for CD8 dysfunction in the context of type 2 diabetes. The next chapter will focus on how these interactions affect glucose regulation, especially in the context of viral infections.

1.2.1. Regulation of blood glucose levels during infection

Combating an infection is an energy-intensive activity that demands peak performance from immune cells. When a virus enters our body, it starts to replicate, and we experience all sorts of symptoms such as fever, loss of appetite, fatigue, and reduced muscle strength. These changes, known as sickness metabolism, are physiological responses coordinated by the interaction between infected tissues and the immune system (46). Glucose is the main fuel, a vital energy source for most cells, and its availability determines many processes in the body, including growth, management of fat storage, and levels of anabolic and catabolic metabolism. Almost all cells in the body take up glucose for metabolic processes, though many tissues can use other carbohydrates such as acetate as a primary source of energy. For instance, the brain itself is responsible for about 60% of blood glucose consumption. Immune cells highly depend on glucose for their metabolism, and it is estimated that the activation of the immune system following infection is energetically extremely costly - it consumes up to 30% of the body's nutrients (47). However, glucose is equally important for pathogens, as many of them utilize it as a nutrient to support their replication (48,49). During an infection, the host therefore faces a dilemma: it must provide enough glucose to support the essential requirements of glucose-dependent organs like the brain and to meet the increased needs of the activated immune system (50), while simultaneously limiting glucose availability to pathogens (51). Therefore, sickness metabolism leads to increased resting time, so that energy-rich fuels can be redirected to support the immune system (52,53).

Under normal conditions, blood glucose levels are carefully maintained above a minimum threshold (~3.9 mmol/l). This ensures the optimal function of glucose-dependent cells and prevents life-threatening conditions such as hypoglycemic coma. Glucose homeostasis is regulated by the pancreatic hormones, insulin and glucagon (54). Changes in glucose metabolism in the context of infection primarily depend on the infection's severity. There appear to be three adapted metabolic states to infection. Euglycemic hyperinsulinemia following mild viral infection and severe hyperglycemia following severe will be discussed in the following chapters. The third metabolic state, referred to as glucose restriction, will be the subject of this research.

1.2.1.1. Mild viral infection

In the case of low to mild infection, virally induced pro-inflammatory cytokines such as IL-1β, TNF, and IFNγ impair systemic insulin sensitivity while maintaining normal blood glucose levels. There is ample evidence that viral infections induce insulin resistance without losing glycemic control (25). Hepatitis C virus (HCV) was shown to impair glucose uptake by downregulating GLUT-2 and GLUT-4 (26) and to induce insulin resistance by altering phosphorylation of insulin receptor substrate proteins 1 and 2 (27). Our group recently showed that local production of IFNγ causes downregulation of the insulin receptor in myocytes as a response to mild viral infection with murine cytomegalovirus (mCMV), lymphocytic choriomeningitis virus (LCMV), and Influenza A. Reduced insulin sensitivity of skeletal muscle cells is then compensated by increased production of insulin by the pancreas, generating a state of hyperinsulinemia. Hyperinsulinemia caused by infection has a dual role; it maintains normal blood glucose levels (euglycemia) and normal distribution of glucose to tissues that critically need it, but it also stimulates the activity of the immune system through the immuno-stimulatory effect of insulin. Elevated levels of insulin in the blood stimulate an anti-viral response via CD8 T lymphocytes, which presents negative feedback that contributes to the control of infection by the immune and endocrine systems (55). This first metabolic state is referred to as euglycemic hyperinsulinemia (56). However, in obese prediabetic subjects, who already have some degree of metabolic dysfunction, viral infection leads to decompensation of blood glucose control and rapid progression of type 2 diabetes (55).

1.2.1.2. Severe viral infection

In case of severe infection, or after severe trauma, alterations in blood glucose levels occur. This metabolic state, characterized by rising blood glucose levels beyond well-defined physiological values, exceeding 10 mmol/l or 180 mg/ml in otherwise healthy people, is known as stress hyperglycemia (57). Severe, potentially lethal infections or major insults such as trauma and heart infarctions trigger a neuroendocrine response, which results in the secretion of stress hormones such as adrenalin, noradrenalin, and corticosteroids. These hormones override insulin-mediated control, promote gluconeogenesis, and in conjunction with IL-1β, TNF, and IFNγ, induce insulin resistance in skeletal muscle (58). At the same time, insulin production by the pancreas is reduced, resulting in an increase in blood glucose levels (59) and disruption of normal glycemic regulation. Short-term and moderate hyperglycemia can be advantageous by providing glucose to immune cells, activating anti-apoptotic pathways, and promoting angiogenesis (60). However, hyperglycemia also adversely affects key components of the innate immune response, such as reducing neutrophil migration and activity (61). During the recent pandemic of severe acute respiratory syndrome coronavirus 2 (SARS-CoV-2), hyperglycemia has been observed to correlate with longer hospitalization periods, less favourable clinical outcomes, and increased mortality. Studies indicate that SARS-CoV-2-induced hyperglycemia is driven by insulin resistance (62). This extreme condition is not an antiviral defence mechanism, but a last-resort survival mechanism that ensures glucose availability to vital tissues by dramatically increasing blood glucose levels.

There is still little knowledge about what is happening in the metabolic state between mild and severe infection. This metabolic state, referred to as glucose restriction, is a case of a strong, non-lethal infection characterized by flu-like symptoms. But what is the purpose and underlying mechanism behind glucose restriction and us feeling sick?

1.2.2 Regulation of endocrine hormone levels during infection

A body of evidence suggests that hormones have a profound impact on immune cell function. Hormones are chemical messengers produced by different cell types that regulate body homeostasis and the cross-talk between systems. Interestingly, many hormone and immune receptors share intracellular signalling pathways, suggesting a functional overlap (63). Endocrine mediators produced by adipose tissue such as leptin and adiponectin are shown to be important for the control of immune cells. Leptin is shown to activate the

JAK/STAT pathway, the same one that is used by the pro-inflammatory cytokine IL-6. Therefore, leptin promotes the activation of the immune cells and increases their proliferation (64,65). Mice deficient in leptin become obese and insulin-resistant, but also have reduced immune cells in circulation and are more susceptible to infection (66).

Hormonal disbalance is linked to abnormal polarization of the immune response and reduced immune cell function during infections. However, the exact impact of many endocrine hormones on the immune system remains unclear. Based on our previous findings on insulin shown by Šestan et al. (55) and Kavazović et al. (45), which are described in chapter 1.2.2.1, we wanted to investigate more in-depth immune modulation by insulin and insulin-like growth factor 1 (IGF-1), hormones responsible for growth and metabolism. Signalling pathways activated by cytokines such as TNFα, and IL-6 also interfere with insulin signalling. Moreover, insulin and IGF-1 are structurally similar and they can both activate both the insulin and IGF-1 receptors.

1.2.2.1 Insulin

Insulin is an endocrine peptide hormone crucial for controlling metabolic fluxes to maintain energy balance and metabolic homeostasis. It is responsible for the regulation of many processes, such as glucose uptake, glycolysis, glycogenesis, lipogenesis, cell proliferation, and survival. Insulin receptors are expressed on many somatic cells, but for maintaining glucose homeostasis insulin has a direct effect on the liver, skeletal muscle, and white adipocytes. The regulation of metabolism by insulin in response to feeding is a highly efficient strategy for managing nutrient availability, a mechanism conserved from insects to humans (54).

Insulin facilitates glucose uptake and promotes its conversion into glycogen and lipids for storage. After the ingestion of food, blood glucose levels rise, which is the signal for pancreatic β-cells to produce insulin. Upon insulin binding, the insulin receptor (INSR) dimerizes and autophosphorylates, which activates the receptor. The activation leads to the phosphorylation of insulin receptor substrate proteins (IRS) that are linked to the activation of downstream signalling pathways. There are two main pathways: the PI3K-AKT/mammalian target of rapamycin (mTOR) pathway and the MAPK pathway. PI3K/AKT/mTOR pathway is important for insulin action on glucose transport via glucose transporter 4 (GLUT4) and glycogen synthesis, while the MAPK pathway is involved in cell growth and survival. Insulin stimulates

muscle cells, adipocytes, and the liver to absorb glucose, effectively lowering plasma glucose levels. The regulation of INSR signalling can occur at multiple levels, including insulin availability, surface receptor expression, post-translational modifications, such as phosphorylation, and intracellular crosstalk with additional pathways, which enhance activity and specificity of INSR (67).

The insulin receptor is also expressed on activated lymphocytes and plays a role in anti-viral responses. Under normal conditions, the insulin receptor on T cells is not expressed. However, during activation of T cells, it contributes to maximizing the functional potential and possibly the migration or recruitment of T cells to target organs (68). Insulin is continuously and systemically present; therefore, it may stimulate T cells when the production of cytokines is lower, since they are primarily produced by specialized immune cells in lymph nodes or at infection sites. A series of studies by Helderman et. al provided evidence of the upregulation of the INSR on the surface of T lymphocytes upon immune activation (69). We and other research groups have shown that insulin can directly promote glucose uptake and stimulate effector T-cell functionality (**Figure 1**) (45,55,70). This is because insulin receptor and CD28 signalling, a key costimulatory molecule for CD8 T cell activation, converge on the major signalling cascade, a PI3K pathway. Therefore, our previous studies suggested that insulin may function as a stimulatory molecule to CD8 T cells, leading to enhanced cytokine production (55).

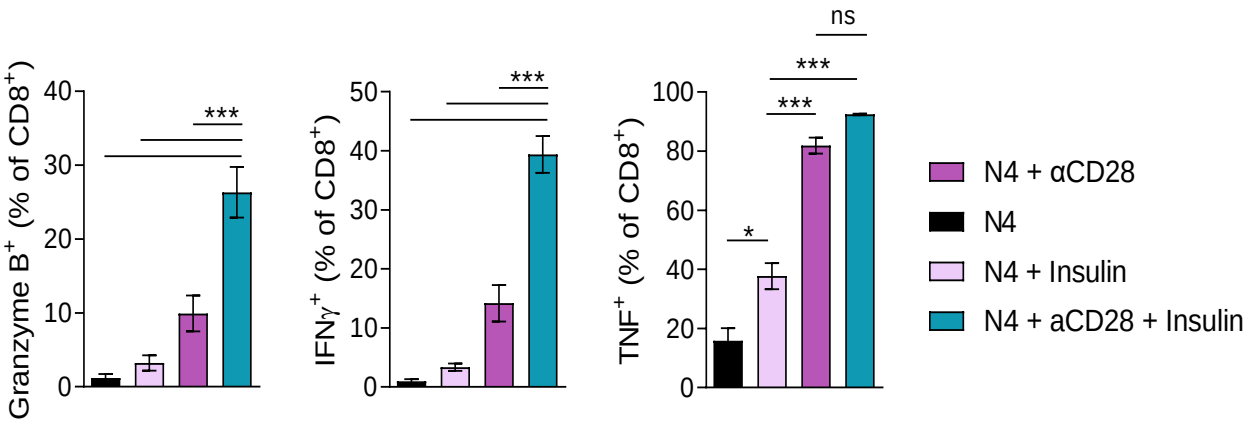

Figure 1. Insulin promotes the antiviral CD8 T cell response. Purified OT-1 cells were stimulated with only N4 peptide or in the presence of insulin and/or anti-CD28. Cells were re-stimulated with N4 peptide 48h after and production of Granzyme B, IFNγ, and TNF was measured by flow cytometry. A representative of three experiments with triplicates is shown. Indicated are means ± s.e.m. and statistical significances at *p < 0.05, **p < 0.01, ***p < 0,001 by ANOVA followed by Bonferroni post-testing. Modified from: Šestan M,

Marinović S, Kavazović I, et al. Virus-Induced Interferon-γ Causes Insulin Resistance in Skeletal Muscle and Derails Glycemic Control in Obesity. *Immunity*. 2018;49(1):164-177

It is thought that this immune-mediated regulation of host metabolism during infection aims to benefit the immune response to infection. Since insulin directly stimulates the antiviral T cell response, both insulin deficiency and a lack of the insulin receptor on T cells, impair the antiviral T cell response. In a mouse model of severe influenza infection, the absence of the insulin receptor in T cells diminished their response, making these mice more vulnerable to the infection. Particularly, INSR-deficient T cells exhibit reduced antigen-specific proliferation, impaired production of pro-inflammatory cytokines, and reduced migration to target organs (70). This phenomenon may help explain why individuals with pre-existing insulin resistance, obesity, and/or diabetes are more susceptible to severe viral infections (71).

1.2.2.2 Insulin-like growth factor 1

IGFs are hormones that mediate growth hormone (GH)-stimulated somatic growth and promote anabolic metabolism. There are two forms, IGF-1 and IGF-2. While IGF-2 plays a role during embryonic development, IGF-1 is mainly involved in enhancing growth and development in childhood and is crucial for metabolic functions in adulthood. The liver hepatocytes produce approximately 75% of IGF-1, whereas adipose tissue contributes to the rest. Synthesis and secretion of IGF-1 happen as a response to GH stimulation from the adenohypophysis. GH production is regulated by growth hormone-releasing hormone (GHRH) or somatostatin, produced by the neurohypophysis. Both insulin and IGF-1 inhibit the release of GH through negative feedback loops to the hypothalamus and hypophysis (72). IGF-1 function is further controlled by several IGF-1 binding proteins, which control the amount of free (and thus active) IGF-1 available.

The receptor for IGF-1 (IGF-1R) is expressed by numerous cell types, resulting in its highly pleiotropic effects. Beyond promoting somatic growth, IGF-1 enhances whole-body protein synthesis, inhibits proteolysis, and stimulates bone formation. Additionally, IGF-1 function partially overlaps with that of insulin, and its administration has been shown to reduce blood glucose levels in humans (73). Due to their structural similarity, both insulin and IGF-1 can bind and activate both the insulin and IGF-1 receptors. These receptors are composed of a homodimer, but even heterodimers of the insulin and IGF-1 receptors are present on certain

cells. However, IGF-1 cannot compensate for insulin deficiency. IGF-1R comprises two extracellular α-chains and two transmembrane β-chains, which include an intracellular tyrosine kinase domain essential for its biological effects. IGF-1R signalling involves autophosphorylation and tyrosine phosphorylation (74) of Shc adapter protein and insulin receptor substrates (IRS)-1, -2, -3, and -4. IRS acts as a docking protein, activating pathways like PI3K, Akt, and MAPK, leading to cell growth, migration, and survival. As mentioned, IGF-1R can form hybrid receptors with insulin receptors, preferentially binding IGF-1. In vascular smooth muscle cells (VSMCs), IGF-1R expression predominates, making them insensitive to insulin, while vascular endothelial cells (ECs) are more sensitive to insulin. Various hormones and growth factors regulate IGF-1, IGF-1R, and IGFBP expression, with potential cross-talk between IGF-1 and other signalling pathways.

IGF-1 plays a vital role in regulating immune cells, as its receptor is expressed on many of them. Exogenous IGF-1 administration stimulates thymocyte development and enhances the repopulation of the atrophic thymus after cyclosporin treatment (75). In human monocytes, IGF-1 has been shown to enhance the production of pro-inflammatory cytokines (76). In B cells, this hormone supports early development and boosts antibody production following immunization (77). In T lymphocytes, IGF-1 activates the PI3K and JNK signalling pathways, enhancing cell survival and cytokine production (78). IGF-1 can either promote regulatory T cell development (79) or drive Th17 polarization (80), depending on the inflammatory context. The specific impact of IGF-1 on CD8 T cell differentiation, memory formation, metabolism, and functionality remains unravelled.

1.3 Diabetes and viral infections

The importance of glucose homeostasis becomes particularly evident when it is permanently disrupted due to disease. The most common diseases that result in blood glucose regulation disorders are type 1 diabetes (T1D) and type 2 diabetes (T2D). T1D is characterized by the autoimmune destruction of insulin-producing pancreatic β-cells, which makes insulin production impossible. Shortage of a hormone essential for regulating blood glucose levels results in hyperglycemia and, without insulin supplementation, can result in death. Unlike T1D, which is an autoimmune disease, T2D is a chronic metabolic disease characterized by insulin resistance (IR). Insulin resistance is a crucial complication of obesity, a global epidemic of modern times due to high-fat, high-calorie foods and a sedentary lifestyle

that negatively affects organs with metabolic and endocrine functions. IR eventually results in hyperglycemia and increased gluconeogenesis. In the beginning, IR is compensated by increased insulin production, but with time, stress on the endoplasmic reticulum, mitochondrial overload, and harmful amyloidosis impair pancreatic beta-cell function, leading to diminished insulin production and, consequently, hyperglycemia and hyperlipidemia (81).

Individuals with T2D, who struggle to maintain normal glucose levels, frequently experience respiratory, urinary tract, and bacterial infections (82). The COVID-19 pandemic highlighted that people with T1D and T2D face an increased risk of severe complications and mortality upon infection due to impaired immune cell function (83). They also exhibit poorer vaccine responses (84), impaired T cell memory response (85), and a higher likelihood of complications during surgeries (82). Chronic hyperglycemia has been shown to directly impair immune cell function by preventing the optimal metabolic changes needed during illness, leading to abnormal antiviral responses (45). For example, hyperglycemia was shown to exacerbate influenza severity by compromising the pulmonary epithelial-endothelial barrier and increasing pulmonary oedema (86), and by leading to reduced immune cell infiltration and an increased viral load in the lungs in a mouse model of respiratory syncytial virus (RSV) infection (87). A study comparing patients with T2D who experienced severe COVID-19 infections revealed that insulin treatment was associated with lower survival rates. This suggests that hormonal imbalances, in addition to hyperglycemia, might negatively impact patients with diabetes (88).

2. RESEARCH GOALS

2. RESEARCH GOALS

This research project aims to investigate immune-endocrine mechanisms behind lowering blood glucose in the context of infection and their impact on the immune control of viral replication. Based on the body of evidence about the effects of mild and severe viral infection on the regulation of systemic blood glucose levels, we want to examine what is happening in acute infections with high, non-lethal virus doses.

Previously, it was shown that both mild and severe viral infections affect insulin sensitivity, leading to an altered glycemic state and therefore toward altered cellular antiviral responsiveness, as well as immune cell responsiveness. Based on our preliminary data, we hypothesize that strong viral infection causes a controlled drop in blood glucose concentration, which induces antiviral cellular mechanisms that contribute to rapid control of the infection. For the regulation of glucose levels, insulin is particularly important. In previous work by Šestan et al. (55) and Kavazović et al. (45), we showed that the endocrine hormone insulin does not only modulate glucose but also has a direct impact on the immune cells and promotes cytokine production by CD8 T cells. Subsequently, we will also investigate the hormonal control of the anti-viral response. We will do this using both our *in vivo* and *in vitro* models.

To answer the main research question, we defined two specific objectives and several sub-objectives:

I. To investigate the glucose control of the antiviral response, we will:

1.1. Determine whether infection-mediated changes in glycemia benefit the antiviral response

1.2. Investigate how infection-mediated changes in glycemia impact cellular anti-viral defence mechanisms

1.3. Determine if this mechanism is disrupted in the context of metabolic disease

II. To investigate the hormonal control of the antiviral response, we will:

2.1. Test the impact of IGF-1 on CD8 T cell differentiation and memory formation

2.2. Investigate the impact of IGF-1 on catabolic CD8 T cell metabolism

2.3. Determine the physiological relevance of IGF-1 on CD8 T cell functionality

3. MATERIAL AND METHODS

3. MATERIALS AND METHODS

3.1. Materials

3.1.1. Laboratoratory mice

Animal experiments were conducted in full compliance with Croatian Animal Ethical regulations ("Ordinance on the protection of animals used for scientific purposes", NN 55/2013, which aligns with Directive 2010/63/EU of the European Parliament and the European Council, as well as the "Law on animal protection" (NN 135/06, 37/13 and 102/17)), and under a project license of prof.dr.sc. Bojan Polić. All animal experiments were done with the approval from the University of Rijeka Medical Faculty Ethics Committee and the Croatian Ministry of Agriculture, Veterinary and Food Safety Directorate, under no. UP/I-322-01/21-01/31.

The experimental mice were bred and maintained in the Laboratory of Mouse Engineering and Breeding Facility (LAMRI) of the Faculty of Medicine, University of Rijeka. Mice were kept under specific pathogen-free (SPF) conditions in an individually ventilated caging system (IVC system) in 12/12-hour light-dark cycles, at 21 °C and 50% humidity. All genetically modified animal models were generated on the C57BL/6J background or backcrossed at least ten times with C57BL/6J mice. Unless stated otherwise, experiments included 8-12-week-old mice fed with a standard rodent diet – normal chow diet (NCD). Mice were strictly age and sex-matched within experiments and handled in accordance with institutional, national, and/or EU guidelines. All experiments were conducted following the 3R principles (Reduction, Refinement, and Replacement). Prior to commencing the studies, the minimum number of animals required to achieve statistically significant results was calculated.

Mouse strains used in this research are listed in **Table 1**. All lines were kept as breeding colonies in our local animal facility, LAMRI.

Table 1. Experimental mouse strains

EXPERIMENTAL MOUSE STRAIN	SOURCE	STRAIN CODE
C57BL/6 (B6; line 664)	Jackson Laboratories	JAX: 000664
C57BL/6J CD45.1 (line 2014)	Jackson Laboratories	JAX: 002014
Ins2Cre (line 3573)	Jackson Laboratories	JAX: 003573

Rosa26 iDTR	Prof. Ari Waisman, Mainz, Germany	JAX: 007900
C57BL/6J OT-1 +/- (line 3831)	Jackson Laboratories	JAX: 003831
CD4Cre	Prof. D. Littman (New York, USA)	JAX: 022071
InsRfl/fl IGF1Rfl/fl	Prof. J. Brüning (Cologne, Germany)	PMID: 18650937
InsRfl/fl IGF1Rfl/fl CD4Cre/+ OT-1tg+/-	Bred in house (LAMRI)	N/A

3.1.2. Cell lines

For most *in vitro* experiments, primary embryonic fibroblasts (mouse embryonic fibroblasts, MEF) isolated from C57BL/6J mice were used. Other primary cell line include bone marrow-derived macrophages (BMDM) isolated from femurs and tibias of C57BL/6J mice. Among the immortalized lines, the seminal vesicle endothelial cells (SVEC4-10) line was utilized. MEF cells were cultivated in a 3% DMEM medium, and SVEC in a 10% DMEM medium until confluence was reached. Tim Sparwasser (TWINCORE, Hannover) provided the ovalbumin (OVA)-transfected murine B16 melanoma cell line (B16-OVA) that was previously described (89). B16-OVA tumour cells were cultured in 10% DMEM (Pan Biotech) supplemented with β-mercaptoethanol (Sigma-Aldrich Corporation) under G418 selection (InvivoGen). A trypsin/EDTA solution was used to detach adherent cells.

3.1.3. Viruses

The murine cytomegalovirus (mCMV) is a bacterial artificial chromosome (BAC) derived virus. MCMV-pSM3fr-MCK-2fl clone 3.3. (in-house produced) has previously been shown to be biologically equivalent to the mCMV Smith strain (VR-1399; ATCC, Manassas, Virginia, USA) and is referred to as wild-type mCMV (90). Other mCMV strains used include the reporter strains mCMV-GFP (91), which expresses green fluorescent protein (GFP), allowing for infection tracking, and the mCMV m157 strain, which lacks the m157 sequence (92). pSM3fr-MCK-2fl clone 3.3 and Δm157 were propagated on MEFs (93). Virus mCMV-SIINFEKL (-N4) was generated as described (94). Lymphocytic choriomeningitis virus (LCMV) Armstrong strain (Armstrong E-350; ATCC) and LCMV-N4 (95) were propagated on baby mouse kidney cells according to standard protocol. Influenza A strain A/PR/8/34 (PR8) was generated in LLC-MK2 cells, and TID50 was determined in C57BL/6J mice.

3.1.4. Cell culture media

- Dulbecco's modified eagle medium - DMEM

DMEM medium (P04-03550, Pan Biotech), 4.5 g/L glucose (25mM), 10 mM HEPES (pH 7.2) (Pan Biotech), 2 mM L-glutamine, 3 or 10% Fetal Bovine Serum (FBS) (Pan Biotech), 0.1 g/L Streptomycin (Pan Biotech) and 10^5 U/L Penicillin (Pan Biotech).

- Dulbecco's modified eagle medium without glucose and glutamine - DMEM w/o glucose, w/o L-glutamine

DMEM medium (P04-01549, Pan Biotech), 3 or 10% Fetal Bovine Serum (FBS) (Pan Biotech), 10 mM HEPES (pH 7.2) (Pan Biotech), 0.1 g/L Streptomycin (Pan Biotech) and 10^5 U/L Penicillin (Pan Biotech).

Before use, 2 mM L-glutamine, and different concentrations of glucose (0.1 mM to 25 mM) or other metabolites, were added as described in Methods.

- Roswell park memorial institute medium - RPMI 1640

RPMI medium (Pan Biotech), 3 or 10% FBS (Pan Biotech), 10 mM HEPES (pH 7.2) (Pan Biotech), 2 mM L-glutamine (Pan Biotech), 10^5 U/L Penicillin (Pan Biotech), 0.1 g/L Streptomycin (Pan Biotech) and β2- mercaptoethanol (Sigma-Aldrich Corporation).

- Cell culture freezing medium

70% RPMI medium (Pan Biotech), 20% FBS (Pan Biotech), 10% dimethyl sulfoxide (DMSO) (Sigma-Aldrich Corporation).

- Flow cytometry medium (FACS medium)

PBS, 1% Bovine serum albumin (BSA) (Thermo Fisher Scientific), 0.1% sodium azide (NaN3) (Sigma-Aldrich Corporation), 1 mM Ethylenediaminetetraacetic acid (EDTA) (Sigma-Aldrich Corporation).

- Methylcellulose medium

DMEM medium (Pan Biotech), 10% FBS (Pan Biotech), 2,2% methylcellulose (Sigma-Aldrich Corporation)

3.1.5. Buffers

- Fluorescence-activated cell sorting (FACS) buffer

PBS (Lonza Group), 1% Bovine serum albumin (BSA) (Thermo Fisher Scientific, Waltham, Massachusetts, USA), 2 mM EDTA (Sigma-Aldrich Corporation).

- Magnetic-activated cell sorting (MACS) buffer

PBS (Lonza Group), 1% FBS (Pan Biotech), 1 mM EDTA (Sigma-Aldrich Corporation).

- Red blood cell lysis buffer (10 x)

140 mM ammonium chloride (NH_4Cl) (Sigma-Aldrich Corporation), 2.7 mM potassium chloride (KCl) (Sigma-Aldrich Corporation), 1.5 mM monopotassium phosphate (KH_2PO_4) (Sigma-Aldrich Corporation), 6.5 mM disodium phosphate (Na_2HPO_4) (Sigma-Aldrich Corporation), 0.7 mM Calcium chloride ($CaCl_2$) (Sigma-Aldrich Corporation). For working solution (1X) 10x buffer is diluted with dH_2O.

- HEPES-buffered saline

Composed of 140 mM NaCl, 20 mM Na-HEPES, 2.5 mM MgSO4, 1 mM CaCl2, and 5 mM KCl, pH 7.4

- 10 x PCR reaction buffer

200 mM Tris/HCl (pH 8.4) (Promega, Madison, Wisconsin, USA), 500 mM KCl (Sigma-Aldrich Corporation).

- Tail lysis buffer

100 mM Tris/HCl, pH 7.5 (Promega), 5 mM EDTA (Sigma-Aldrich Corporation), 0.2% (w/v) SDS (Sigma-Aldrich Corporation), 200 mM NaCl (Sigma-Aldrich Corporation). Add 100 µg/ml Proteinase K (Sigma-Aldrich Corporation) to 400 µL of the tail buffer.

- TE buffer (Tris-EDTA buffer)

Melt 294.5 g sodium acetate in 500 ml H_2O, 1 mM EDTA (Sigma-Aldrich Corporation), 10 mM Tris/HCl pH 8.0. Adjust pH with NaOH on 5.5 and add H_2O up to 1 L.

- TAE buffer (Tris-acetat-EDTA pufer, 50x)

57.1 ml glacial acetic acid (Sigma-Aldrich Corporation), 242 g Tris base (Sigma-Aldrich Corporation), 100 ml 0.5 M EDTA (pH 8.0) (Sigma-Aldrich Corporation), fill with qH_2O up to 100 ml.

- Percoll stock solution

54 ml Percoll (GE Healthcare, Little Chalfont, UK), 6 ml 10X phosphate-buffered saline (PBS) (Lonza Group, Basel, Switzerland).

Percoll 80%

40 ml Percoll stock solution, 10 ml 1X PBS (Lonza Group)

Percoll 40%

20 ml Percoll stock solution, 30 ml 3% DMEM (Pan Biotech)

3.1.6. Antibodies, peptides, chemicals, and kits

Antibodies were purchased from suppliers as indicated in **Table 2**.

Table 2. Antibodies, peptides, chemicals, and kits used in experiments

REAGENT or RESOURCE	SOURCE	IDENTIFIER
ANTIBODIES		
Rat Anti-mouse Monoclonal Antibody IFN-γ PE (Clone: XMG1.2)	eBioscience	#12-7311-82
Rat Anti-Mouse Monoclonal Antibody IFN-γ APC (Clone: XMG1.2)	eBioscience	#17-7311-82
Rat Anti-Mouse Monoclonal Antibody TNF alpha FITC (Clone: MP6-XT22)	eBioscience	#11-7321-82
Rat Anti-Mouse Monoclonal Antibody IL-2 PE-Cyanine7 (Clone: JES6-5H4)	eBioscience	#25-7021-82
Syrian hamster Anti-mouse monoclonal KLRG1 FITC (Clone: 2F1)	eBioscience	#11-5893-80
Rat Anti-mouse monoclonal CD8a-PercpCy5.5 (Clone: 53-6.7)	eBioscience	#45-0081-80
Mouse Anti-Mouse Monoclonal Antibody CD45.1 FITC (Clone: A20)	eBioscience	#11-0453-82
Mouse Anti-Mouse Monoclonal Antibody CD45.2 PercpCy5.5 (Clone: 104)	eBioscience	#45-0454-82
Rat Anti-Mouse Monoclonal Antibody CD25 APC (Clone: PC61.5)	eBioscience	#17-0251-81
Rat Anti-Mouse Monoclonal Antibody CD127 PE (Clone: A7R34)	eBioscience	#12-1271-83
Rat Anti-mouse Monoclonal Antibody CD4 PE (Clone: GK 1.5)	eBioscience	#12-0041-85
Rat Anti-mouse Monoclonal Antibody CD62L PerCP-Cyanine5.5 (Clone: MEL-14)	eBioscience	#45-0621-82
Rat Anti- mouse Monoclonal Antibody CD44 APC-eFluor™ 780 (Clone: IM7)	eBioscience	#47-0441-82

Armenian hamster Anti-mouse Monoclonal Antibody CD3e PE-Cyanine7 (Clone: 145-2C11)	eBioscience	#25-0031-82
Armenian hamster Anti-mouse Monoclonal Antibody CD69 PE-Cyanine7 (Clone: H1.2F3)	eBioscience	#25-0691-82
Mouse Anti-mouse Monoclonal Antibody NK1.1 PerCP-Cyanine5.5 (Clone: PK136)	eBioscience	#45-5941-82
Mouse Anti-mouse Monoclonal Antibody TCR V alpha 2 APC (Clone: B20.1)	eBioscience	#17-5812-82
Mouse Anti-mouse Monoclonal Antibody CD28 (Clone: 37.51)	Invitrogen	#14-0281-82
Mouse IGF-1 Recombinant Protein	PeproTech	#250-19-50UG
Fixable Viability Dye eFluor™ 780	eBioscience	#65-0865-14
Fixable Viability Dye eFluor™ 506	eBioscience	#65-0865-14
Rat anti-mouse CD16/32 mAb (93)	eBioscience	#16-0161-82
Anti-NK1.1 (Klon PK136)	BioXCell	BP0036
PEPTIDES		
SIINFEKL (N4)	GenScript	Custom
CHEMICALS AND KITS		
2-Deoxy-D-glucose (2DG)	Sigma Aldrich	D6134
Acetate	Sigma Aldrich	S2889
Albumin fraction V	Roth	T844.3
β-Mercaptoethanol	Pan Biotech	P07-05100
Brefeldin A	eBioscience	#00-4506-51
CFSE	Sigma	150347-59-4
Citrate	Kemika	1405407
CD8a (Ly-2) MicroBeads	Miltenyi Biotec	130-117-044
DMEM (4.5 g/L glucose, w L-glutamine)	Pan Biotech	P04-03550
DMEM (w/o glucose, w/o L-glutamine)	Pan Biotech	P04-01549
DMSO (Dimethyl sulphoxide)	Gram-mol	P04-03550
Diphteria Toxin	Sigma Aldrich	#322326
DPBS (Dulbecco's phosphate-buffered saline)	Pan Biotech	P120601
EDTA	Kemika	1136808
Ethidium-bromide (EtBr)	Carl Roth	2218.1

Fetal Bovine Serum (FBS Standard)	Pan Biotech	P30-3306
Fixation/Permeabilization Concentrate	Invitrogen	P30-3306
Fixation/Permeabilization Diluent	Invitrogen	00-5123
FoxP3 staining buffer set	eBioscience	00-5523-00
Fix/Perm kit	BD Biosciences	554714
Galactose (D+ galactose)	Sigma Aldrich	G5388
G418 (Geneticin)	InvivoGen	108321-42-2
Glucose (D+ glucose)	CarlRoth GmbH	X997.2
Glucose (HK) Assay Kit	Sigma Aldrich	GAHK20-1KT
Glutamine (L-glutamine)	Pan Biotech	P04-80100
HEPES	Sigma Aldrich	7365-45-9
IC Fixation Buffer	Invitrogen	P04-80100
Insulin Aspart NovoRapid FlexPen	Novo Nordisk	
Ionomycin	Sigma Aldrich	407952
L-Lactate Assay Kit (Colorimetric)	Abcam	ab65331
LS columns	Miltenyi Biotec	130-042-401
Mouse Insulin ELISA	Alpco	80-INSMS-E01
Mouse IGF1 ELISA Kit	Abcam	ab108874
NucleoZOL	Macherey-Nagel	593-84-0
Oligomycin A	MedChemExpress	HY-16589
o-Phenylenediamine dihydrochloride (OPD)	Sigma Aldrich	740404
Penicillin-Streptomycin	Pan Biotech	P4664
Percoll	Cytiva	P06-07100
Permeabilization Buffer (10x)	Invitrogen	17089101
PMA (Phorbol 12-myristate 13-acetate)	Sigma Aldrich	P1839
RBC Lysis Buffer	eBioscience	00-4333-57
Reverse Transcription Core Kit	Eurogentec	RT-RTCK-03
RPMI 1640	Pan Biotech	P04-18047
SD CodeFree automatic glucometer	SD Biosensor	
SD CodeFree Blood Glucose Test Strips	SD Biosensor	
Sodium pyruvate	Sigma Aldrich	P2256
Sodium oxamate	Cayman Chemical	19057
SYBR Green dye	Eurogentec	UF-NSMT-B0701

Takyon No Rox SYBR MasterMix dTTP Blue	Eurogentec	43-695
Tris buffer	Roth	4855.2
Trypsin/EDTA (10x)	Pan Biotech	T3605
Tween 20	Sigma Aldrich	P10-024100

3.2 Methods

3.2.1. Mouse genotyping

3.2.1.1. DNA isolation from the murine tail

Freshly cut or frozen biopsies of ~ 4 mm murine tail placed in 1.5 mL Eppendorf tubes were incubated overnight in a thermo-block at 56°C with 0.5 mL of tail lysis buffer and proteinase K (1:50). Next day, tubes were centrifuged in a small table centrifuge (5 min at 13680 x *g*) to pellet cellular debris. The supernatant was transferred into a clean 1.5 mL tube. DNA was precipitated by the addition of 0.5 ml of isopropanol and mixed gently by rotation of the tube. The samples were then centrifuged (5 min at 13680 x *g*), and the supernatant was removed. Precipitated DNA was washed twice with 0.6 mL of 70% EtOH. Samples were then pelleted (5 min at 13680 x *g*), dried, and DNA was dissolved in 150 µL TE buffer and incubated for 15 min at 56°C. Genomic DNA was stored at 4^{o}C.

3.2.1.2. Polymerase chain reaction (PCR)

The PCR reaction mix included 10x reaction buffer, $MgCl_2$ (50 mM) (NEB, Ipswich, Massachusetts, USA), dNTP (5 mM) (Metabion, Munich, Germany), forward primer (Metabion), reverse primer (Metabion), Taq polymerase (0.025 U/µL) (NEB) and dH_2O, making a total volume of 25 µL. To each Eppendorf tube containing the PCR reaction mix, 1 µl of DNA of interest was added. The PCR reaction was carried out in a PCR thermo-block (Bio-Rad, Hercules, California, USA). This method was used to determine the genotype of the animals used in the experiments, with different sets of primers applied based on the genotype (see **Table 3**).

Table 3. List of primers used for PCR

Ins2Cre	Tg FWD: 5`-GTG AAA CAG CAT TGC TGT CAC TT-3' Tg REV: 5`-GCG GTC TGG CAG TAA AAA CTA TC-3' Ctrl FWD: 5`-CTA GGC CAC AGA ATT GAA AGA TCT-3' Ctrl REV: 5`-GTA GGT GGA AAT TCT AGC ATC ATC C-3'
CD4Cre	SC-1: 5'-GTC CAA TTT ACT GAC CGT ACA-3' SC-3: 5'-CTG TCA CTT GGT CGT GGC AGC-3'

OT-1	OT1 TCR1 F: 5’-CAG CAG CAG GTG AGA CAA AGT-3' OT1 TCR1 R: 5’-GGC TTT ATA ATT AGC TTG GTC C-3' OT1 Ctrl. F: 5’-CAA ATG TTG CTT GTC TGG TG-3' OT1 Ctrl. R: 5’-GTC AGT CGA GTG CAC AGT TT-3'
IGF1r	IGF1r-FIFwd: 5’TCC CTC AGG CTT CAT CCG CAA-3' IGF1r-FIRev: 5’CTT CAG CTT TGC AGG TGC ACG-3'

3.2.1.3. Agarose gel electrophoresis

To determine the size of amplified DNA fragments, we used agarose gel electrophoresis. A 1.8% agarose gel was prepared by dissolving agarose in boiling 1xTAE buffer. Once the gel cooled to approximately 50°C, 2 µL of ethidium bromide (EtBr) (Sigma-Aldrich Corporation) was added per 50 mL of gel solution and then poured into a gel container. Combs were placed in the liquid gel to form wells as the gel polymerized. After polymerization, a molecular-weight size marker was added to the first well to determine the size of the individual DNA fragments. The DNA bands were visualized using the gelLITE Gel Documentation System (Cleaver Scientific, Rugby, United Kingdom).

3.2.2. Immune cell isolation protocols

3.2.2.1. Isolation of splenic lymphocytes

Splenocytes were isolated as previously described (96). The spleen was harvested and homogenized through a 100 µm cell strainer (Thermo Fisher Scientific) using 3% DMEM. The homogenate was then centrifuged at 1500 rpm for 5 minutes. The resulting pellet was resuspended in 3 mL of erythrocyte lysis buffer to lyse the erythrocytes. After a 5-minute incubation on ice, 7 ml of 3% DMEM was added. The suspension was centrifuged again at 1500 rpm for 5 minutes, the supernatant was discarded, and the pellet was resuspended in 5 mL of 3% RPMI.

3.2.2.2. Isolation of hepatic lymphocytes

The entire liver, excluding the gall bladder, was harvested and homogenized through a 70 µm cell strainer into a 50 ml tube. Each liver was processed with 5–10 ml of 3% DMEM to create a single-cell suspension. This cell suspension was centrifuged for 5 min at 1700 rpm,

the supernatant discarded, and the pellet resuspended in 5 mL of 40% Percoll solution. The resuspended pellet was carefully layered over an equal volume of 80% Percoll solution and centrifuged at 1800 rpm for 30 minutes at room temperature (RT). After centrifugation, the sample was separated into layers based on density differences. The ring of leukocytes was carefully collected from the gradient and washed with 5 ml of 3% DMEM. This suspension was centrifuged again at 1700 rpm for 5 minutes, and the cell pellet was resuspended in 1 ml of erythrocyte lysis buffer. After a few minutes at RT, the lysis buffer was neutralized by adding 2 mL of 3% DMEM and centrifuged again for 5 min. Finally, the supernatant was removed and the pellet resuspended in 1 mL of 3% DMEM. Samples from this cell suspension were taken for cell counting and analysis.

3.2.2.3. Isolation of bone marrow-derived macrophages

BMDMs were isolated using established protocols (97). Femurs and tibias were harvested from C57BL/6J mice, and bone marrow was flushed out. The bone marrow was then filtered through a 70 µm cell strainer (Greiner Bio-One) to create a single-cell suspension. Cells were cultured in non-tissue culture-treated Petri dishes (Corning, 430597) with RPMI medium supplemented with 10% fetal Bovine serum and 20% L929-conditioned supernatant. On day 3, an additional 30 mL of fresh medium was added, and by day 7, the BMDMs were ready for *in vitro* experiments.

3.2.3. Cell counting

The number of cells per millilitre of the isolation suspension was determined using the Corning Cell Counter (Corning, New York, USA). Cells were mixed with trypan blue stain in a 1:1 ratio, which allowed us to determine live from dead cells.

3.2.4. Flow cytometry

For phenotypic cell analysis, cells were labelled with fluorochrome-conjugated antibodies, and results were acquired through flow cytometry using a FACSVerse (BD) and a MACSQuant Analyzer 16 (Miltenyi Biotec). Additionally, flow cytometry was used to determine the viral load in experiments involving cells infected with a mCMV virus expressing a

fluorescent protein (eGFP). Data analysis was performed with FlowJo software (FlowJo LLC, Ashland, Oregon, USA).

3.2.4.1. Cell surface staining

Flow cytometric analysis was performed using fluorophore-labeled antibodies specific to certain markers. Single-cell suspensions from the spleen, liver, or cell lines were prepared. Labeling antibodies were diluted in 40 µL of FACS medium, along with the Fc receptor block (CD16/32, clone 2.4G2) that prevents nonspecific binding of antibodies. After a 30-minute incubation at 4°C, the cells were washed with FACS medium, centrifuged for 5 minutes at 4000 rpm, and resuspended in 120 µL of FACS medium. Samples were analyzed on the same day.

3.2.4.2. Cytoplasmic intracellular staining

For cytoplasmic intracellular cytokine staining, cells were first stimulated *in vitro* with PMA (50ng/mL) and ionomycin (500 ng/mL) (Sigma-Aldrich), or restimulated *in vitro* with 10ng/mL peptide (N4, SIINFEKL) in complete RPMI, in the presence of brefeldin A (eBioscience) for 4 hours at 37°C. Intracellular staining was performed using an IC Fix/Perm kit (BD Biosciences) according to the manufacturer's instructions. Briefly, cells were first stained for surface markers, then fixed for 30 minutes at room temperature with fixation buffer, and washed in Perm/Wash permeabilization buffer. After centrifugation, cells were incubated with 40 µL of an antibody mix prepared in Perm/Wash buffer for 30 minutes at 4°C. The cells were then washed, centrifuged, resuspended in FACS buffer, and analyzed on the flow cytometer either the same day or stored overnight at +4 °C and analyzed the following day.

3.2.4.3. Intranuclear staining

Cells were stained for surface markers, then fixed and permeabilized using a Nuclear Fixation/Permeabilization kit (eBioscience, FoxP3) containing diluent and concentrate for 30 minutes at room temperature. They were washed in Perm/Wash permeabilization buffer. After centrifugation, the cells were incubated with 40 µl of an antibody mix for 1 hour at 4°C. The cells were then washed, centrifuged, resuspended in 120 µl FACS buffer, and analyzed either the same day or the next day.

3.2.4.4. CFSE staining

For proliferation assays, cells were labeled with carboxyfluorescein succinimidyl ester (CFSE) according to the manufacturer's protocol. Cells cultured in a medium with FBS were washed three times with PBS to remove residual proteins. The cells were then resuspended in PBS, adjusting the volume to achieve a maximum concentration (10^7) of cells/ml. They were mixed with CFSE diluted in PBS at a 1:1 ratio, resulting in a final concentration of 5 µM CFSE. The CFSE-labeled cells were incubated in the dark at 37°C for 10 minutes, then washed twice with 5 ml of 10% DMEM. CFSE dilution was assessed by flow cytometry after 3 and 6 days.

3.2.4.5. Viability staining

Fixable Viability Dyes eFluor 780 (eBioscience) or Fixable Viability Dye eFluor™ 506 (eBioscience) were used to exclude dead cells. Viability Dye eFluor 780 was used at a dilution factor of 1:1000, and Viability Dye eFluor™ 506 at 1:200 in FACS medium, together with cell surface staining antibodies. Cells were stained for 30 minutes at +4°C.

3.2.5. *In vitro* experiments

3.2.5.1 Cell lines

A total of 80,000 mouse MEFs, BMDMs, and SVEC cells per well were plated in a 24-well plate and preincubated with increasing glucose concentrations (1 mM to 25 mM) for 20 hours in complete DMEM (supplemented with 10% FBS, 1% HEPES, sodium pyruvate, glutamine, streptomycin, and penicillin). When experiments requiring specific glucose or metabolite concentrations were performed, fresh media was prepared by adding glucose, glutamine (final concentration 2 mM), or other metabolites to DMEM without glucose and glutamine (P04-01549, Pan Biotech). When indicated, metabolites such as 5 mM citrate (1405407, Kemika), 5 mM acetate (S2889, Sigma-Aldrich), 25 mM galactose (G5388, Sigma-Aldrich), pyruvate (P2256, Sigma-Aldrich) up to 100 mM were used to supplement low-glucose (1 mM) medium. 20 mM sodium oxamate (19057, Cayman Chemical), a specific lactate dehydrogenase A (LDHA) inhibitor, was used to inhibit lactate formation. Subsequently, cells were infected with mCMV-eGFP or mCMV at 0.01 MOI. At indicated time-points, cells or supernatants were analyzed for viral replication using confocal microscopy (Leica TCS SP8 confocal laser scanning microscope and LasX acquisition software) or by

measuring GFP expression within the cells, or IFNβ levels in the supernatant after 24h incubation. To assess cell proliferation, cells were stained with the proliferation dye eFluor450 (65-0842-85, eBioscience).

3.2.5.2 CD8 T cell stimulation

CD8 OT-1 T cells were isolated from the spleen and purified by positive selection using Ly-2 magnetic beads (Miltenyi Biotec) according to the manufacturer's protocol. Cells were cultured in RPMI 1640 medium (PAN-Biotech), supplemented with 10% FBS (PAN-Biotech). For *in vitro* differentiation, $3x10^4$ cells per well in U-bottom 96 well plate (Cellstar) were stimulated for 30h with 1 ng/mL of SIINFEKL (N4) peptide in the presence of 0.5 µg/mL of αCD28 (37.51, eBioscience), with or without different concentrations of IGF-1 (PeproTech). After 30h of stimulation, cells were washed and cultured for 3 days with 50 ng/mL IL-2 (PreproTech) in the presence or absence of IGF-1 to generate effector CD8 T cells. For *in vitro* memory differentiation, cells were washed and cultured for an additional 5 days with 50 ng/mL IL-15 (PreproTech) in the presence or absence of IGF-1. For proliferation assays, cells were labeled with CFSE, and its dilution was assessed by flow cytometry after 3 days and/or 6 days. For cytokine production, cells were re-stimulated with 10 ng/mL N4 peptide in the presence of Brefeldin A. Cytokines were measured 4 hours later by intracellular flow cytometry.

3.2.6. *In vivo* experiments

3.2.6.1. Metabolic tests

Metabolic measurements were done as previously described (55). For fasting plasma glucose (FPG) measurement, animals were fasted for 6 hours, unless stated otherwise. Glucose levels were measured in blood taken from the *v. saphena* with an automated glucometer (SD, Codefree). To induce hyperglycemia following infection, a 5% (w/v) glucose solution was added to the water.

3.2.6.2. Virus infections, adaptive transfers, and tumour model

All viruses and the tumour model were described in section 3.1.2. and 3.1.3. All used mCMV strains were propagated on MEF and purified using standard protocols (93). Adult mice, 8-12 weeks old, were intravenously (i.v.) infected with $2x10^5$ PFU mCMV, mCMV-Δm157, or mCMV-N4 in 500 µL of pure DMEM, or $2x10^7$ PFU mCMV for strong infection. Virus titers were determined on MEF by a standard plaque assay. Adult animals were intraperitoneally (i.p.) infected with a normal dose of $1x10^6$ inclusion-forming units (IFU) of LCMV or LCMV-N4 in 500 µL of pure DMEM, or $2x10^7$ IFU of LCMV in 500 µL of pure DMEM for strong infection. For survival experiments, mice were infected intranasally with 20% of an LD50 dose of Influenza A under ketamine/xylazine anaesthesia. Regarding the tumour model, B16-OVA cells were cultured in 10% DMEM supplemented with β-mercaptoethanol and under G418 selection. Mice were i.v. injected with 10^5 B16-OVA cells, and survival was monitored. CD8 T cells were purified by positive selection using magnetic beads (Miltenyi Biotec) according to the manufacturer's protocol. Mice were i.v. injected with $2x10^4$ – $4x10^4$ of OT-1 and/or IR^{CKO} $IGF1R^{CKO}$ OT-1 CD8 T cells (dependent on the experiment) in a volume of 500 µL of pure DMEM.

3.2.6.3. Cell depletion and streptozotocin treatment

To deplete pancreatic β cells in Ins2CreiDTR mice, an i.p. injection of 25 ng/ g of DT (Sigma Aldrich) was administered 48 and 24 hours before infection. Hyperglycemia was induced with 125 mg/kg of streptozotocin (STZ) (Sigma-Aldrich Corporation), a chemical selectively toxic to the β cells of the pancreatic islets used to induce type I diabetes. STZ was dissolved in PBS every five days until hyperglycemia was achieved, which was determined by measuring FPG after 6 hours of fasting. The depletion of NK cells in vivo was performed by i.p. injection of 250 µg of αNK1.1 (BioX cell; PK136) one day before infection with mCMV-N4.

3.2.6.4. Diet-induced obesity

As previously described (98), WT male mice (8-12 weeks old) were fed *ad libitum* with a high-fat diet (HFD), where 60% of the calories were derived from animal fat (Bregi). The HFD causes the onset of liver insulin resistance after 6 weeks, elevated FPG levels, and increased pyruvate intolerance, but normal glucose and insulin tolerance, resembling the state of human prediabetes. After 10-12 weeks of feeding HFD results in IR and glucose intolerance

(GI) development. Animals remained on this diet for 12 weeks, and the onset of diabetes was assessed by measuring the increase in FPG levels compared to control animals. Control animals were fed a normal chow diet (NCD) containing 5-6% fat (SSNIFF, Spezialdiaten, GmbH, Soest, Germany). Following this, we isolated serum from the blood taken from *v. bucales*, and IGF-1 levels were measured in the serum using ELISA.

3.2.7. ELISA

To analyze serum insulin levels, animals were fasted for 16h. Blood was isolated from the facial vein using heparin-coated plastics. Plasma insulin was measured using the mouse ultrasensitive insulin ELISA kit (Alpco). To assess plasma and/or supernatant IFNβ levels, we used a rat monoclonal capture antibody (clone 7F-D3, Abcam), a rabbit polyclonal detection antibody (32400-1, Pbl assay science), and the anti-hIgG-HRP antibody (111-035-003; Jackson Immunoresearch). To determine serum IGF1 levels, a mouse insulin-like growth factor 1 (IGF1) ELISA kit (ab108874, Abcam) was used. Absorbance was determined by a microplate reader (TriStar LB 941 Multimode Microplate Reader; Berthold Technologies) and analyzed using MicroWin v5.24 (Berthold Technologies).

3.2.8. L-lactate assay and inhibition of lactate production

Lactate content was measured *in vitro* in SVEC cells infected with 0.01 MOI mCMV, cultured in a medium containing different glucose concentrations, with or without glutamine or oxamate, 3 days p.i. The measurements were performed using the colorimetric L-Lactate Assay Kit (Abcam) according to the manufacturer's instructions. The same kit was used to quantify lactate production *in vivo* in the spleen and liver of C57BL/6J mice infected with 2×10^7 IFU LCMV. The mice were fasted and given either normal water or water supplemented with 5% glucose for 3 days p.i. To inhibit lactate dehydrogenase (LDH), mice received daily intraperitoneal injections of 750 mg kg−1 of sodium oxamate (Cayman Chemical), starting one day before infection.

3.2.9. Glucose uptake

SVEC cells were plated at a density of 80,000 cells per well in 24-well plates using 10% DMEM medium, as described. After 24 hours, the cells were infected with mCMV at 0.1

MOI, and incubated in DMEM containing 1 mM, 5 mM, or 25 mM glucose. Following a 24-hour incubation, cells were washed twice with HEPES-buffered saline. Cells were then incubated for 5 minutes in HEPES-buffered saline containing 10 µM unlabeled 2-Deoxy-D-glucose (2DG) and 0.2 µCi/ml 2-deoxy-[14C] glucose (PerkinElmer). The reaction was stopped by washing the cells three times with ice-cold 0.9% NaCl. Nonspecific uptake was measured in the presence of 50 µM cytochalasin B. Radioactivity was quantified by liquid scintillation counting after lysing the cells in 0.05 N NaOH. The counts were normalized to protein content, which was determined using the BCA assay. To evaluate tissue-specific glucose uptake *in vivo*, a bolus of 10 µCi 2-[1-14C] deoxyglucose was administered via a catheter after the steady-state period. Blood samples were collected at 2-, 15-, 25-, and 35-minute post-bolus administration. The area under the curve (AUC) of the disappearing plasma 2-[1-14C] deoxyglucose, along with the tissue concentration of phosphorylated 2-[1-14C] deoxyglucose, was used to calculate glucose uptake.

3.2.10. Hyperinsulinemic-euglycemic clamping

Hyperinsulinemic-euglycemic clamping was performed on freely moving mice as described by Wueest et al. (99), in collaboration with the group of Prof. Daniel Konrad from the Division of Pediatric Endocrinology and Diabetology, University Children's Hospital, Switzerland. WT mice were anesthetized with isoflurane, and eye ointment was administered to both eyes. A catheter (MRE 025, Braintree Scientific) was inserted into the right jugular vein and exteriorized at the back of the neck. Two days post-surgery, either DMEM (control) or $2x10^5$ PFU MCMV virus in pure DMEM was injected via the catheter. Five days post-injection, the hyperinsulinemic-euglycemic clamping procedure was performed in mice after 5 hours of fasting. To assess basal glucose turnover, mice were infused with 3-[3H] glucose (1 µCi bolus and 0.05 µCi/min, PerkinElmer) for 80 minutes. Following blood collection from the tail vein, hyperinsulinemia was induced by a constant insulin infusion rate of 12 mU/kg∗min, alongside 3-[3H] glucose infusion (2 µCi bolus and 0.1 µCi/min). Steady-state glucose infusion rate was calculated once glucose infusion reached a constant rate for 15–20 min maintaining blood glucose concentrations at 5-6 mmol/l. The glucose turnover rate was determined by dividing the rate of [3-3H] glucose infusion by the plasma [3-3H] glucose-specific activity. Endogenous glucose production during the clamping was calculated by subtracting the glucose infusion rate from the glucose turnover rate.

3.2.11. Virus plaque assay

Animals were sacrificed at indicated time points, organs were harvested and viral particles were determined by a standard plaque-forming assay (93). Briefly, after sacrificing the mice, spleens and livers were collected under sterile conditions, stored in 2 mL Eppendorf tubes filled with 1 mL of 3% DMEM medium, and frozen at -20°C. The day before the plaque assay, primary MEF cells were cultured on 48-well cell culture plates at a concentration of $2x10^5$ cells/well to reach an 80% to 90% confluent cell monolayer on the day of testing. The organs were thawed at RT and homogenized using metal beads and a tissue homogenizer (MillMix 20, Domel). Serial dilutions ranging from 10^2 to 10^5 were prepared by mixing with fresh 3% DMEM. The medium was aspirated from the previously prepared MEF cells, and 100 µl of each serial dilution was added in duplicate to the 48-well plate. The plates were incubated for 30 minutes at 37°C in an incubator to facilitate virus attachment, centrifuged to synchronize and facilitate virus entry into the cell (30 min, 800 x *g*), and incubated again for 30 minutes at 37°C. To prevent the spread of the virus over supernatant and facilitate only cell-to-cell spread, we added ~0.5 mL of methylcellulose medium. The plates were incubated at 37°C for 4 days or until the appearance of viral plaques. The number of plaques was counted in at least two dilutions using an inverted microscope, and the number of plaque-forming units (PFU) was calculated based on the number of plaques in the individual dilutions of the organ homogenates, with a lower detection limit of 100 PFU/organ.

3.2.12. Quantitative RT-PCR

Quantitative reverse-transcription PCR (RT-PCR) was performed as previously described (100). According to the manufacturer's instructions, total RNA from infected tissues was extracted using NucleoZOL (Macherey-Nagel). RNA concentration was measured using NanoPhotometer Pearl (Implen). Reverse transcription Core Kit (Eurogentec, Seraig, Belgium) was used to generate cDNA according to the manufacturer's protocol in a PCR thermo-block (ProFlex™ PCR system, Applied Biosystems™). Quantitative real-time reverse-transcription PCR was performed in a 7500 Fast Real-Time PCR machine (ABI) with Hprt as a housekeeping gene. For the expression of Lcmvgp33, qPCR was performed by measuring in real-time the increase in fluorescence of the SYBR Green dye (Eurogentec) according to the manufacturer's protocol. The relative mRNA expression was normalized by quantification of Hrpt. Analysis was obtained with QuantStudio Design and Analysis Software v1.4.2

(Applied Biosystems) and performed using the comparative CT method (2−ΔCT). Primers used in this study are described in **Table 4**.

Table 4. Primers used for qPCR measurement of gene expression

Primer	Supplier	
HPRT forward 5'-TGAAGAGCTACTGTAATGATCAGTCAAC-3'	Metabion International AG	Custom
HPRT reverse 5'-AGCAAGCTTGCAACCTTAACCA-3'	Metabion International AG	Custom
Lcmvgp forward 5'-CATTCACCTGGACTTTGTCAGACTC -3'	Metabion International AG	Custom
Lcmvgp reverse 5'-GCAACTGCTGTGTTCCCG AAAC-3'	Metabion International AG	Custom

3.2.13. Extracellular flux assay

Extracellular flux assay (Seahorse assay) was performed in collaboration with the group of Prof. Daniel Konrad from the Division of Pediatric Endocrinology and Diabetology, University Children's Hospital, Switzerland. ATP production rates were measured using the Seahorse XF Real-Time ATP Rate Assay Kit (Agilent Technologies) following the manufacturer's guidelines. To determine metabolic changes in infected cells, MEF cells were seeded at 5,000 per well in 96-well Seahorse cell culture microplates with the described culture medium. After 24 hours, cells were infected with MCMV at 0.01 MOI and incubated in DMEM supplemented with either 1 mM or 25 mM glucose. Twenty to 24 hours post-infection, the medium was replaced with Seahorse XF DMEM Medium pH 7.4, supplemented with 1 mM or 25 mM glucose, 2 mM glutamine, and 1 mM pyruvate. To assess the ATP production rates of effector and/or memory CD8 T cells treated with IGF-1, cultivated cells were transferred from U-bottom 96-well plates onto 96-well Seahorse cell culture microplates (10^5 cells per well) coated with Cell-Tak (BD Bioscience) to enhance T cell attachment, one day before Seahorse measurements. 24h later, cells were resuspended in Seahorse XF RPMI Medium pH 7.4 supplemented with 11 mM glucose, 2 mM glutamine, and different concentrations of IGF-1. Following the change of the medium, the plate was degassed in a non-CO2 incubator at 37 °C for 1 h. After measuring basal oxygen consumption rate (OCR) and extracellular acidification rate (ECAR) in a Seahorse XF Pro Extracellular Flux Analyzer

(Agilent Technologies), cells were sequentially treated with Oligomycin (1.5 µM) and antimycin A (0.5 µM). Experiments with the Seahorse system were done with the following assay conditions: 2 min mixture; 2 minutes wait and 4 min measurement. ATP production from glycolysis (glycoATP) and mitochondria (mitoATP) was calculated using Seahorse Analytics software (Agilent).

3.2.14. Quantification and statistical analysis

Unless otherwise noted, data are shown as mean ± SEM. Statistical analysis was performed with GraphPad Prism 8 software (GraphPad Software, Inc.). Statistical significance was determined by Student's t-test, one-way ANOVA with Bonferroni post-testing, or Mann-Whitney's U test. The Kruskal-Wallis test was used to determine significant differences between groups in the survival experiments. Statistically significant differences were considered with P values of <0.05 (*$p < 0.05$, **$p < 0.01$, and ***$p < 0.001$).

4. RESULTS

4. RESULTS

SECTION 1 - Glucose control of the antiviral response

While our previous study (55) has demonstrated that mild viral infections do not impact systemic blood glucose levels, severe infections have been shown to cause changes in glycemia. To date, most attention has been directed to infection-induced stress hyperglycemia (101), but strong, non-lethal, viral infection may also cause a drop in blood glucose levels. However, much less is known about infection-induced hypoglycemia. In this first section, we therefore focused on the impact of strong viral infection on blood glucose regulation and the underlying molecular processes controlling the system.

4.1. Strong viral infection induces transient relative hypoglycemia

To gain more insight in the underlying processes of infection-mediated changes to blood glucose levels, we infected C57BL/6J mice with increasing doses of murine cytomegalovirus (mCMV), and three days post-infection, measured fasting plasma glucose (FPG) concentrations in the blood. In agreement with our previous findings (55), a low dose ($2x10^5$ PFU) of murine cytomegalovirus (mCMV) did not affect FPG levels. However, infection with a higher, non-lethal dose of mCMV ($2x10^7$ PFU) resulted in a significant drop in FPG levels. Since this drop does not reach levels that would be defined as clinical hypoglycemia in humans (FPG < 3 mmol/l), we referred to this state as relative hypoglycemia (RHG) (**Figure 2a**). To confirm that RHG is a result of viral replication and not of the initial viral load used for infection, animals were infected with a relatively low dose ($2x10^5$ PFU) of a more virulent strain of mCMV (mCMV-*Δm157*). Due to the deletion of the viral gene encoding the m157 protein, this virus avoids recognition by NK cells through the Ly49h receptor, resulting in a tenfold higher viral burden upon infection compared to that accomplished by wild-type (WT) mCMV after infection with the same dose (10). Moreover, we harvested livers from these infected mice and performed a standard plaque-forming assay. As a result, we confirmed that $2x10^5$ of mCMV-*Δm157* virus is more virulent than the same dose of WT mCMV, and causes higher viral load upon infection, accompanied by notable glucose restriction (**Figure 2b**). We observed that even a low dose of this virulent strain induced RHG, indicating that this effect is mediated by viral replication rather than the initial dose used for infection (**Figure 2a**).

We wondered whether RHG was a specific response to mCMV infection or may be a general response to strong viral infection. To investigate this, we infected mice with lymphocytic choriomeningitis virus (LCMV) Armstrong strain, with both lower ($1x10^6$ IFU) and higher doses ($2x10^7$ IFU). As observed with mCMV, the lower dose had no effect on FPG levels, but the higher dose significantly reduced FPG levels three days post-infection (**Figure 2c**). Similarly, a non-lethal infection with a virulent strain of influenza A virus (A/PR8/34) also resulted in RHG (**Figure 2d**). Therefore, we concluded that RHG is a general response to strong viral infection. By measuring FPG at multiple time points post-infection, we aimed to determine the kinetics of the infection-induced relative hypoglycemia. Results showed that the effect was induced rapidly and was transient. RHG was initiated already 18 hours after infection, reaching the lowest level after 3 days. RHG lasted for at least 7 days before FPG levels returned to the level of uninfected controls (**Figure 2e**).

All these findings together suggest that strong viral infection induces transient relative hypoglycemia.

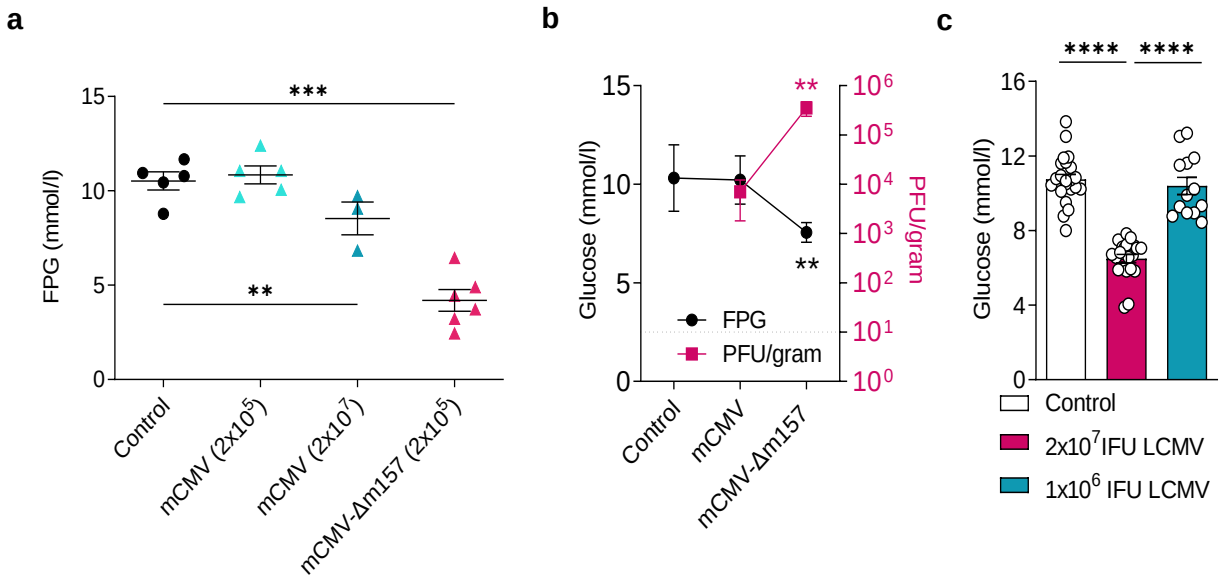

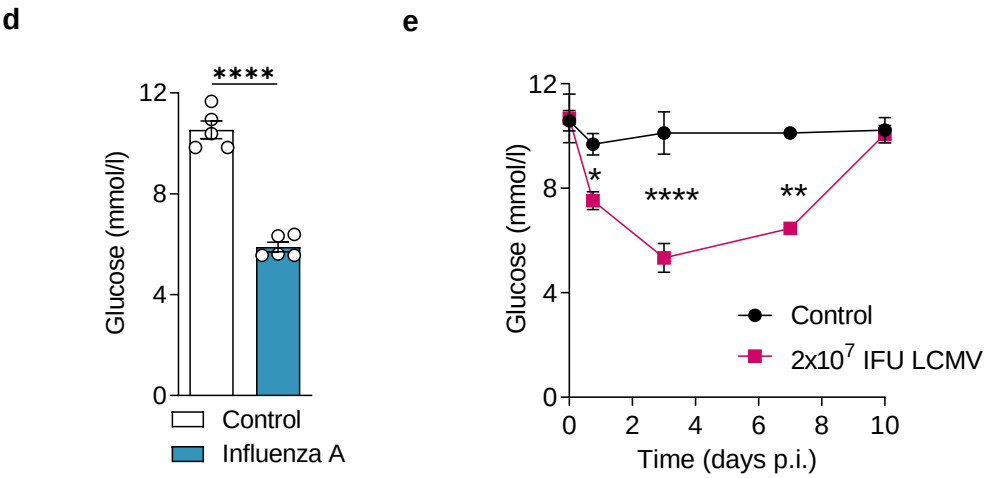

Figure 2. Strong viral infection induces transient relative hypoglycemia. C57BL/6J mice were infected with **(a)** $2x10^5$ PFU (n=5) or $2x10^7$ PFU mCMV (n=3), or $2x10^5$ PFU mCMV-*Δm157* (n=6), **(b)** $2x10^5$ PFU mCMV or mCMV-*Δm157* (n=5), or **(c)** with $2x10^7$ IFU (n=21) or $1x10^6$ IFU LCMV (n=13). Three days post-infection **(a, c)** FPG levels, or **(b)** FPG and viral load in the liver were measured after 6h of fasting (n=5). **(d)** C57BL/6J mice were infected with 10xIC50 (inhibitory concentration 50%) influenza A/PR/8/34 virus and three days p.i. FPG levels were measured after 6h of fasting (n=5). **(e)** C57BL/6J mice were infected with $2x10^7$ IFU LCMV. At indicated time points p.i. FPG levels were measured after 6 hours of fasting (n=3). Data show means ± (s.e.m.) and statistical significances. Indicated are statistical significances using **(a, c)** one-way ANOVA followed by Bonferroni post-testing, or **(b, e)** two-way ANOVA, or **(d)** Student's t-test *p<0.05, ** p<0.01, ***p<0.001, ****p<0.0001. **(a, b, d, e)** Representative of three independent experiments or **(c)** pooled data from three independent experiments is shown.

4.2. Relative hypoglycemia is not a sex-dependent phenomenon

Many studies show evidence of sexual dimorphism in response to infection (102). Gender can significantly impact susceptibility to infection and immunological responses. To determine whether RHG is a sex-dependent phenomenon, we infected female C57BL/6J mice with increasing doses of mCMV (**Figure 3a**), $2x10^5$ PFU mCMV-*Δm157* (**Figure 3b**), and $2x10^7$ IFU of LCMV (**Figure 3c**). We observed that female mice showed a reduction in FPG levels following strong mCMV or LCMV infection which was highly comparable to male mice.

Therefore, sexual dimorphism does not appear to play a major role in infection-induced RHG.

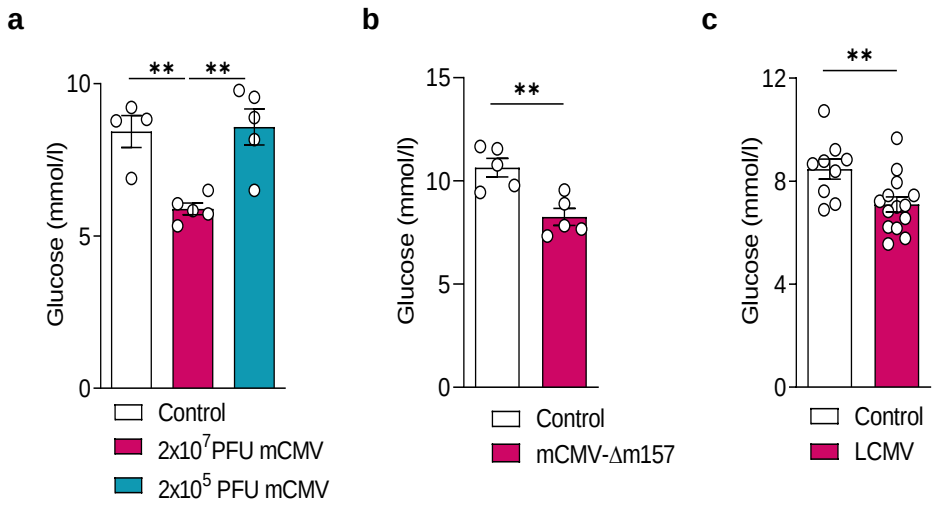

Figure 3. Infection-induced relative hypoglycemia occurs independently of sex. Female C57BL/6J mice were infected with **(a)** $2x10^5$ PFU or $2x10^7$ PFU mCMV (n=5), **(b)** $2x10^5$ PFU mCMV-*Δm157* (n=5), or **(c)** with $2x10^7$ IFU LCMV. Three days p.i., FPG levels were measured after 6 hours of fasting using an automatic glucometer. Data show means ± s.e.m. and statistical significances. Indicated are statistical significances using **(a)** one-way ANOVA followed by Bonferroni post-testing, or **(b, c)** Student's t-test *p<0.05, ** p<0.01, ***p<0.001, ****p<0.0001. **(a, b)** A representative of three experiments is shown, or **(c)** pooled data from three independent experiments.

4.3. Relative hypoglycemia benefits the antiviral response

We questioned whether prevention of glucose restriction during infection would have a detrimental effect on the antiviral response. To investigate this *in vivo*, mice were infected with $2x10^7$ IFU of LCMV while being fasted for 3 days. Infected mice were divided into two groups. One group was provided with normal drinking water *ad libitum*, while the other group was brought into a chronic hyperglycemic state by providing drinking water containing glucose, which was confirmed in blood using an automated glucometer (**Figure 4a**). Next, we investigated viral load in these animals using qPCR. Our observations showed that hyperglycemia causes increased viral loads following a strong LCMV infection (**Figure 4b**). To determine whether increased viral titers have a clinical impact, mice were placed on normal or glucose-spiked drinking water and infected with 20% of an LD_{50} dose of Influenza A. Whereas almost all animals on normal drinking water survived, 70% of hyperglycemic animals succumbed to the infection (**Figure 4c**).

These results indicate that a state of RHG benefits the antiviral immune response.

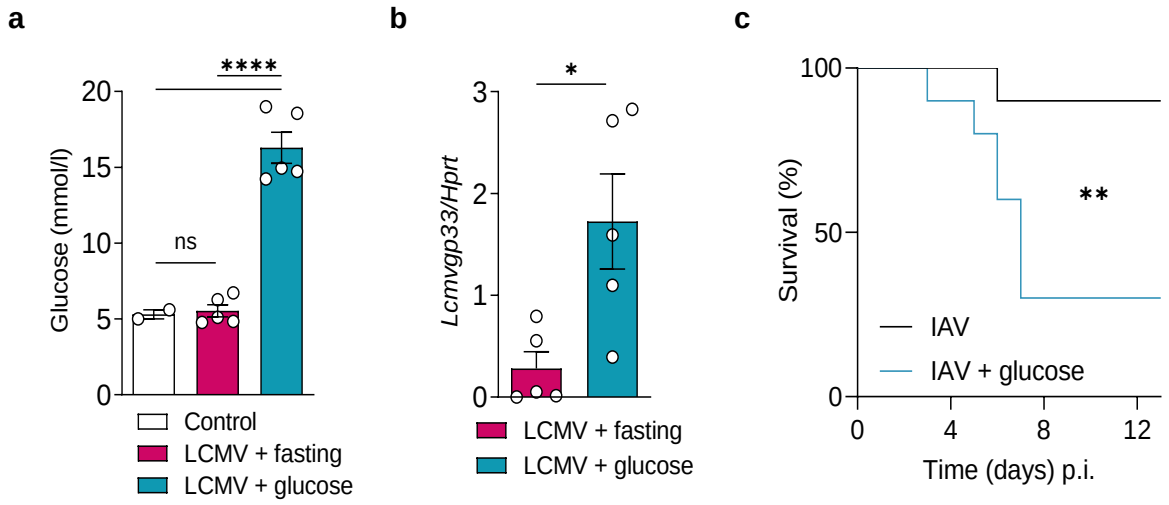

Figure 4. Prevention of glucose restriction negatively impacts the antiviral response. (a, b) C57BL/6J mice were infected with $2x10^7$ IFU LCMV. Following infection, mice were fasted and one group of animals received normal water while the other received water supplemented with 5% glucose. Three days p.i. we measured **(a)** FPG levels and **(b)** viral load in the liver was determined by qPCR (n=5). **(c)** C57BL/6J mice were infected with 20& of an LD^{50} influenza A virus. After infection, animals received normal water or water supplemented with 5% glucose, and their survival was monitored over time (n = 10). Data show means ± s.e.m. and statistical significances. Indicated are statistical significances using **(a)** one-way ANOVA followed by Bonferroni post-testing, **(b)** Student's t-test, or **(c)** Kaplan–Meier model, *p<0.05, ** p<0.01, ***p<0.001, ****p<0.0001. For all panels, a representative of three experiments is shown.

4.4. Low glucose concentrations impair viral replication *in vitro*

Glucose is a vital energy source for most cells, and its availability determines many bodily processes, including growth, management of fat storage, and levels of anabolic and catabolic metabolism. We hypothesized that limited glucose availability restricts viral replication in target cells. To assess the impact of restricted glucose levels on viral replication, we made use of *in vitro* models. Mouse embryonic fibroblasts (MEF) were infected *in vitro* with a modified strain of mCMV that expresses green fluorescent protein (mCMV-*GFP*), allowing us to follow the course of infection using confocal microscopy or flow cytometry. Infected cells were cultivated in the presence of increasing concentrations of glucose, ranging from 0,1 mM to 25 mM glucose. The percentage of GFP^+ cells, corresponding to the percentage of infected cells, was measured three days post-infection using flow cytometry (**Figure 5a**). We observed that viral replication was greatly diminished when cells were cultured under low glucose concentrations. Results obtained using flow cytometry were confirmed by confocal microscopy (**Figure 5b, e**). We were curious whether this mechanism

is present in different cell types. Therefore, we infected murine stromal vascular endothelial cells (SVECs) (**Figure 5d**) and bone marrow-derived macrophages (BMDMs) (**Figure 5h**) with mCMV-*GFP in vitro* and cultivated them in the presence of normal (25mM), low (1mM), or very low (0,1mM) glucose concentrations. The results were consistent with those obtained in MEF cells, where low glucose concentrations caused a reduction in viral replication. Neither viability (**Figure 5c, f**) nor proliferation of the cells (**Figure 5g**) was affected, indicating that the difference in viral replication is due to intracellular mechanisms rather than a direct consequence of reduced glucose concentrations in the medium on cell survival. Based on these results, we concluded that reduced glucose availability inhibits viral replication.

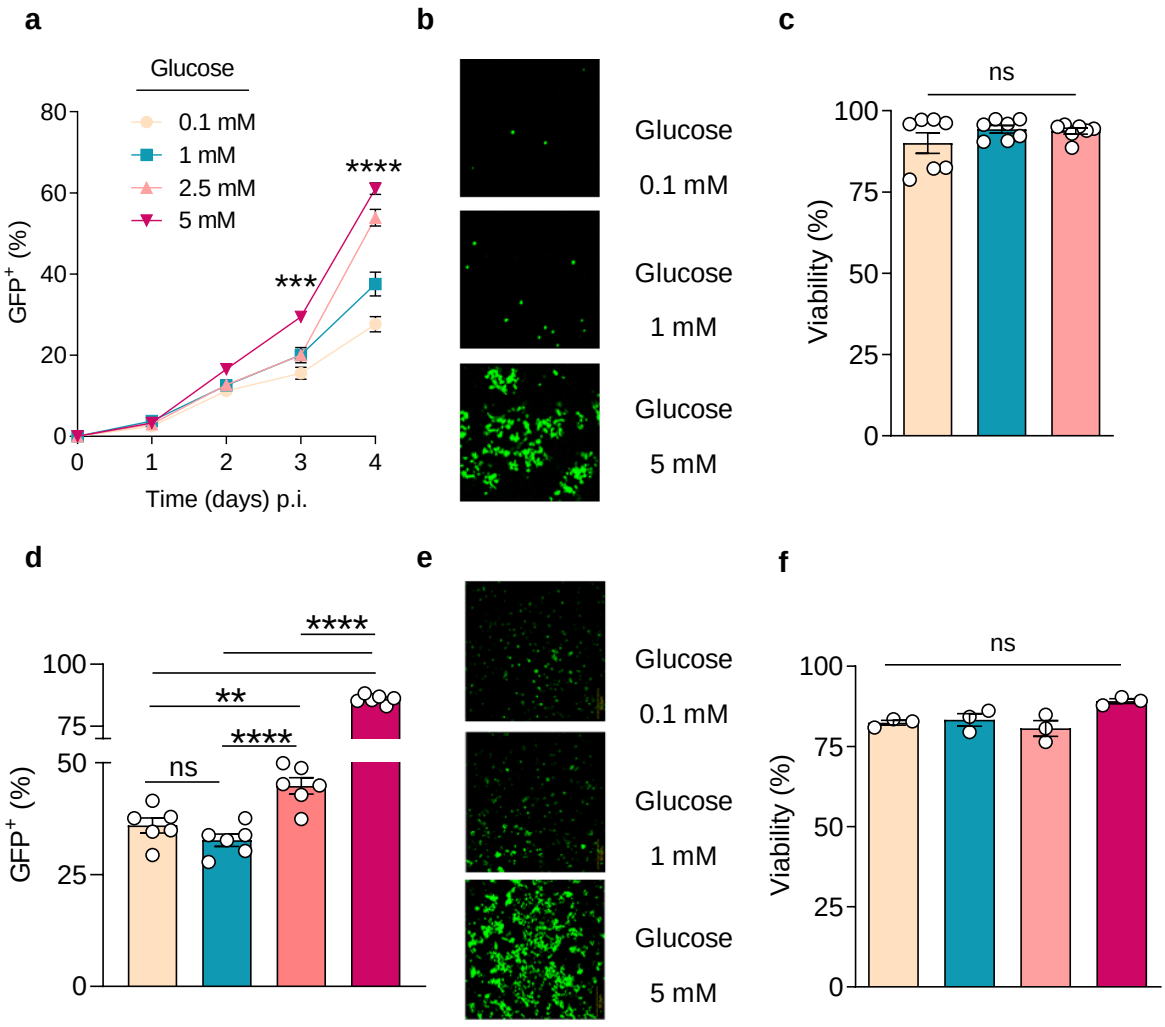

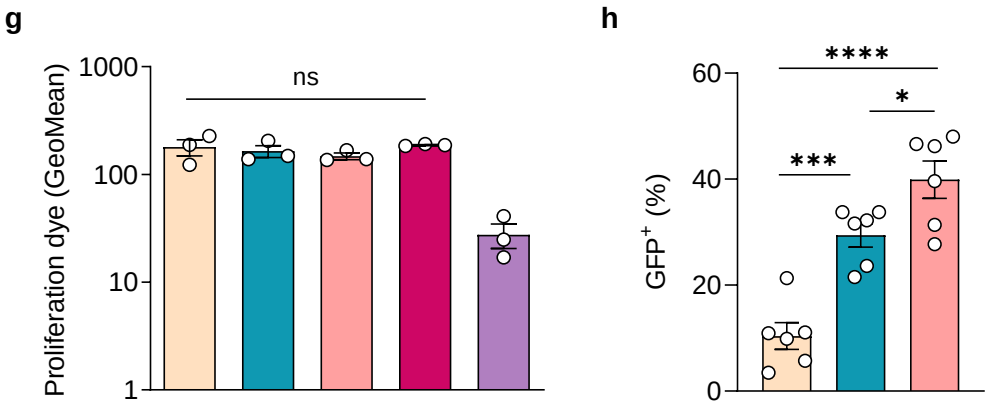

Figure 5. Hypoglycemia impairs viral replication *in vitro*. (a-c) MEFs or **(d-g)** SVECs or **(h)** BMDMs were infected with mCMV-ε*GFP* at 0.01 MOI and cultured in media with indicated glucose concentrations. **(a, d, h)** Viral load, **(c, f)** cell viability, and **(g)** proliferation were determined by measuring the percentage of εGFP+ cells using flow cytometry at indicated time points. **(b, e)** Representative confocal images are shown (n=7). Data show means ± s.e.m. and statistical significances. Indicated are statistical significances using **(a)** two-way ANOVA, or **(c, d, f-h)** one-way ANOVA followed by Bonferroni post-testing *p<0.05, ** p<0.01, ***p<0.001, ****p<0.0001. For all panels, a representative of three experiments is shown.

4.5. Metabolic deficiency is not the cause of an impaired viral infection

Glucose acts as a source of fuel in glycolysis and its metabolites may further be used in the Krebs cycle. Infection has been shown to increase the glucose dependence of cells to fulfill the increased metabolic demand of producing viral particles, which is a highly energy-intensive process (48). Therefore, we hypothesized that low glucose levels reduce viral replication by preventing the cell from meeting its metabolic requirements. First, we determined whether its uptake becomes rate-limiting for viral replication under low-glucose conditions. Therefore, we infected SVECs with 0.1 MOI mCMV-*GFP*, and three days post-infection we determined glucose uptake in uninfected and infected cells cultivated under increasing glucose concentrations. Neither mCMV infection nor low glucose concentration in the medium affected the rate of glucose uptake into the cell, indicating that this parameter was not affected by limiting glucose availability (**Figure 6a**).

Next, we asked ourselves whether metabolic deficiency is the cause of the impaired viral replication. This time, infected MEF and SVEC cells with 0.01 MOI *GFP*-mCMV cultivated in 10% DMEM with different glucose concentrations were supplemented with nutrients that

feed into metabolic energy pathways downstream of glucose. Medium containing low glucose concentration was supplemented with 5 mM citrate, 5 mM acetate, or 25 mM galactose. The percentage of GFP^+ cells was measured three days post-infection using flow cytometry, and the results showed that none of these alternative carbon sources managed to compensate for the effect of limited glucose (**Figure 6b**). Next, we cultured infected SVECs under different pyruvate concentrations in the presence of low or high glucose levels. The results from flow cytometry showed that pyruvate was not able to negate the differences in viral replication between low and high glucose levels (**Figure 6c**). Based on these results, we concluded that this metabolite has no role in impaired viral replication under reduced glucose conditions. Glutamine is an essential carbon source for many cells and is usually provided at a concentration of 2 mM in a standard culture medium. Decreasing or increasing the amount of available glutamine negatively impacted viral replication, however, it failed to negate the difference between cells cultured under high- or low-glucose concentrations (**Figure 6d**).

To summarize, impaired viral replication under conditions of limited glucose availability is not the result of metabolic deficiency.

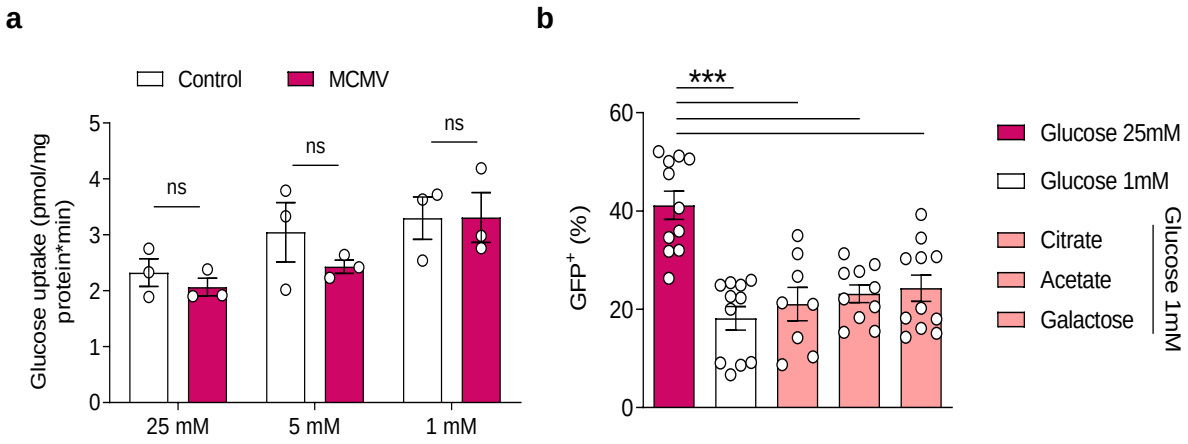

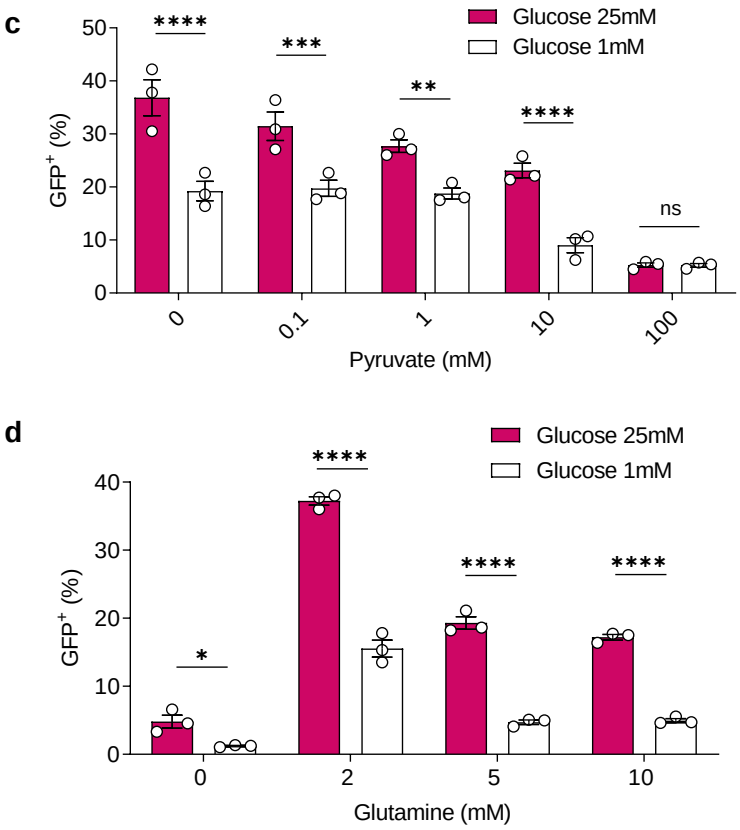

Figure 6. Metabolic deficiency does not cause impaired viral infection. (a-d) SVECs cells were infected with mCMV-*GFP* at 0.1 MOI or **(b-d)** 0.01 MOI and grown in a medium with indicated glucose concentrations, which was supplemented with **(b)** citrate (5mM), acetate (5mM), or galactose (25mM), or with indicated **(c)** pyruvate (n=3) or **(d)** glutamine concentrations (n=3). Three days p.i. **(a)** glucose uptake was determined by liquid scintillation (n=3), and **(b-d)** viral load was determined using flow cytometry. Data show means ± s.e.m. and statistical significances. Indicated are statistical significances using **(a, c, d)** two-way ANOVA and **(b)** one-way ANOVA followed by Bonferroni post-testing, *p<0.05, ** p<0.01, ***p<0.001, ****p<0.0001. A representative of three experiments, or pooled data **(b)** from three independent experiments, are shown.

4.6. Glucose restriction affects viral replication through modification of cellular metabolism

Given that providing alternative carbon sources to cells in low glucose conditions did not eliminate the glucose-dependent variations in viral replication, we hypothesized that glucose limitation might influence viral replication by altering cellular metabolism. Growing evidence indicates that metabolism can regulate signalling pathways and gene expression, thereby affecting diverse biological outcomes and phenotypes (103). Adenosine triphosphate

(ATP) is a key energy carrier produced by cellular catabolic metabolism, essential for the fundamental functions of all living cells. In mammalian metabolism, the two primary ATP-generating pathways are oxidative phosphorylation and glycolysis. The Seahorse extracellular flux analyzer is a powerful tool and gold standard for simultaneously measuring glycolysis and oxidative phosphorylation in the same cell (104). Therefore, MEF cells were infected with 0.01 MOI mCMV and cultured under high and low glucose concentrations and Seahorse XF Real-Time ATP Rate Assay was performed one day p.i.. We observed that cells under low glucose concentrations have an increased oxygen consumption rate (OCR), whereas their production of lactate was low, as shown by a low level of extracellular acidification (**Figure 7a**). This is different in cells cultured under high glucose, which have an increased extracellular acidification rate (ECAR) and reduced OCR (**Figure 7b**).

Thus, glucose restriction promoted its utilization in the tricyclic acid cycle, thus allowing for more ATP production from a single glucose molecule, as indicated by the increased membrane potential of their mitochondria, both in uninfected and infected cells. In contrast, when glucose is readily available, pyruvate formed during glycolysis is not shuttled into the Krebs cycle as efficiently but is instead excreted from the cell.

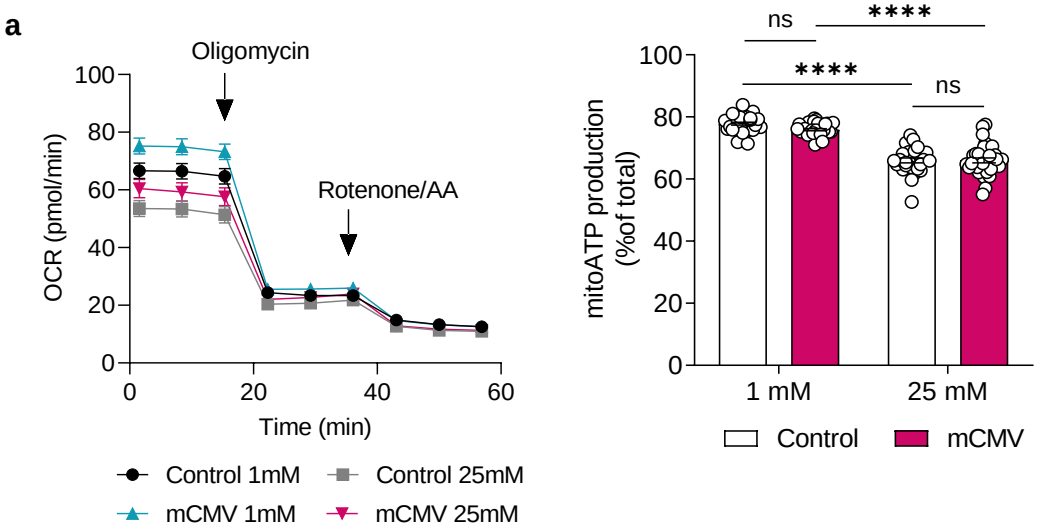

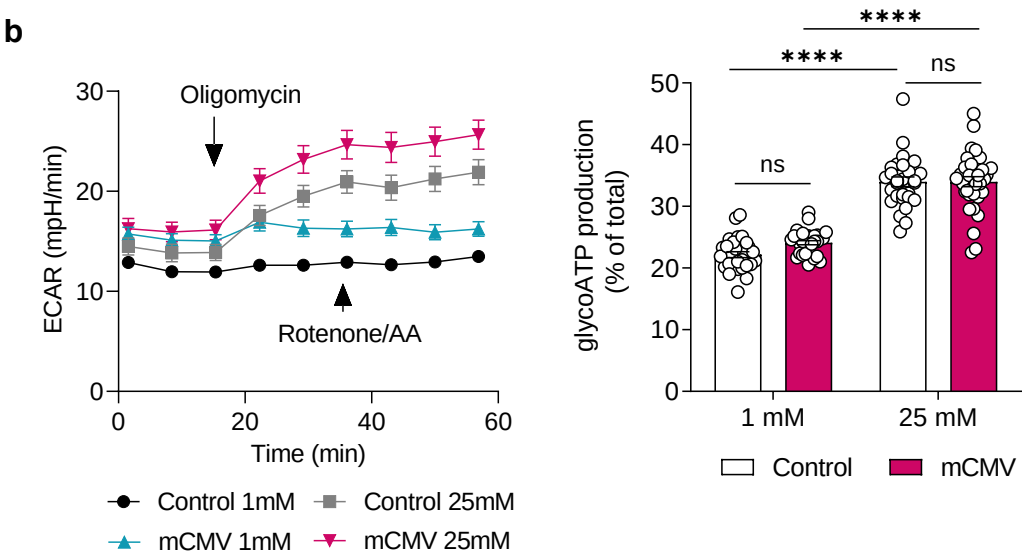

Figure 7. Limiting glucose affects viral replication by altering cellular metabolism. MEF cells were infected with mCMV at 0.01 MOI and grown in a medium with high (25mM) or low (1mM) glucose concentrations. **(a)** OCR (left panel) and mitochondrial ATP production (right panel), and **(b)** ECAR (left panel) and glycolytic ATP production were measured by Seahorse one day p.i. (control 1mM n= 30, control 25mM n= 29, mCMV 1mM n= 31, mCMV 25mM n= 34). Indicated are means ± s.e.m. and statistical significances using two-way ANOVA, *p<0.05, ** p<0.01, ***p<0.001, ****p<0.0001. Pooled data from two independent experiments are shown.

4.7. Low glucose concentrations inhibit viral replication by limiting lactate production

Using our established *in vitro* model systems shown in Figure 5, we aimed to uncover the mechanism beneath impaired infection under limited glucose availability. Recent findings have identified lactate as a crucial metabolite responsible for glycolysis-mediated inhibition of RLR signalling and, therefore, impairment of IFN-I production in response to viral infection (7). Zhang et al. demonstrated that inhibiting lactate dehydrogenase A with sodium oxamate reduces lactate levels and increases type I IFN production, thereby protecting mice from viral infections (7). If plenty of glucose is available, lactate is formed from pyruvate at the end of glycolysis, and then exported out of the cell, helping to maintain redox balance or acidify the environment. However, when glucose availability is limited, pyruvate is converted into Acetyl-CoA and shuttled into the TCA cycle.

To determine whether glucose availability regulates IFN-I production through a lactate-dependent mechanism, infected MEFs and SVECs were cultivated under low- or high glucose concentrations. In addition, cells were supplemented with sodium oxamate (25 mM), a specific LDHA inhibitor that blocks the conversion of pyruvate into lactate. Three days post-infection we used an L-Lactate Assay Kit to quantify lactate production in cell lysates. Results showed that lactate formation is higher in infected cells cultured under high-glucose conditions, as these cells predominantly use glycolysis to fulfill their energetic needs and depend less on OXPHOS (**Figure 7**). Accordingly, limited glucose availability and supplementation with sodium oxamate reduced lactate production (**Figure 8a**). Next, we determined whether oxamate could inhibit viral replication. Results showed that the level of viral replication was significantly reduced when cells were cultured under low glucose conditions, or high glucose conditions in the presence of sodium oxamate (**Figure 8b**). Next, we wanted to investigate whether lactate inhibits type I interferon production. To analyze the ability of cells cultured under normal or hypoglycemic conditions to produce IFNβ, supernatants were collected 24 hours post-infection. IFNβ levels were determined using ELISA. As the results show, targeting LDHA and reducing lactate levels enhanced type I interferon production, which resulted in suppressed viral replication in low glucose conditions, or high glucose conditions in the presence of sodium oxamate (**Figure 8c**). To investigate whether limited glucose availability impairs lactate-mediated inhibition of the antiviral response *in vivo*, we infected mice with a high dose of LCMV. Mice were fasted and received either normal water or water containing glucose for three days. Three days p.i. lactate content was determined in the spleen and liver using an L-Lactate Assay Kit. The obtained results showed that induced hyperglycemia caused an increase in lactate levels in both organs (**Figure 8d, e**). Complementary to our *in vitro* data, IFNβ levels in the serum of these mice were reduced following hyperglycemia (**Figure 8f**). Finally, infected animals provided with glucose-spiked drinking water were treated with sodium oxamate *in vivo*. We could show that this treatment resulted in increased levels of IFNβ (**Figure 8g**) and consequently lower viral load, as determined by qPCR (**Figure 8h**).

Thus, we concluded that glucose restriction impairs viral replication by promoting OXPHOS and reducing lactate production. This relaxes lactate-mediated inhibition of type I interferon signalling and impairs viral replication.

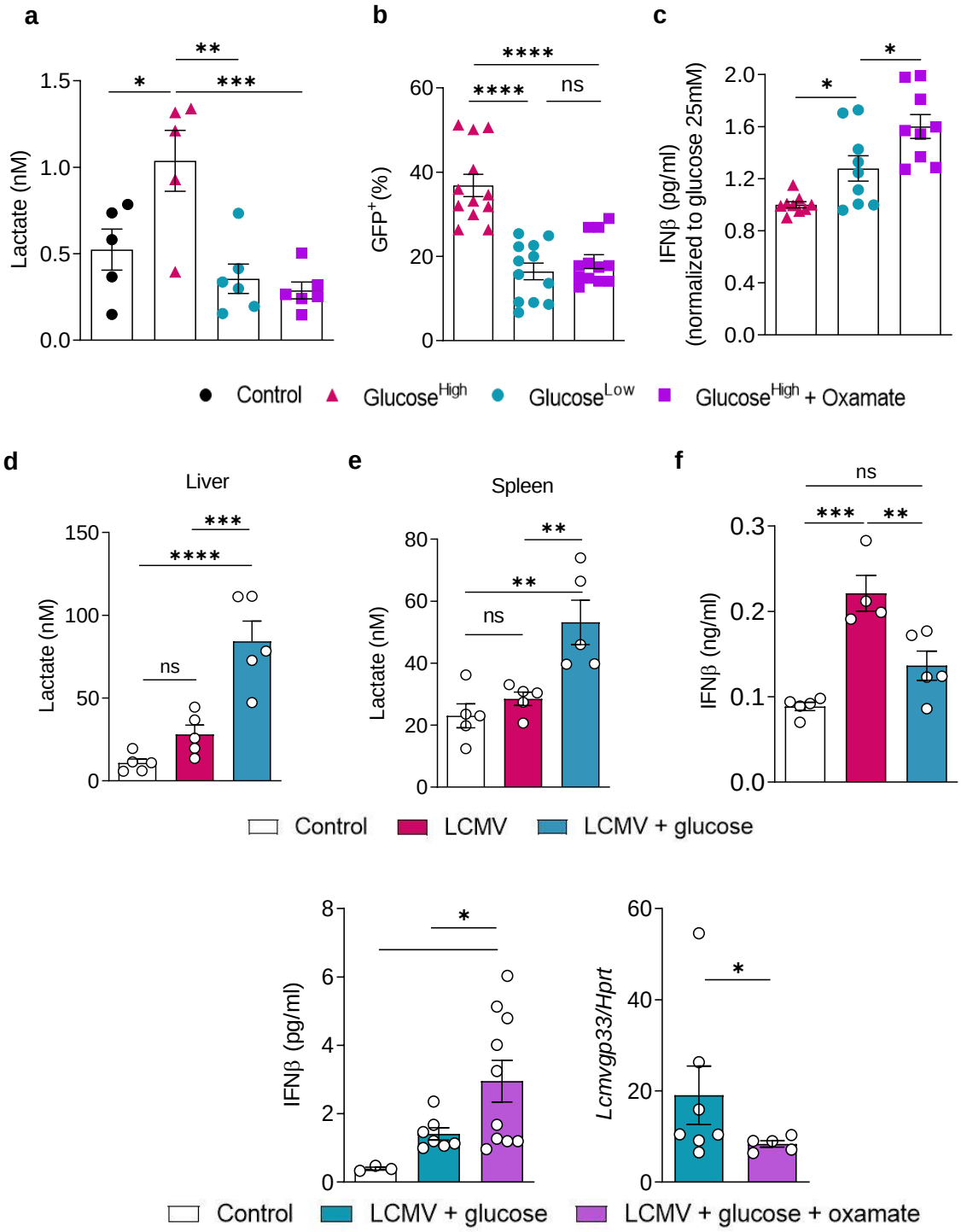

Figure 8. Glucose restriction impairs lactate-mediated inhibition of the antiviral response. (a-c) SVEC cells were infected with mCMV at an MOI of 0.01 and grown in media with high (25 mM), low (1 mM) glucose concentrations, or medium with high glucose supplemented with 25 mM sodium oxamate. Three days p.i. **(a)** lactate content was determined in cell lysates (noninfected n= 5, glucose 25mM n= 5, glucose 1mM n= 6, glucose 25mM + oxamate n= 6) and **(b)** the percentage of mCMV-GFP^{+} cells was measured using flow

cytometry (n = 12)**. (c)** One day p.i. IFNβ levels in supernatants were measured using ELISA (n=9)**. (d-h)** C57BL/6J mice were infected with 2×10^7 IFU LCMV. In addition, animals were fasted and received either normal water or water supplemented with 5%of glucose **(d-f)** or **(g, h)** and were treated with oxamate. Three days p.i., lactate content was measured in **(d)** the liver and **(e)** the spleen (n = 5), and **(f)** serum IFNβ levels were measured 18 h p.i. (n=5). Three days p.i., **(g)** plasma IFNβ levels were determined by ELISA, and **(h)** viral replication in the spleen was analyzed by qPCR (n= 3-10). Indicated are means ± s.e.m. One-way ANOVA followed by Bonferroni post-testing **(a-g)** or two-sided Student t-test **(h)** was used to determine statistically significant differences *p<0.05, ** p<0.01, ***p<0.001, ****p<0.0001. Representative of three independent experiments **(a, d-h)** or pooled data from three independent experiments **(b, c)** is shown.

4.8. Infection-induced glucose restriction is the result of increased insulin release from the pancreas

Insulin is an endocrine hormone produced by pancreatic β-cells. Given its role as a key regulator of blood glucose levels, we hypothesized that infection-induced relative hypoglycemia is mediated by insulin. Therefore, we decided to determine insulin levels during viral infection. C57BL/6J mice were infected with low and high doses of LCMV and FPG, and insulin levels were measured in the blood 3 days post-infection. Results showed that insulin concentrations positively correlated with the dose of the virus used (**Figure 9a**). Additionally, systemic insulin levels were increased in mice infected with a low dose of the virulent strain mCMV-*Δm157*. This increase was evident at both 18 hours (**Figure 9b**) and 3 days post-infection (**Figure 9c**). After observing that infection increases blood insulin levels, the next step was determining the glycemic index of infected mice. The glycemic index, which is a measure of pancreatic β-cell function, is determined as the ratio of the areas under the glucose and insulin curves in the blood. Compared to uninfected controls, the glycemic index was elevated in animals infected with a high dose of the LCMV (**Figure 9d**), indicating that insulin secretion is at a level that is higher than necessary for maintaining glucose homeostasis. To confirm the role of insulin in mediating infection-induced RHG, we eliminated the cells producing this hormone. To deplete pancreatic β-cells we used Insulin2Cre (Ins2Cre) mice that were crossed with animals expressing a Cre-inducible diphtheria toxin (DT) receptor (iDTR). When these mice are treated with diphtheria toxin, it induces selective elimination of pancreatic cells and permanently destroys the body's ability to produce insulin (105). After diphtheria toxin treatment, mice were infected with a high dose of the LCMV, and blood glucose levels were measured three days post-infection. Strong infection of Ins2Cre iDTR

mice treated with diphtheria toxin did not show a reduction in blood glucose but instead demonstrated an increase in blood glucose levels. In contrast, untreated controls showed the occurrence of RHG (**Figure 9e**).

These results indicate that infection-induced relative hypoglycemia depends on increased insulin secretion from the pancreas

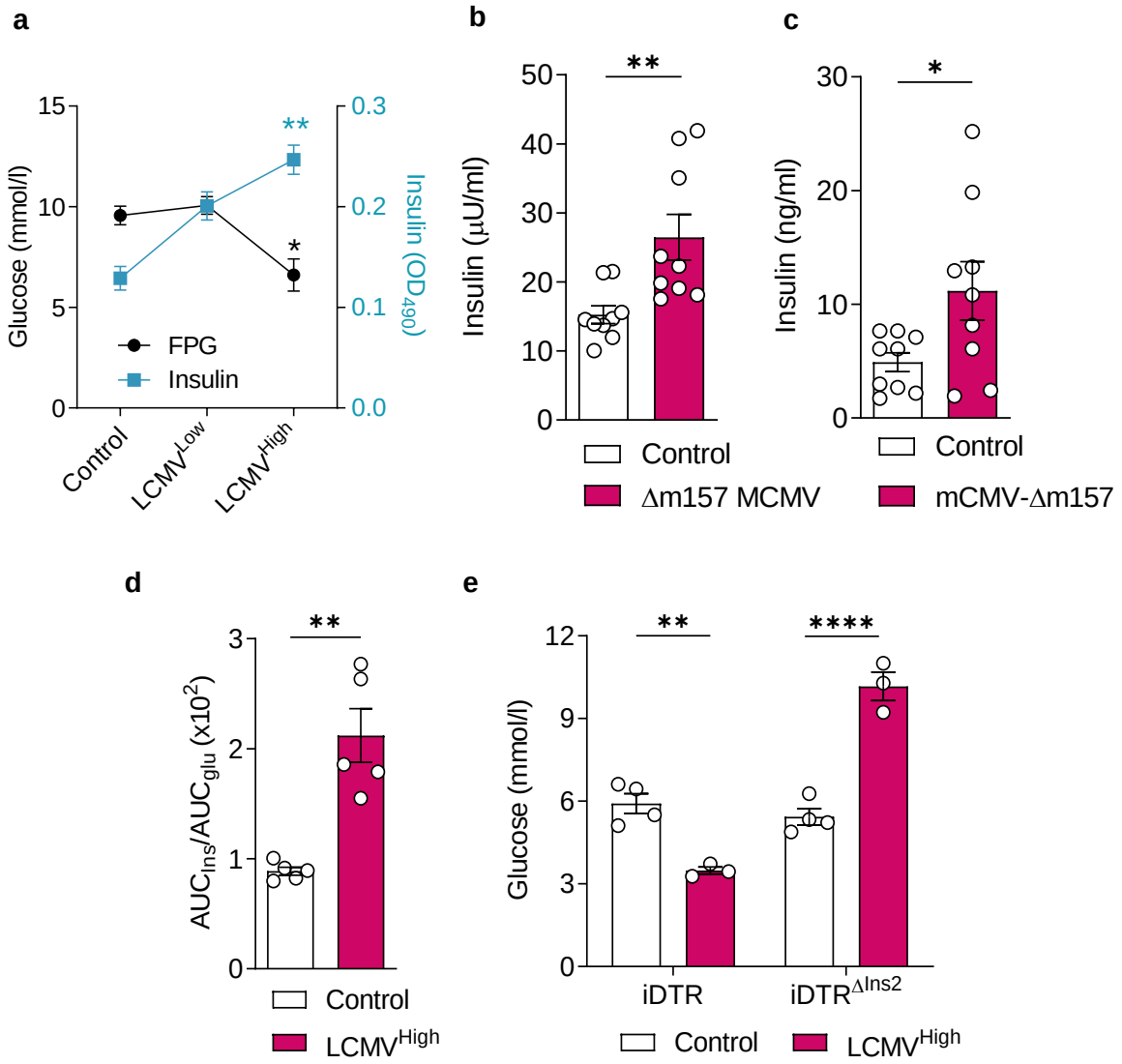

Figure 9. Relative hypoglycemia is a result of increased insulin production by the pancreas. C57BL/6J mice were infected with **(a)** 1×10^6 IFU or 2×10^7 IFU LCMV, or **(b, c)** 2×10^5 PFU mCMV-*Δm157*. **(a)** FPG levels and plasma insulin levels were measured three days p.i. after 6 hours of fasting (n=5). **(b, c)** Plasma insulin levels were determined **(b)** 18 hours p.i. or **(c)** three days p.i. after 6 hours of fasting (n=9). **(d)** Three days after infection of C57BL/6J mice with 2×10^7 IFU LCMV insulinogenic index was calculated. **(e)** Ins2CreiDTR or littermate controls were infected with 2×10^7 IFU of LCMV. Three days p.i., FPG levels

were measured after 6 h of fasting (iDTR control n= 4, iDTR LCMV n= 3, Ins2CreiDTR control n= 4, Ins2CreiDTR LCMV n= 3). Indicated are means ± s.e.m. **(a, e)** Two-way ANOVA and **(b-d)** two-sided Student's t-test was used to determine statistically significant differences *p<0.05, ** p<0.01, ***p<0.001, ****p<0.0001. For all panels, a representative of three independent experiments is shown.

4.9. Relative hypoglycemia is the result of inhibited glycogenolysis in the liver

Blood glucose levels during fasting are mainly maintained by the liver, which releases glucose into the blood in a process that is limited by insulin (54). To investigate whether infection impacts hepatic glucose metabolism, we assessed the level of glucose secretion by the liver under basal conditions and upon insulin stimulation. C57BL/6J mice were infected with the mCMV-*m157* virus and subjected, along with uninfected controls, to hyperinsulinemic-euglycemic clamping. Hyperinsulinemic–euglycemic clamping showed that basal glucose secretion by the liver is reduced in infected animals (**Figure 10a**). In contrast, after insulin stimulation, both groups of animals showed equal glucose output, which implies that the difference in basal glucose secretion is not due to a change in the sensitivity of liver cells to insulin (**Figure 10b**) but rather reduced output of glucose from the liver. Next, in the clamping experiment, radiolabeled glucose was injected to determine whether infection impacts glucose uptake. We did not observe any changes in the rate with which adipose tissue and skeletal muscle tissue take up glucose from the blood. In contrast, we observed a significant increase in glucose uptake in the spleen (**Figure 10c**). The spleen is known to play a crucial role in the body's immune response, and increased glucose uptake might signify heightened activity of the immune cells. Based on the course of the immune activation, lymphocyte proliferation rises on the fifth day after infection, including the expansion of the antigen-specific CD8 T cells (106). Therefore, we hypothesize that a drop in blood glucose following infection may be partially explained by increased glucose consumption by activated immune cells in secondary lymphoid organs. Glucose output by the liver depends on the combined effect of gluconeogenesis and glycogenolysis, of which the latter is particularly sensitive to insulin (54). To investigate whether infection impacts glycogenolysis, the level of glycogen in the liver was determined after fasting in mice infected with a lower or higher dose of the virus. Mice infected with a high, but not a low dose of the virus had significantly higher amounts of glycogen in the liver upon a six-hour fast (**Figure 10d**).

To sum up these findings, infection-induced glucose restriction is mediated through reduced hepatic glycogenolysis and increased glucose uptake by immune cells.

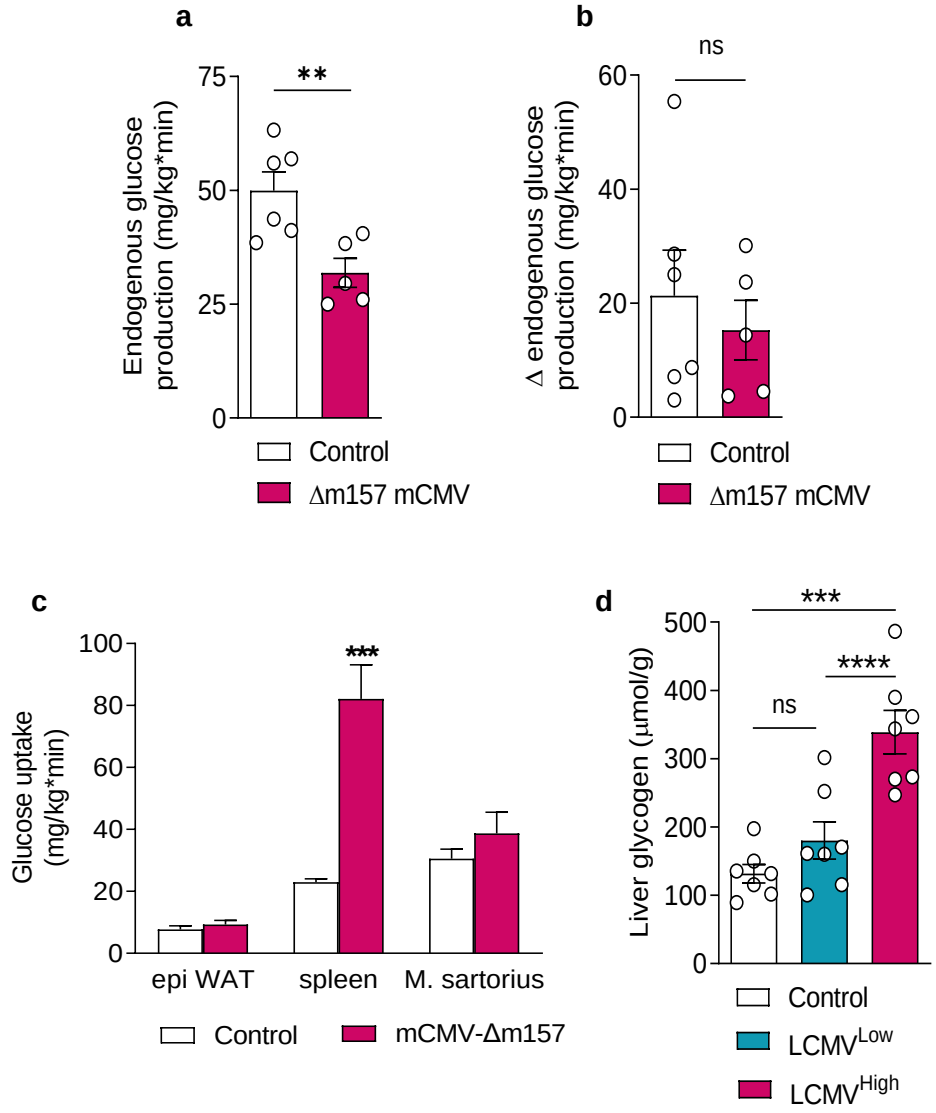

Figure 10. Infection-induced relative hypoglycemia depends on decreased hepatic glycogenolysis. C57BL/6J mice were infected with 2x10^5 PFU of mCMV-*Δm157* and after 5 days, a hyperinsulinemic-euglycemic clamp was performed. Hepatic glucose production was measured under **(a)** basal conditions or **(b)** after insulin infusion at plateau conditions (n=5-6). **(c)** C57BL/6J mice were infected with 2x10^5 PFU of mCMV-*Δm157* and 5 days p.i. tissue-specific glucose uptake *in vivo* was performed in the epididymal white adipose tissue (epi WAT), spleen, and muscle sartorius. **(d)** C57BL/6J mice were infected with 1×10^6 IFU (low) or 2×10^7 IFU (high) LCMV. Three days p.i., hepatic glycogen storage was measured (n=7). Data show means ± s.e.m. and statistical significances. Indicated are statistical significances using **(a, b)** Student's t-

test, **(c)** two-way ANOVA, or **(d)** one-way ANOVA followed by Bonferroni post-testing, *p<0.05, ** p<0.01, ***p<0.001, ****p<0.0001. For all panels, a representative of three experiments is shown.

4.10. Hyperglycemia in the context of diabetes negatively impacts the ability of mice to control viral replication

Our research showed that hyperglycemia negatively impacts the immune response to infection. Chronic hyperglycemia is characteristic of patients with diabetes, who are also more prone to viral infections (82). We wondered whether these two aspects of the disease are in a cause-effect relationship. To investigate this, we eliminated pancreatic β-cells using streptozotocin (STZ) to model type 1 diabetes. STZ is a strong cytotoxic agent that destroys pancreatic β-cells, resulting in insulin deficiency, hyperglycemia, excessive thirst (polydipsia), and frequent urination (polyuria), all hallmark symptoms of human T1D (107). After achieving hyperglycemia in mice via i.p. injections of STZ (**Figure 11a**), mice were infected with $2x10^5$ of mCMV-*Δm157*. Three days p.i. blood was taken to isolate serum and spleens were harvested to determine the viral titres. Hyperglycemic animals showed reduced systemic IFNβ levels (**Figure 11b**) and higher viral loads in tissues than controls (**Figure 11c**).

In summary, hyperglycemia disrupts infection-induced glucose restriction, weakening the antiviral IFN-I response and increasing susceptibility to pathogens.

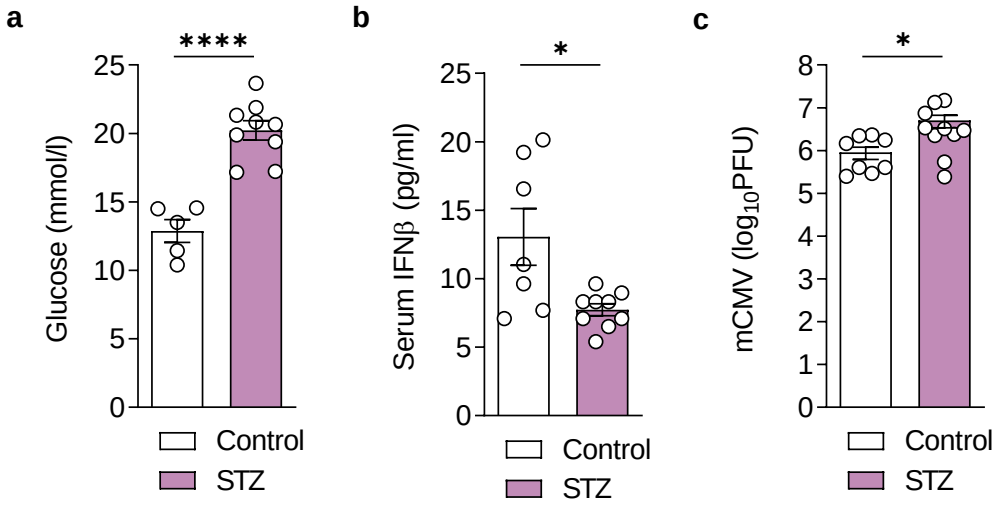

Figure 11. Type 1 diabetes impairs viral control. (a) C57BL/6J animals were treated with STZ, and FPG levels were measured after 6h of fasting. Three days p.i. with 2× 10^5 PFU mCMV-*Δm157*, **(b)** serum IFNβ

levels were measured using ELISA, and **(c)** viral titres were determined in the spleen by plaque assay (n=5-10). Data show means ± s.e.m. and statistical significances. Indicated are statistical significances using **(a, b)** Student's t-test and **(c)** Mann-Whitney test, *p<0.05, ** p<0.01, ***p<0.001, ****p<0.0001. For all panels, a representative of three independent experiments is shown.

Summary section 1

In summary, we show that lowering blood sugar levels during severe infections is a natural physiological response designed to enhance the body's ability to combat viral pathogens. Infection-induced relative hypoglycemia depends on increased insulin secretion from the pancreas. Hyperinsulinemia lessens hepatic glucose output by reducing glycogenolysis of hepatocytes during fasting. Glucose restriction enhances type-I interferon production by mitigating lactate-mediated inhibition of type-I interferon signalling. However, this immune-endocrine mechanism is disrupted in cases of hyperglycemia, possibly explaining why individuals with metabolic diseases, such as type 1 diabetes, are more vulnerable to viral infections.

SECTION 2 – Hormonal control of the antiviral response

In the previous section, we investigated how the immune system modulates the early antiviral response through the modulation of endocrine signalling, most notably of insulin. However, previous studies from our lab have shown that endocrine hormones such as insulin do not only modulate glucose but also directly impact immune cells (105). In this section, we investigated the hormonal dimension of the anti-viral response, with a focus on their impact on CD8 T cells.

4.11. Insulin does not impact the anti-viral CD8 T cell response through the insulin receptor

Previously, we and others have shown that insulin is able to promote the antiviral CD8 T cell response (45,70,105). However, the insulin concentrations that are required to cause an increase in cytokine production by CD8 T cells are super-physiological. We therefore questioned whether insulin promotes CD8 T cell responses through the insulin receptor, or has off-target effects at the concentrations used. Therefore, we made use of CD4Cre InsrFL/FL (IR^{CKO}) mice, which have T cell-specific deficiency of the insulin receptor. In addition, we made use of an *in vitro* model of CD8 T cell stimulation (13). CD8 T cells were purified from the spleens of OT-1 mice. These animals express a transgenic T cell receptor specific for the SIINFEKL (N4) epitope of ovalbumin. Using this tool, CD8 T cells can be stimulated *in vitro* via their antigen receptor using N4 peptides and subsequently differentiated into effector or memory cells using IL-2 or IL-15, respectively. OT-1 cells were differentiated *in vitro* into memory cells in the presence or absence of 1 unit/mL fast-acting insulin, a supraphysiological concentration. The ability of memory OT-1 cells to produce cytokines was determined using intracellular flow cytometry. As observed previously, insulin stimulation caused an increase in IFNγ production by these cells. However, we observed that the increase in IFNγ production was comparable between WT and IR^{CKO} cells (**Figure 12a**). The same results were observed for TNFα and IL-2 production (**Figure 12b, c**). Thus, insulin does not stimulate CD8 T cells via the insulin receptor.

Insulin has more than 50% structural and sequence homology with insulin-like growth factor 1 (IGF-1), an endocrine hormone produced by the liver (72). Importantly, insulin and IGF-1 can bind to each other's receptor, though with much-reduced affinity. Importantly, both the

insulin and IGF-1 receptors consist of a homodimer, but their monomers can bind to each other, forming an IGF1R-IR heterodimer that can bind both insulin and IGF-1. We therefore decided to investigate whether IGF-1 may impact CD8 T cell biology. First, we questioned whether the IGF-1 receptor is expressed on CD8 T cells. We used our *in vitro* model for effector and memory cell differentiation. As shown previously (45), we observed that the IGF-1 receptor is expressed on naïve CD8 T cells. In activated T cells, at 30 and 72 hours after stimulation with ovalbumin (N4) peptide and αCD28, we observed a mild induction of the IGF-1R (**Figure 12d**). Importantly, at 144 hours after stimulation, when cells have obtained a memory phenotype, we observed that the expression of the IGF-1R was induced almost twofold compared to naïve cells (**Figure 12d**).

In summary, insulin does not stimulate CD8 T cells via the insulin receptor. Instead, we hypothesize that the IGF1 receptor plays a role in T cell activation following CD8 T cell stimulation, in particular for memory cells.

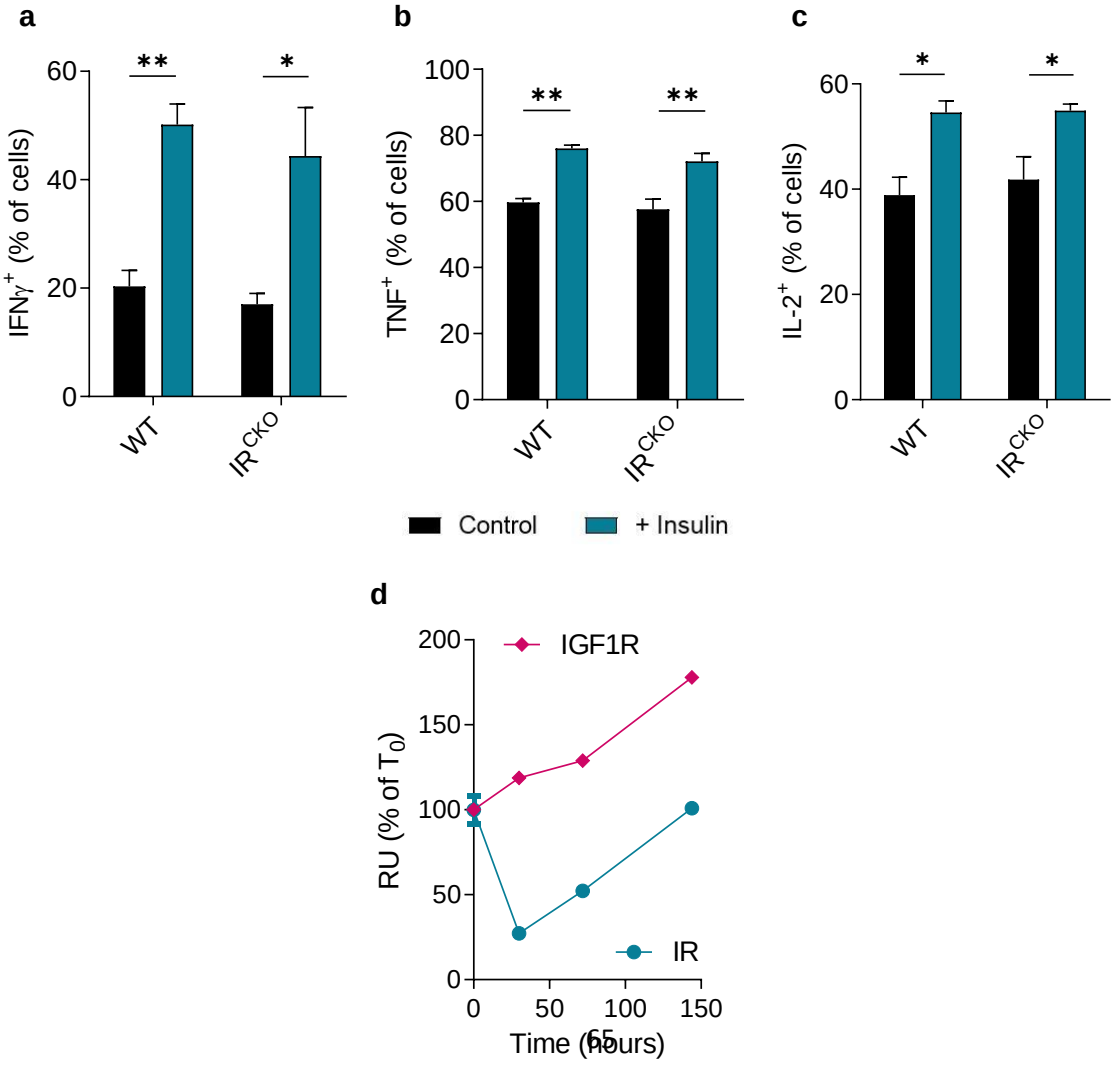

Figure 12. Insulin does not influence the anti-viral CD8 T cell response via its receptor. (a) WT OT-1 and IR^{CKO} OT-1 cells were stimulated *in vitro* with ovalbumin (N4) peptide and anti-CD28 for 30 h in the presence or absence of insulin. The next day, the cells were washed with 10% RPMI and incubated with 50ng/ml of IL-15 for 5 days to generate memory cells. On day 6, the ability of these cells to produce cytokines **(a)** IFNγ, **(b)** TNFα, and **(c)** IL-2 was determined using intracellular flow cytometry. **(d)** OT-1 cells were activated and differentiated to memory cells *in vitro*, and hormone receptor expression was determined by microarray. Indicated are means ± s.e.m. and statistical significances using two-way ANOVA, *p<0.05, ** p<0.01, ***p<0.001, ****p<0.0001. **(a-c)** A representative of three independent experiments or **(d)** data from transcriptome analysis of three biologically independent samples is shown.

4.12. IGF-1 concentrations change during infection

To gain more insight in the role of IGF-1 in CD8 T cell biology, first we investigated IGF-1 hormone levels *in vivo* following viral infection. We infected C57BL/6J mice with a low dose ($2x10^5$ PFU) of murine mCMV and mCMV-*Δm157*. Three days p.i. we collected a drop of blood from the buccal vein (*v. bucalis*) and determined IGF-1 concentrations using ELISA. We found a significant decrease in serum IGF-1 concentrations in infected mice compared with control mice. Furthermore, infection with a more virulent strain mCMV-*Δm157* resulted in even lower levels of IGF-1 than infection with mCMV (**Figure 13a**). These results prompted us to determine how long this effect lasts and what happens to IGF-1 concentrations at later time points when the viral infection is cleared. To determine the kinetics of the IGF1 hormone *in vivo*, we infected C57BL/6J mice with $2x10^5$ PFU of mCMV and collected a drop of blood at specific time points – day 0 before infection and days 3, 7, 14, and 28 after infection. ELISA results on serum samples showed that IGF1 concentrations are reduced three days post-infection but return to baseline within a week after infection (**Figure 13b**). This kinetics suggests that IGF-1 does not play a role in effector CD8 T cell formation, but may be involved in the regulation of CD8 memory T cell biology.

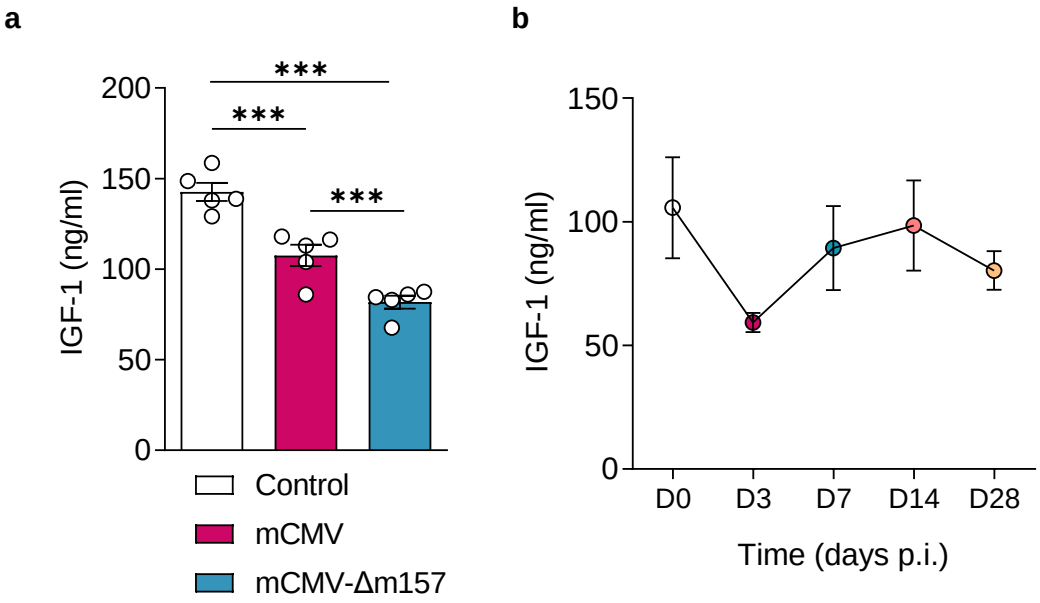

Figure 13. Kinetics of serum IGF-1 concentrations following viral infection. (a) C57BL/6J animals were infected with 2× 10^5 PFU mCMV or mCMV-*Δm157*. Three days p.i. serum IGF-1 levels were measured using ELISA (n=5). **(b)** C57BL/6J animals were infected with 2× 10^5 PFU mCMV, and serum was isolated from blood at indicated time points. IGF-1 levels were measured using ELISA (n=5). Data show means ± s.e.m. and statistical significances. Indicated are statistical significances using one-way ANOVA followed by Bonferroni post-testing, *p<0.05, ** p<0.01, ***p<0.001, ****p<0.0001. For all panels, a representative of two independent experiments is shown.

4.13. IGF-1 stimulation has no impact on the proliferation of effector and memory CD8 T cells *in vitro*

To characterize the role of IGF-1 in effector and memory CD8 T cells, we used the *in vitro* model of CD8 T cell stimulation. CD8 T cells were purified from the spleens of OT-1 mice. Effector and memory cells were generated *in vitro* by culturing them briefly with N4 peptide and anti-CD28, followed by IL-2 or IL-15 stimulation. To determine the impact of IGF-1, cells were stimulated in the presence or absence of this hormone in a concentration range from 0 to 250 ng/ml. Using flow cytometry, we determined the biological properties of these cells stimulated with IGF-1, such as proliferation, phenotype, and cytokine production.

To visualize T cell proliferation *in vitro*, we labeled OT1 cells with the fluorescent, cell-permeable dye carboxyl fluorescein succinimidyl ester (CFSE) to quantify the number of cell

divisions. CFSE is equally partitioned during cell division, causing the fluorescent intensity to halve with each successive generation (108). This technique allows visual monitoring of up to seven cell divisions before the cells become CFSE-negative. Analysis of CFSE dilution revealed no differences in the rate of proliferation between cells stimulated with different concentrations of IGF-1 and cells stimulated only with N4 and anti-CD28. These results were observed for both effector (**Figure 14a**) and memory cells (**Figure 14b**).

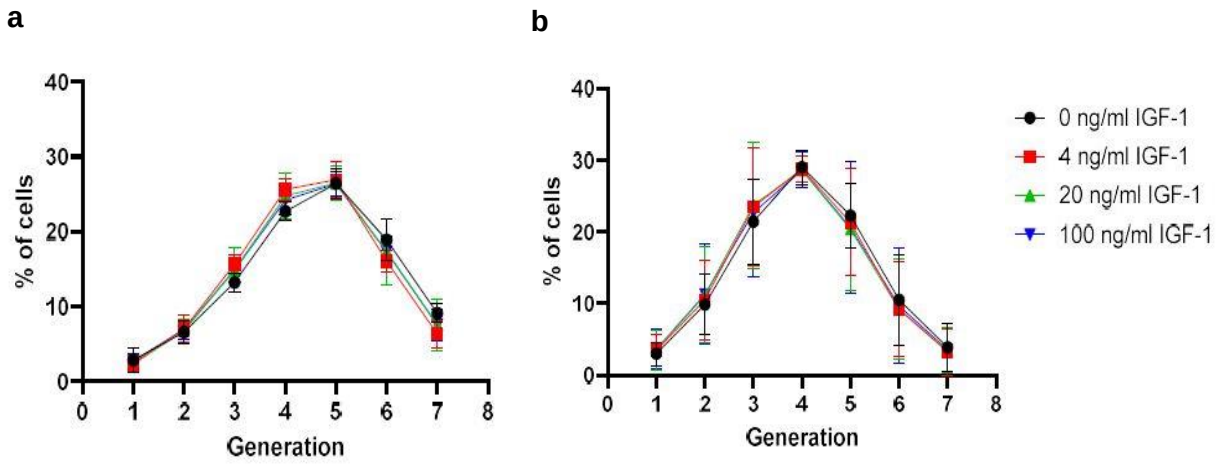

Figure 14. The proliferation of effector and memory CD8 T cells in vitro is not affected by IGF-1 stimulation. Purified CD8 OT-1 cells were CFSE-labeled and activated *in vitro* with ovalbumin (N4) peptide and anti-CD28 for 30 h in the presence or absence of different IGF-1 concentrations. The next day, the cells were washed with 10% RPMI and incubated with 50ng/ml of IL-2 for 2 days to generate effector cells or 50ng/ml of IL-15 for 5 days to generate memory cells. Cells were analyzed by flow cytometry on **(a)** day 3 and **(b)** day 6 after the start of stimulation. Indicated are means ± s.e.m. and statistical significances using one-way ANOVA followed by Bonferroni post-testing, *p<0.05, ** p<0.01, ***p<0.001, ****p<0.0001. For all panels, a representative of three independent experiments is shown.

4.14. IGF-1 stimulation has no impact on the phenotype of effector and memory CD8 T cells *in vitro*

Next, we questioned whether IGF-1 stimulation impacts the phenotype of *in vitro* generated effector and memory CD8 T cells. We used the same *in vitro* CD8 T cell stimulation model with N4/αCD28 in the presence or absence of varying concentrations of IGF-1. After 3 days in culture with IL-2, or 6 days with IL-15, we performed surface staining of CD8 T cells to determine the phenotype of these cells using flow cytometry. Surface markers that were

used are CD44, CD25, CD69, CD127 and CD62L. On effector T cells, we found typically high levels of CD25, as it is a marker of activation and proliferation, as well as high levels of CD44, which distinguishes them from naïve cells. There was no significant difference between cells stimulated with different concentrations of IGF-1 and cells stimulated only with N4 and anti-CD28 (**Figure 15a**). We found comparable levels of memory-associated markers CD127 and CD62L, as well as similar expression of CD44 on memory CD8 T cells, regardless of stimulation with IGF-1 (**Figure 15b**). The only significant difference observed was the downregulation of CD62L between 2 ng/mL and 50 ng/mL of IGF-1, which suggests that these cells may have obtained a phenotype that leans more towards effector memory rather than central memory cells.

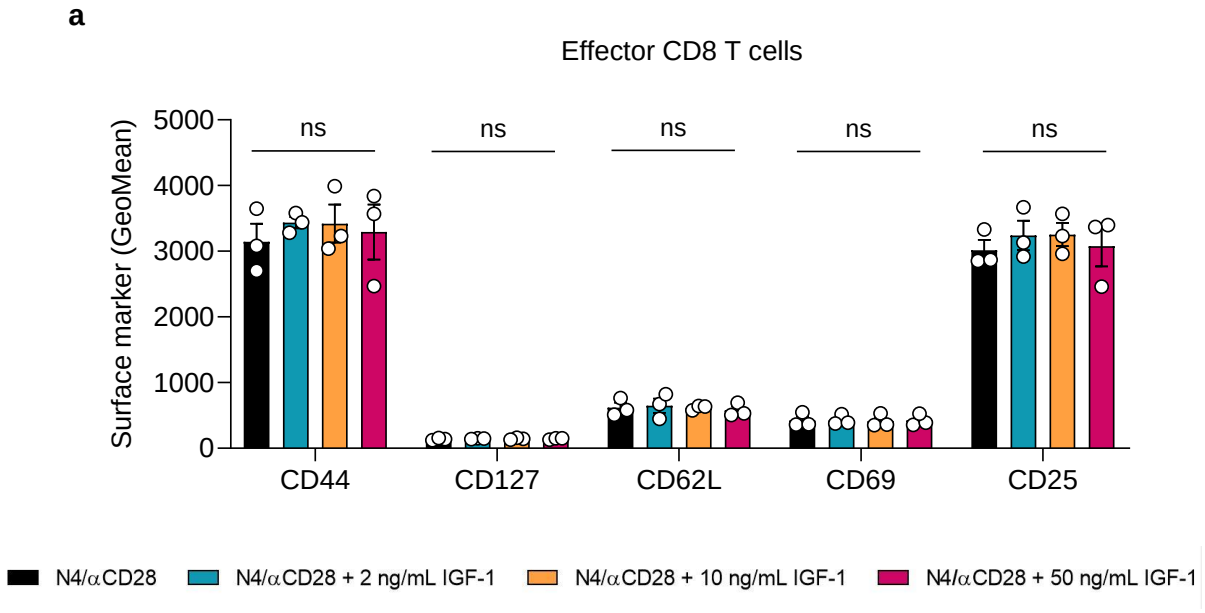

Figure 15. The phenotype of effector and memory CD8 T cells *in vitro* is not affected by IGF-1 stimulation. Purified CD8 OT-1 cells were activated *in vitro* with ovalbumin (N4) peptide and anti-CD28 for 30 h in the presence or absence of different IGF-1 concentrations. The next day, the cells were washed with 10% RPMI and incubated with 50ng/ml of IL-2 for 2 days to generate effector cells or 50ng/ml of IL-15 for 5 days to generate memory cells. Cell surface marker expression was analyzed by flow cytometry on **(a)** day 3 and **(b)** day 6 after the start of stimulation. Indicated are means ± s.e.m. and statistical significances using two-way ANOVA, *p<0.05, ** p<0.01, ***p<0.001, ****p<0.0001. For all panels, a representative of three independent experiments is shown.

4.15. IGF-1 stimulation increased IFNγ production by memory CD8 T cells *in vitro*

Previously, we demonstrated that high insulin concentrations promoted cytokine production by CD8 T cells (45,105), but that effect is also observed in cells deficient for the insulin receptor (**Figure 12a-c**). Using the same *in vitro* model of CD8 T cell stimulation, we wanted to investigate whether IGF-1 affects effector and memory T cell functionality. Cells were restimulated with 10ng/mL of N4 *in vitro* after 3 days in culture with IL-2, or 6 days in culture with IL-15 in the presence or absence of varying concentrations of IGF-1. After 4h of stimulation, surface, and intracellular stainings were performed. Using flow cytometry, we measured their ability to produce cytokines. Cytokine production by effector cells was assessed on day 3, while cytokine production by memory cells was measured on day 6. Stimulation using IGF-1 hormone did not affect the functionality of effector cells, as we found comparable levels of IFNγ, TNFα, and IL-2 production on IGF-1 stimulated and unstimulated CD8 T cells (**Figure 16a**). However, flow cytometry data on cytokine production on day 6 showed that even very low concentrations of IGF-1 promoted IFNγ production after restimulation (**Figure 16b**).

Therefore, we concluded that the functionality of memory CD8 T cells cultured with different concentrations of IGF-1 was enhanced, in particular with regards to IFNγ production.

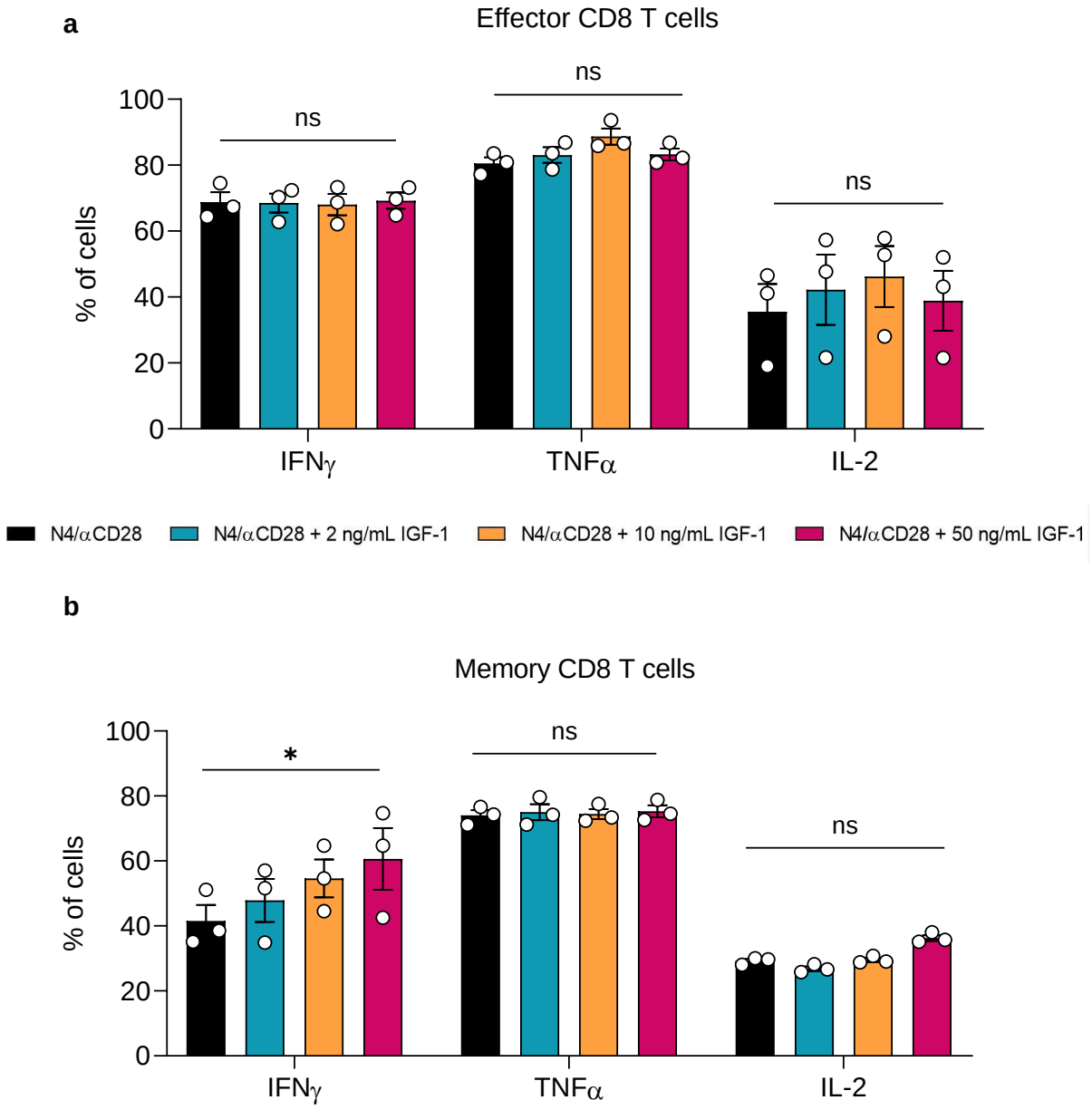

Figure 16. *In vitro* IGF-1 stimulation increased IFNγ production by memory, but not effector CD8 T cells. Purified CD8 OT-1 cells were stimulated *in vitro* with ovalbumin (N4) peptide and anti-CD28 for 30 h in the presence or absence of different IGF-1 concentrations. The next day, the cells were washed with 10% RPMI and incubated with 50ng/ml of IL-2 for 2 days to generate effector cells or 50ng/ml of IL-15 for 5 days to generate memory cells. Cytokine production was assessed using flow cytometry on **(a)** day 3 and **(b)** day 6 after restimulation with N4. Indicated are means ± s.e.m. and statistical significances using two-way ANOVA, *p<0.05, ** p<0.01, ***p<0.001, ****p<0.0001. For all panels, a representative of three independent experiments is shown.

4.16. IGF-1 promotes glycolytic metabolism in memory CD8 T cells

Although IGF-1 is traditionally recognized as a key growth factor due to its ability to stimulate the growth of all cell types and is a potent stimulant of protein synthesis it also has significant metabolic effects (73). We questioned whether this hormone significantly influences catabolic CD8 T cell metabolism. Purified WT OT-1 cells were stimulated *in vitro* with N4 peptide, anti-CD28, and varying concentrations of IGF-1 for 30 hours. The following day, cells were washed with 10% RPMI and cultured for an additional 5 days with IL-15 to generate memory CD8 T cells, in the presence or absence of IGF-1. On day 6, the cells obtained phenotypic and functional features of memory cells. Their metabolic profiles were analyzed using a Seahorse extracellular flux analyzer. In memory CD8 T cells, ATP production primarily relies on mitochondrial activity, with glycolytic activity being completely diminished (**Figure 17a**), consistent with existing literature (35). Measurements of OCR and ECAR revealed that IGF-1-treated cells had decreased OCR (**Figure 17b**), and increased ECAR (**Figure 17c**). Moreover, IGF-1 was found to enhance both glycolytic metabolism and overall ATP production in a dose-dependent fashion (**Figure 17d**).

In conclusion, metabolic profiling indicates that IGF-1 enhances glycolytic capacity, thereby increasing overall ATP production and potentiating the functionality of memory CD8 T cells.

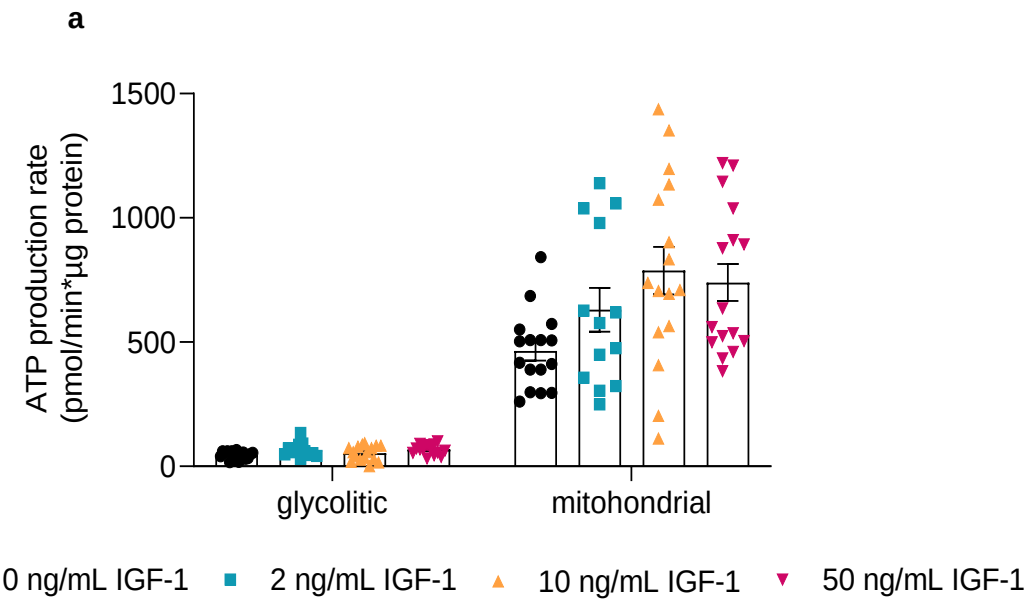

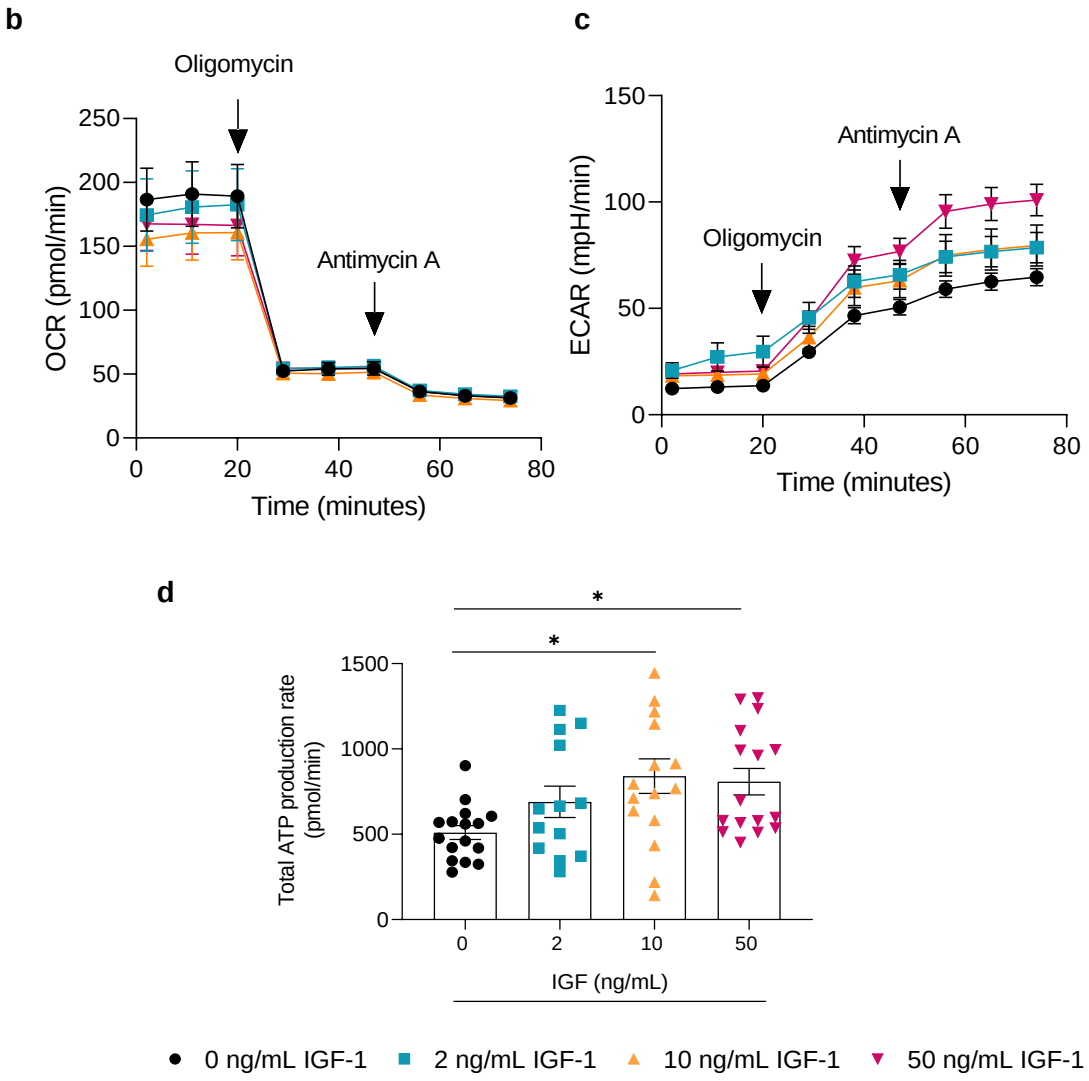

Figure 17. IGF-1 promotes glycolytic metabolism, increasing overall ATP production and improving the functionality of memory CD8 T cells. Purified CD8 OT-1 cells were stimulated *in vitro* with ovalbumin (N4) peptide and anti-CD28 for 30 h in the presence or absence of different IGF-1 concentrations. The next day, the cells were washed with 10% RPMI and incubated with 50ng/ml of IL-15 for 5 days to generate memory cells. Cells were analyzed by Seahorse on day 6 after the start of stimulation. **(a)** ATP production rate. **(b)** OCR as a measure of oxidative phosphorylation, and **(c)** ECAR as a measurement of glycolysis. **(d)** Total ATP production rate calculated. (n=16). Indicated are means ± s.e.m. and statistical significances using one-way ANOVA followed by Bonferroni post-testing, *p<0.05, ** p<0.01, ***p<0.001, ****p<0.0001. For all panels, a representative of three independent experiments is shown.

4.17. IGF-1 signalling is important for the generation of CD8 memory T cells

Subsequently, we aimed to investigate whether the functional and metabolic changes observed after IGF-1 stimulation in vitro translated to altered functionality *in vivo*. To do so, we made use of genetically modified animals that generate OVA-specific CD8 T cells which are deficient both for insulin and for the IGF-1 receptor (IR^{CKO} $IGF1R^{CKO}$), whereas all other tissues in the body are responsive to this hormone. Our lab has congenic mouse strains with CD45.1 and/or CD45.2 alleles, enabling easy detection of donor OT-1 cells after transfer into recipients (13). C57BL/6J mice ($CD45.2^{+}$) were recipients of a mixture of donor cells. Naïve WT OT-1 cells ($CD45.1/2^{+}$) were mixed with an equal number of naïve IR^{CKO} $IGF1R^{CKO}$ OT-1 cells ($CD45.1^{+}$) and $4x10^{4}$ cells were i.v. injected into recipients. This model allows the tracking of virus-specific cells. The next day recipients were infected with $2x10^{5}$ of an mCMV strain expressing the N4 peptide (mCMV-N4), and transferred cells were followed in the blood.

At the acute phase of the antiviral T cell response, on day 8 after infection, donor CD8 T cells were analyzed in the spleen, liver, and blood. Results showed a significant decrease in the relative numbers of donor cells lacking the IGF-1 receptor (**Figure 18a**). The same analysis was performed 35 days p.i. at the memory phase of the antiviral response. At this time point, the percentage of donor cells was lower than in the acute phase, as the effector pool contracts with the clearance of the pathogen. Nevertheless, the difference in cell ratios remained preserved and there was still a notable reduction in the percentage of donor cells deficient in the IGF-1 receptor (**Figure 18b**). Finally, to examine how memory cells react to a subsequent viral encounter, mice that had received OT-1 cells and were primed with mCMV-N4 were reinfected after 40 days with LCMV-N4. In this model, only N4-specific cells respond to the secondary infection, enabling a detailed analysis of memory responses. The recall response was measured 6 days p.i. Both WT OT-1 and IR^{CKO} $IGF1R^{CKO}$ OT-1 cells showed the ability to form secondary effector cells, however, the difference in the percentage of donor cells remained statistically different (**Figure 18c**). Day six after recall is at the peak of the T cell responses and therefore shows the ability of cells to form secondary effector cells. To determine whether a lack of IGF-1 signalling also impacts secondary memory formation, we analyzed mice on days 15 (**Figure 18d**) and 50 post-recall (**Figure 18e**) with LCMV-N4, which correspond with days 55 and 90 post-priming. WT OT-1 cells still had a competitive advantage over IR^{CKO} $IGF1R^{CKO}$ indicating an important role of IGF-1 in promoting secondary memory CD8 T cells fitness.

In conclusion, IGF-1 receptor deficiency impacts the ability to form both primary and secondary effector and memory cells.

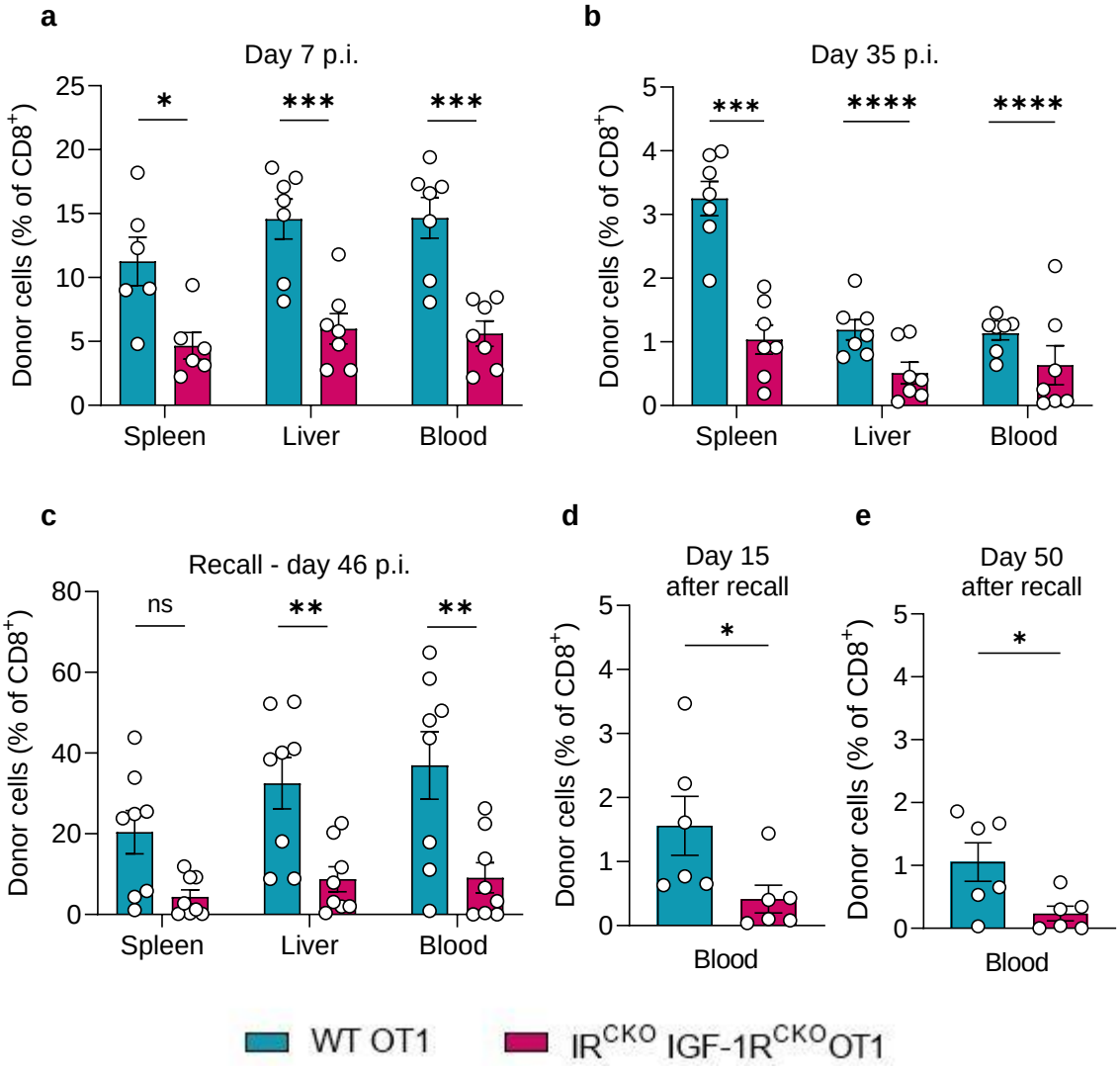

Figure 18. IGF-1 signalling promotes CD8 memory T cell formation *in vivo*. C57BL/6J mice were i.v. injected 4x10^4 of IR^{CKO} IGF1R^{CKO} OT-1 and WT OT-1 CD8 T cells mix. Recipient mice were infected with mCMV-N4 the following day. OT1 cells were isolated from the spleen, liver, and blood and sorted at different time points p.i. Donor cells as a fraction of CD8 T cells in indicated organs were measured using flow cytometry at **(a)** 7 days p.i, **(b)** 35 days p.i., **(c)** 6 days after recall with LCMV-N4, **(d)** 15 days and **(e)** 50 days after recall. Data show means ± s.e.m. and statistical significances. Indicated are statistical significances using (**a-c**) two-way ANOVA, or (**d, e**) Student's t-test at * $p < 0.05$, ** $p < 0.01$, ***$p<0.001$, ****$p<0.0001$. A representative of two independent experiments is shown.

4.18. The functionality of T cells lacking the IGF-1 receptor is not affected *in vivo*

Using the same *in vivo* experimental setup as in Figure 18, we aimed to determine the impact of IGF-1 deficiency on CD8 T cell functionality. A mixture of WT OT-1 cells (CD45.1/2^{+}) and IR^{CKO} IGF1R^{CKO} OT-1 cells (CD45.1^{+}) in a ratio 1:1 was i.v. injected into CD45.2^{+} recipients, that were infected with 2x10^{5} mCMV-N4 the next day. OT-1 cells were isolated from the spleen, liver, and blood at different time points after priming. Following *in vitro* stimulation with N4, intracellular measurement of cytokines such as IFNγ, TNF, and IL-2 was assessed using flow cytometry. Surprisingly, in contrast to our *in vitro* experiments (Figure 16), cytokine production was not different between WT OT-1 and IR^{CKO} IGF1R^{CKO} OT-1 cells at 7 days (**Figure 19a**) and 35 days p.i. (**Figure 19b**), indicating that the functionality of these cells was not affected by the lack of IGF-1 receptor. To examine how memory cells react to a subsequent viral encounter, mice that had received a mix of WT and IR^{CKO} IGF1R^{CKO} OT-1 cells and were primed with mCMV-N4 were reinfected after 40 days with LCMV-N4. In this model, only N4-specific cells respond to the secondary infection, enabling a detailed analysis of memory responses. Recall responses were assessed after 6 days. We did not observe any difference in the capacity of WT and IR^{CKO} IGF1R^{CKO} OT-1 cells to produce IFNγ, TNFα, and IL-2 even after recall (**Figure 19c**).

Although IGF-receptor deficient T cells showed reduced capacity to form memory cells, their functionality and recall capacity were not notably impacted *in vivo*.

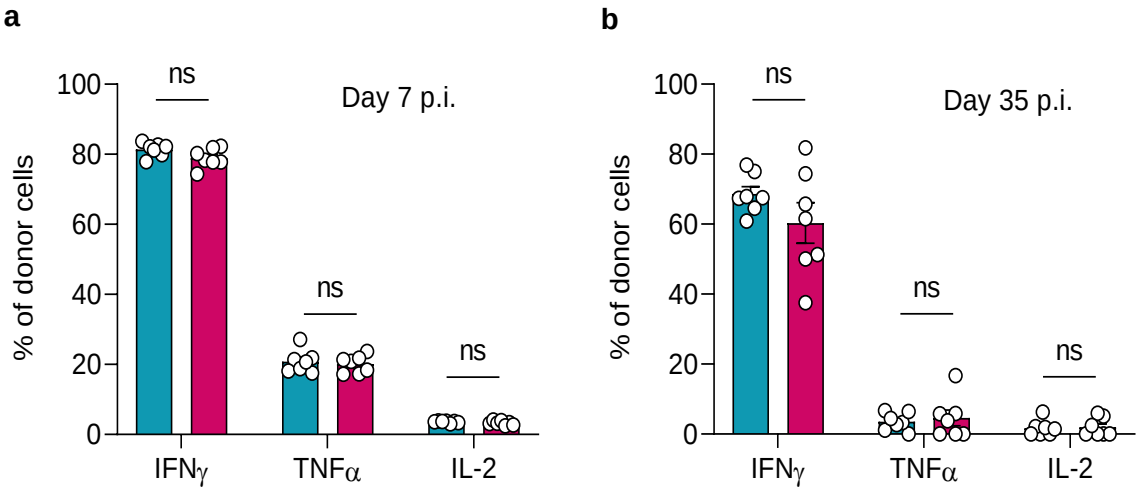

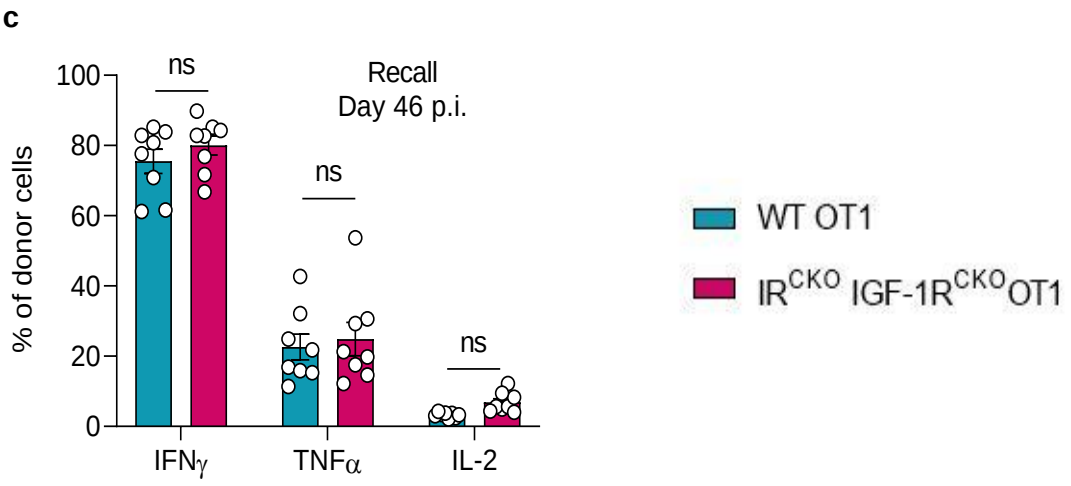

Figure 19. Deficiency of the IGF-1 receptor has no significant impact on the functionality and recall capacity of CD8 T cells *in vivo*. C57BL/6J mice were i.v. injected 4x10^4 of IR^{CKO} IGF1R^{CKO} OT-1 and WT OT-1 CD8 T cells mix. Recipient mice were infected with mCMV-N4 the following day. OT1 cells were isolated from the spleen, liver, and blood and sorted at different time points p.i. Cytokine production after *in vitro* restimulation with N4 was measured using flow cytometry at **(a)** 7 days p.i, **(b)** 35 days p.i., and **(c)** 6 days after recall. Data show means ± s.e.m. and statistical significances. Indicated are statistical significances using two-way ANOVA * $p < 0.05$, ** $p < 0.01$, ***$p<0.001$, ****$p<0.0001$. A representative of two independent experiments is shown.

4.19. IGF-1 receptor signalling is not required for memory CD8 T cell-mediated control of viral replication

To determine the physiological relevance of IGF-1 on memory CD8 T cell functionality, C57BL/6J mice were transferred with 2x10^4 IR^{CKO} IGF1R^{CKO} OT-1 or WT OT-1 CD8 T cells. One day after transfer, mice were infected i.p. with 1x10^6 IFU of LCMV-N4. After 30 days, mice were reinfected with 2x10^5 PFU of mCMV-N4. To ensure that the influence of IGF-1 on CD8 T cell biology is not confounded by the presence of NK cells, which also play a crucial role in controlling mCMV, we depleted NK cells *in vivo* by i.p. injection of αNK1.1 one day before mCMV infection. This approach allowed us to specifically assess the effects of IGF-1 on CD8 T cells without interference from NK cell activity. To determine viral titers in the spleen and liver, organs were collected 5 days p.i., and a standard plaque-forming assay was performed. Results showed no difference in viral infectivity in both the spleen (**Figure 20a**)

and liver (**Figure 20b**). The results showed no difference in the viral load of mice that received IGF-1 receptor-deficient OT-1 cells compared to the control WT OT-1 cells.

These results indicate that IGF-1 receptor signalling is not essential for the ability of memory CD8 T cells to control viral replication *in vivo*.

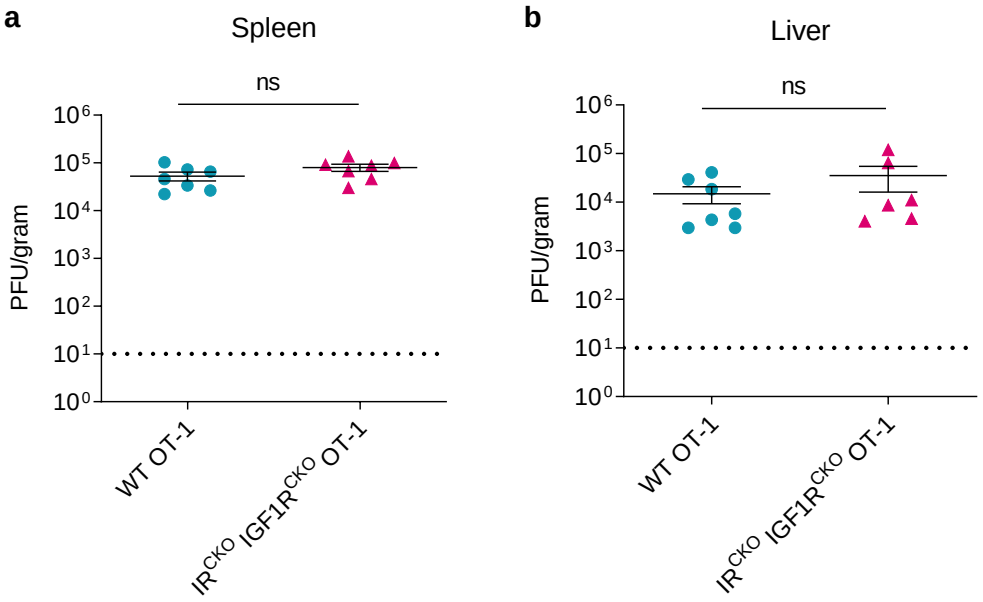

Figure 20. IGF-1 has no significant impact on CD8 T cell biology in the absence of NK cells. C57BL/6J mice received 2x10^4 either IR^{CKO} IGF1R^{CKO} OT-1 or WT OT-1 CD8 T cells and were infected with LCMV-N4. Before recall infection with 2x10^5 PFU mCMV-N4, NK cells were depleted. Viral titers were determined 5 days p.i. in **(a)** spleens and **(b)** livers. Data show means ± s.e.m. and statistical significances. Indicated are statistical significances at Mann-Whitney test * p < 0.05, ** p < 0.01, ***p<0.001, ****p<0.0001.

4.20. IGF-1 receptor signalling is important for memory CD8 T cell-mediated control of melanoma cells

Viral infection represents a very strong immunological stimulus and differences in responsiveness between wild-type and IGF-1R deficient cells may therefore be lost. Therefore, we decided to investigate the functionality of these cells in a tumour model, which represents a milder stimulus. C57BL/6J mice were transferred with 2x10^4 IR^{CKO} IGF1R^{CKO} OT-1 or WT OT-1 CD8 T cells. One day after transfer, mice were infected i.p. with 1x10^6 IFU of

LCMV-N4. As found previously, after 40 days we observed that IGF-1 cells had generated significantly fewer memory cells than their wild-type counterparts (**Figure 21a**). To test the ability of these cells to control melanoma cells, mice were i.v. injected with 10^5 B16 melanoma cells overexpressing the N4 peptide (B16-OVA). B16 melanoma is spontaneously derived from C57BL/6J mice, poorly immunogenic, and used as a model for human tumours (109). After injecting the B16-OVA tumour cells, survival was followed (**Figure 21b**). Our results showed that only a minor fraction of animals with wild-type OT-1 cells developed tumours. In contrast, the majority of mice transferred with IGF1R^{CKO} succumbed to melanoma. In addition, the onset of disease was observed much earlier than in animals transferred with WT cells.

These results indicate that IGF-1 signalling promotes the ability of memory CD8 T cells to control tumours *in vivo*.

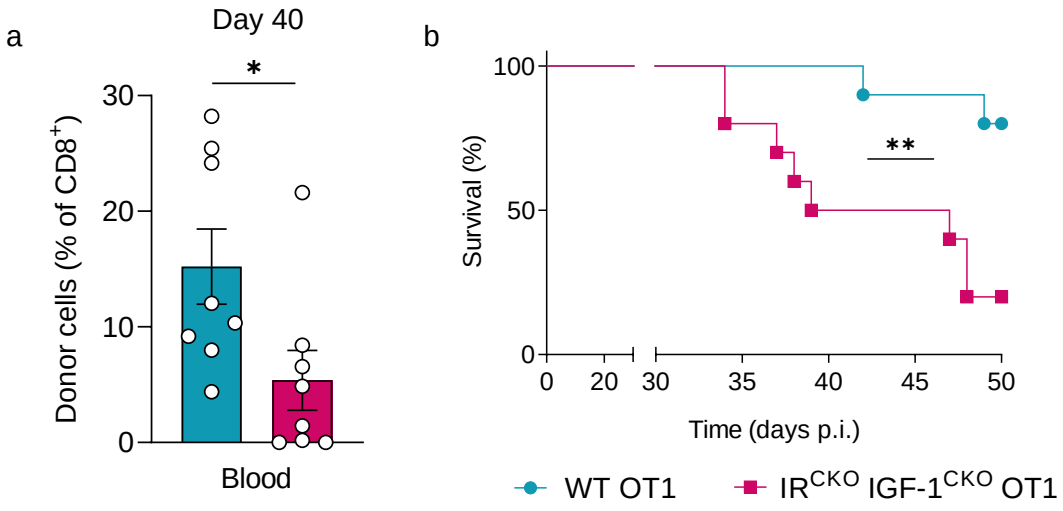

Figure 21. IGF-1R deficiency impairs the ability of memory CD8 T cells to control B16 melanoma tumour growth. C57BL/6J mice received 2x10^4 either IR^{CKO} IGF1R^{CKO} OT-1 or WT OT-1 CD8 T cells and were infected with LCMV-N4. After 30 days, mice were i.v. injected with 10^5 B16-OVA melanoma cells (n=10 per group). **(a)** Donor cells as a fraction of CD8 T cells in the blood were measured 40 days p.i, before i.v. injection of B16-OVA cells. **(b)** Survival curve of mice transferred with IR^{CKO} IGF1R^{CKO} OT-1 or WT OT-1 CD8 T cells after i.v. injection of B16-OVA cells. Each symbol represents an individual mouse. Data show means ± s.e.m. and statistical significances. Indicated are statistical significances using **(a)** Student's t-test, and **(b)** to analyze the survival curves Kaplan-Meier model, followed by the log-rank (Mantel-Cox) test, was used at * $p < 0.05$ and **$p < 0.01$.

Summary section 2

Although we previously demonstrated that insulin stimulation enhances cytokine production by CD8 T-cells, in this thesis, we show that insulin itself does not impact the anti-viral CD8 T cell response through the insulin receptor. Instead, our data revealed that CD8 T cells in the memory phase express high levels of the IGF1R, which binds insulin with low affinity. Stimulation with IGF-1 enhanced IFNγ production and glycolytic activity in memory CD8 T cells. *In vivo*, IGF-1 signaling was critical for the generation of functional memory CD8 T cells. Mice lacking IR and IGF1R on CD8 T cells showed impaired memory responses and failed to control B16 melanoma. Together, these findings identify IGF-1 as an important regulator of memory CD8 T cell function and tumour control.

5. DISCUSSION

5. DISCUSSION

The research described in this thesis explored how various aspects associated with nutrient homeostasis are important for the immune response against viral infection, with a focus on how glucose and the IGF-1 hormone modulate the antiviral immune response. In the first section, we discovered that a strong, but non-lethal infection leads to systemic restriction of glucose availability by increasing pancreatic insulin production. Hyperinsulinemia inhibited hepatic glycogenolysis during fasting and limited glucose availability. This resulted in reduced lactate production and promoted secretion of IFN-I. Preventing glucose restriction by induced hyperglycemia nullified this mechanism, leading to increased lactate levels, reduced type-I IFN production, and higher viral loads following infection. Dysregulation of this mechanism in the context of hyperglycemia may explain why people with diabetes are more susceptible to viral infections. Thus, we identified a new mechanism by which the immune system regulates systemic blood glucose to control viral infection better (71).

In the second section, we focused on the impact of the receptors binding hormone insulin on the anti-viral immune response. We discovered that insulin does not impact the antiviral CD8 T cell response through insulin receptors. Instead, we showed that the IGF-1 receptor, a molecule that binds insulin with low affinity, is highly expressed on CD8 T cells in the memory phase. Stimulation of CD8 T cells with IGF-1 promoted the production of IFNγ and glycolytic metabolism in memory cells. *In vivo*, we could show that IGF-1 is important for generating CD8 memory T cells. Deficiency of the IGF-1 receptor significantly impaired the ability of memory CD8 T cells to protect mice from B16 melanoma development. This research therefore, showed that the hormone IGF-1 has an important role in promoting memory CD8 T cell functionality.

In order to function, our body requires maintaining homeostasis - whether that involves regulating blood glucose concentrations, pH levels, temperature, oxygen, or a large number of other nutrients, proteins and electrolytes. However, homeostatic values are altered in the context of infection. Viral infection therefore has a major impact on systemic metabolism, and the interplay between the immune and endocrine systems is crucial for the host's defence against infection. Of particular interest is the regulation of blood glucose, since this is both an essential nutrient for optimal functioning of activated immune cells, and a molecule which infected cells use for enhanced viral replication. While intensive research has been done on

the impact of both mild and severe viral infection on the regulation of systemic blood glucose levels, how strong infection affects glucose metabolism was still unclear. Insulin is a major glucose-lowering endocrine hormone and plays a key role in orchestrating glucose homeostasis. Previously, Šestan et al. showed that mild viral infection causes transient IR in skeletal muscle, but not in the liver and adipose tissue of lean mice. This is due to virus-induced IFNγ that downregulates insulin receptors on muscle cells. In mild infection, systemic IR does not lead to an increase of blood glucose levels, because euglycemia is preserved by compensatory hyperinsulinemia (105). Nevertheless, hypoglycemia following infection with more agressive pathogens, such as malaria (110) and mumps (111) had been observed, but its physiological role was unclear.

We proved that glucose restriction benefits the antiviral response since its prevention in vivo resulted in higher viral loads in the tissue following LCMV infection and a higher mortality rate following influenza infection. Although it may seem that our findings contradict a previous study that oral glucose gavage improves survival in influenza-infected animals, the possible explanation lies in the experimental setup. While Wang et al. (112) provided glucose twice a day through oral gavage, in our experimental setup animals are constantly exposed to glucose in drinking water. Even during infection, a boost of glucose triggers insulin release from pancreatic β-cells, restoring blood glucose levels to baseline within two hours. Therefore, twice-a-day glucose administration primarily replenishes nutrient stores, making them more resistant to infection without sustaining elevated glucose levels. In our experiments, mice have a permanent increase in their glucose levels in the blood. These increased glucose levels are mimicking a condition of hyperglycemia, a feature of metabolic diseases such as diabetes. STZ-treated mice lose their pancreatic β cells and therefore exhibit the same pathological and molecular signatures as T1D patients (113). As we showed, STZ-induced hyperglycemia prevents glucose restriction and has a detrimental effect on antiviral immune response. Since the COVID-19 pandemic pointed out the increased susceptibility of diabetic patients to severe viral disease (83), our findings could explain why individuals with metabolic diseases and chronic hyperglycemia experience increased infection severity.

Restriction of glucose availability was shown to impair HCMV replication (114), and blocking of glycolysis using 2DG, a glucose analog, reduced pseudorabies virus (PRV) replication in vitro (115). The final product of glycolysis is lactate, previously mostly regarded as a metabolic waste product. Recently, the importance of lactate as both a nutrient and a signalling molecule

has become appreciated (116). Lactate is a key metabolite in the impairment of type-I IFN production through the inhibition of the RLR-signalling pathway (7). Lowering the glucose levels *in vitro* reduced lactate production and promoted type I IFN production during infection. Moreover, blocking of LDHA using sodium oxamate, a specific LDHA inhibitor, resulted in increased IFNβ expression and virus clearance in various tissues following VSV infection (7). However, whether glucose availability was limited following viral infection *in vivo*, thus promoting the antiviral response by restricting lactate availability, was left unexplored. We confirmed both *in vitro* and *in vivo* that by reducing lactate levels using sodium oxamate, IFNβ production was increased, and viral replication was suppressed. This was performed either by supplementing high-glucose medium with oxamate or through daily i.p. injection of oxamate in mice. Thus, the body indeed lowers lactate production during viral infection by lowering systemic glucose availability.

The reciprocal action of insulin and glucagon is responsible for the control of systemic glucose availability. Previously, the immune system was shown to control pancreatic glucagon production in a type-2-like immune response (117). Here, in a Th1-type response, a role for insulin is elucidated since our findings imply that infection-induced glucose restriction is mediated by insulin. Systemic insulin levels were increased in the serum of infected mice after 18 hours post-infection, indicating increased insulin secretion from the pancreas. Hyperinsulinemia reduces hepatic glucose output by restricting glycogenolysis, which systemically lowers lactate levels in the circulation and promotes type I IFN production. Hyperinsulinemia not only lowers systemic glucose levels; it also directs this nutrient to other organs. Previously, infection was proposed to redirect glucose to the immune system, but whether and how this happens was left unexplored (118). We investigated glucose flux in infected animals using hyperinsulinemic-euglycemic clamping. Besides reduced hepatic glucose output, we discovered that glucose uptake is significantly increased in the spleen, 5 days post-infection. We hypothesized this is due to immune activation and lymphocyte proliferation that increases on the fifth day after infection, including the expansion of CD8 T cells. Activation of CD8 T cells is accompanied by a sharp rise in glucose demand to support their growth, proliferation, and effector functions (119). Immune cells express the insulin receptor. As stated previously, major organs associated with insulin-dependent glucose uptake, such as skeletal muscle, reduce their sensitivity to this hormone following infection. Therefore, our findings suggest that hyperinsulinemia in the context of infection does not only

lower systemic glucose availability, but also redirects this nutrient specifically to the immune system.

The role of insulin signalling in immune stimulation may reach beyond that of purely redirecting glucose. Immune-mediated hyperinsulinemia following mild infection was proven to be beneficial since it directly enhanced the expansion and activity of virus-specific CD8 T lymphocytes (105). This occurs because the insulin receptor and CD28 signalling, a crucial costimulatory pathway for CD8 T cell activation, converge on the PI3K signalling cascade. A study by Tsai et al. showed that both insulin deficiency and a deficiency of the insulin receptor on T cells impaired the antiviral T cell response, making mice more vulnerable to the infection (70). Thus, infection-induced hyperinsulinemia promotes the antiviral immune response in multiple ways.

Notably, whereas CD8 T cells do have the insulin receptor on their cell surface, its level of expression is relatively low (45). It was therefore questioned whether insulin uses its main receptor to stimulate these cells. We used mice that generate T cells deficient for insulin receptors (IR^{CKO}). By stimulating purified WT and KO OT1 cells with N4 and insulin we showed that insulin increased IFNγ production, however, both in WT and insulin receptor-deficient cells. In addition to having insulin receptors, CD8 cells also express receptors for numerous other hormones, including IGF-1R (120). The transcription of hormone receptor genes revealed that IGF-1R is highly expressed on CD8 T cells in the memory phase. Insulin and INSR share structural homology with IGF-1 and IGF-1R; these two hormones are involved in numerous overlapping signalling pathways. While insulin primarily controls metabolic processes, IGFs regulate long-term cell fate decisions. The importance of IGF-1 for development and growth was shown in many studies and complete deficiency of IGF-1 is linked to postnatal lethality or growth and developmental defects (121). IGF-1 was proven to play a role in various physiological processes, including lifespan and immune function. Stimulation with physiological concentrations of IGF-1 proved its role in cytokine production because it induced macrophage TNF release (122). Here, we demonstrate that even very low concentrations of IGF-1 could promote the production of IFNγ by CD8 memory T cells, while supraphysiological concentrations of insulin were used to achieve a similar effect. Thus, disruption of IGF-1 signalling has significant impact on CD8 T cell biological functions.

Under normal conditions, most immune cells use OXPHOS to fulfill their energetic needs because it generates the maximum amount of ATP from a single molecule of glucose. However, immune cells switch their metabolism from using primarily OXPHOS to glycolysis to support growth, proliferation, and cytokine production during infection (123). During memory formation, CD8 T cells switch metabolism back from glycolysis to OXPHOS (35). Which mechanism controls this careful balance is mostly unclear. Our findings suggest that IGF-1 signalling is an important mediator of metabolic checkpoint in differentiating CD8 T cells. Stimulation with IGF-1 resulted in a dose-dependent increase in ECAR that suggests that IGF-1 promotes glycolysis and effector-like metabolism in memory cells. Specific IGF-1 binding to IGF-1R on the cell surface leads to the downstream activation of PI3K and MAPK signalling pathways, which is required for increased bioactivities of IGF-1 such as proliferation, differentiation, and survival (124). Moreover, PI3K and MAPK pro-growth signalling pathways are shown to promote cellular use of glycolytic metabolism, confirming the dominant role of glycolysis in rapidly proliferating cells (123). In the absence of pathogens, memory cells must adopt a type of energy-efficient metabolism that prevents excessive use of nutrients. At the same time, these cells must be able to rapidly respond upon re-encounter of pathogens. Our findings suggest that IGF-1 is important for preventing memory cells from adopting an excessively quiescent state and retain their potential for rapid responsiveness.

In vivo, we demonstrated that IGF-1 is important for generating CD8 memory T cells. This aligns with previous findings that the mTOR pathway is involved in the regulation of CD8 T cell memory formation (125). Notably, mTOR facilitates the phosphorylation of key proteins, including IGF-1R, and this pathway is disrupted in cells deficient for IGF-1 receptor, therefore formation of memory is impaired. Opposite to our *in vitro* data, IGF1R-deficient CD8 T cells did not show any difference in cytokine production compared to WT OT1 cells, meaning that the functionality of T cells lacking the IGF-1R is not impacted *in vivo*. A possible explanation for the discrepancy between our *in vitro* findings and those *in vivo* may lay in the fact that *in vitro* we are using increased levels of IGF-1 to stimulate cells, while *in vivo* there is a complete lack of signal since cells are deficient both for insulin and IGF-1 receptor. Moreover, another limitation of these findings is the lack of data on whether insulin can stimulate the IGF-1 receptor and therefore modulate CD8 T-cell response.

The *in vivo* role of IGF-1 is unclear, especially in regards to tumours. We have found that although IGF-1R signalling deficiency on memory CD8 T cells did not impact cytokine

production, it was required for a proper response against tumours. There are longstanding controversies in oncology about the role of IGF-1 in tumourigenesis, and whether it has a pro- or anti-oncogenic effect. However, a recent study suggested that IGF-1 might act as a tumour suppressor by enhancing T lymphocyte proliferation and activity both in the peripheral lymphoid system and within the tumour microenvironment (126). Our findings are in accordance with this model.

This work emphasizes how the endocrine and immune systems are interconnected and work together in maintaining homeostasis, both under steady-state conditions and following infection. These findings provide valuable insights into the metabolic-immune interplay during viral infections or tumor growth, which may help explain why individuals with metabolic disorders, such as diabetes, exhibit impaired immune responses. Understanding these mechanisms opens new avenues for therapeutic interventions targeting metabolic pathways to improve antiviral immunity.

6. CONCLUSIONS

6. CONCLUSIONS

During an infection, major changes in systemic metabolism and its regulation are induced, including alterations in glucose and hormone levels. However, exactly how these changes benefit the antiviral response is still largely unclear.

Our findings reveal an immune-endocrine circuit in which **strong viral infections induce transient glucose restriction, enhancing the innate antiviral immune response**. Moreover, we began to unravel the role of hormonal control of antiviral response by discovering that **IGF-1 signalling plays a pivotal role in shaping memory T cell function and tumour control**. These findings provide valuable insights into the metabolic-immune interplay during viral infections and tumours. Disruption of glucose and/or hormonal control of the antiviral response in the context of metabolic disease might explain increased susceptibility to pathogens in individuals with metabolic disorders, such as diabetes. To summarize, the main novel findings shown in this thesis are:

- Strong viral infection induces transient relative hypoglycemia, which benefits the antiviral immune response
- Glucose restriction impairs viral replication *in vitro* by limiting lactate production and enhancing the production of type-I interferons
- Infection-induced glucose restriction depends on increased insulin secretion and inhibited glycogenolysis
- Insulin does not influence the anti-viral CD8 response through the insulin receptor
- IGF-1 stimulation promoted IFNγ production and glycolytic metabolism by memory CD8 T cells *in vitro*
- IGF-1 signalling plays a crucial role in CD8 memory T cell formation and tumour control *in vivo*

7. LITERATURE

7. LITERATURE

1. Li D, Wu M. Pattern recognition receptors in health and diseases. Signal Transduct Target Ther. 2021 Aug 4;6(1):291.

2. Marshall JS, Warrington R, Watson W, Kim HL. An introduction to immunology and immunopathology. Allergy Asthma Clin Immunol. 2018 Sep;14(S2):49.

3. Vantourout P, Hayday A. Six-of-the-best: unique contributions of γδ T cells to immunology. Nat Rev Immunol. 2013 Feb;13(2):88–100.

4. Bonneville M, O'Brien RL, Born WK. γδ T cell effector functions: a blend of innate programming and acquired plasticity. Nat Rev Immunol. 2010 Jul;10(7):467–78.

5. Cella M, Jarrossay D, Facchetti F, Alebardi O, Nakajima H, Lanzavecchia A, et al. Plasmacytoid monocytes migrate to inflamed lymph nodes and produce large amounts of type I interferon. Nat Med. 1999 Aug;5(8):919–23.

6. McNab F, Mayer-Barber K, Sher A, Wack A, O'Garra A. Type I interferons in infectious disease. Nat Rev Immunol. 2015 Feb;15(2):87–103.

7. Zhang W, Wang G, Xu ZG, Tu H, Hu F, Dai J, et al. Lactate Is a Natural Suppressor of RLR Signaling by Targeting MAVS. Cell. 2019 Jun 27;178(1):176-189.e15.

8. Mack EA, Kallal LE, Demers DA, Biron CA. Type 1 Interferon Induction of Natural Killer Cell Gamma Interferon Production for Defense during Lymphocytic Choriomeningitis Virus Infection. Griffin DE, editor. mBio. 2011 Sep;2(4):e00169-11.

9. O'Brien TR, Prokunina-Olsson L, Donnelly RP. IFN-λ4: The Paradoxical New Member of the Interferon Lambda Family. J Interferon Cytokine Res. 2014 Nov;34(11):829–38.

10. Innate immunity: impact on the adaptive immune response - ScienceDirect [Internet]. [cited 2025 Feb 2]. Available from: https://www.sciencedirect.com/science/article/pii/S0952791597801525?via%3Dihub

11. Platanias LC. Mechanisms of type-I- and type-II-interferon-mediated signalling. Nat Rev Immunol. 2005 May 1;5(5):375–86.

12. Kaech SM, Wherry EJ. Heterogeneity and Cell-Fate Decisions in Effector and Memory CD8+ T Cell Differentiation during Viral Infection. Immunity. 2007 Sep;27(3):393–405.

13. Kavazović I, Han H, Balzaretti G, Slinger E, Lemmermann NAW, Brinke A ten, et al. Eomes broadens the scope of CD8 T-cell memory by inhibiting apoptosis in cells of low affinity. PLOS Biol. 2020 Mar 17;18(3):e3000648.

14. Jung S, Unutmaz D, Wong P, Sano GI, De Los Santos K, Sparwasser T, et al. In Vivo Depletion of CD11c+ Dendritic Cells Abrogates Priming of CD8+ T Cells by Exogenous Cell-Associated Antigens. Immunity. 2002 Aug;17(2):211–20.

15. Williams MA, Bevan MJ. Effector and Memory CTL Differentiation. Annu Rev Immunol. 2007 Apr 1;25(1):171–92.

16. Liu Y, Wenger RH, Zhao M, Nielsen PJ. Distinct Costimulatory Molecules Are Required for the Induction of Effector and Memory Cytotoxic T Lymphocytes. J Exp Med. 1997 Jan 20;185(2):251–62.

17. Manjunath N, Shankar P, Wan J, Weninger W, Crowley MA, Hieshima K, et al. Effector differentiation is not prerequisite for generation of memory cytotoxic T lymphocytes. J Clin Invest. 2001 Sep 15;108(6):871–8.

18. Kaech SM, Cui W. Transcriptional control of effector and memory CD8+ T cell differentiation. Nat Rev Immunol. 2012 Nov;12(11):749–61.

19. Ziegler SF, Ramsdell F, Alderson MR. The activation antigen CD69. STEM CELLS. 1994 Jan;12(5):456–65.

20. Adamczyk M, Bartosińska J, Raczkiewicz D, Kowal M, Surdacka A, Krasowska D, et al. The Expression of Activation Markers CD25 and CD69 Increases during Biologic Treatment of Psoriasis. J Clin Med. 2023 Oct 17;12(20):6573.

21. Baaten BJG, Tinoco R, Chen AT, Bradley LM. Regulation of Antigen-Experienced T Cells: Lessons from the Quintessential Memory Marker CD44. Front Immunol [Internet]. 2012 [cited 2025 Feb 4];3. Available from: http://journal.frontiersin.org/article/10.3389/fimmu.2012.00023/abstract

22. Osborn JF, Hobbs SJ, Mooster JL, Khan TN, Kilgore AM, Harbour JC, et al. Central memory CD8+ T cells become CD69+ tissue-residents during viral skin infection independent of CD62L-mediated lymph node surveillance. Bhaduri-McIntosh S, editor. PLOS Pathog. 2019 Mar 15;15(3):e1007633.

23. Sterry SJ, Kelly JM, Turner SJ, Carbone FR. T cell receptor Va bias can be determined by TCR-contact residues within an MHC-bound peptide.

24. Goyal P, Rajala MS. Reprogramming of glucose metabolism in virus infected cells. Mol Cell Biochem. 2023 Nov;478(11):2409–18.

25. Fernández-Real JM, López-Bermejo A, Vendrell J, Ferri MJ, Recasens M, Ricart W. Burden of Infection and Insulin Resistance in Healthy Middle-Aged Men. Diabetes Care. 2006 May 1;29(5):1058–64.

26. Kasai D, Adachi T, Deng L, Nagano-Fujii M, Sada K, Ikeda M, et al. HCV replication suppresses cellular glucose uptake through down-regulation of cell surface expression of glucose transporters. J Hepatol. 2009 May;50(5):883–94.

27. Banerjee S, Saito K, Ait-Goughoulte M, Meyer K, Ray RB, Ray R. Hepatitis C Virus Core Protein Upregulates Serine Phosphorylation of Insulin Receptor Substrate-1 and Impairs the Downstream Akt/Protein Kinase B Signaling Pathway for Insulin Resistance. J Virol. 2008 Mar 15;82(6):2606–12.

28. Li X, Yang Y, Zhang B, Lin X, Fu X, An Y, et al. Lactate metabolism in human health and disease. Signal Transduct Target Ther. 2022 Sep 1;7(1):305.

29. Pearce EL, Pearce EJ. Metabolic Pathways in Immune Cell Activation and Quiescence. Immunity. 2013 Apr;38(4):633–43.

30. Fox CJ, Hammerman PS, Thompson CB. Fuel feeds function: energy metabolism and the T-cell response. Nat Rev Immunol. 2005 Nov;5(11):844–52.

31. Krawczyk CM, Holowka T, Sun J, Blagih J, Amiel E, DeBerardinis RJ, et al. Toll-like receptor–induced changes in glycolytic metabolism regulate dendritic cell activation. Blood. 2010 Jun 10;115(23):4742–9.

32. Gubser PM, Bantug GR, Razik L, Fischer M, Dimeloe S, Hoenger G, et al. Rapid effector function of memory CD8+ T cells requires an immediate-early glycolytic switch. Nat Immunol. 2013 Oct;14(10):1064–72.

33. Frauwirth KA, Riley JL, Harris MH, Parry RV, Rathmell JC, Plas DR, et al. The CD28 Signaling Pathway Regulates Glucose Metabolism. Immunity. 2002 Jun;16(6):769–77.

34. Reina-Campos M, Scharping NE, Goldrath AW. CD8+ T cell metabolism in infection and cancer. Nat Rev Immunol. 2021 Nov;21(11):718–38.

35. van der Windt GJW, Everts B, Chang CH, Curtis JD, Freitas TC, Amiel E, et al. Mitochondrial Respiratory Capacity Is a Critical Regulator of CD8+ T Cell Memory Development. Immunity. 2012 Jan;36(1):68–78.

36. Riganti C, Gazzano E, Polimeni M, Aldieri E, Ghigo D. The pentose phosphate pathway: An antioxidant defense and a crossroad in tumor cell fate. Free Radic Biol Med. 2012 Aug;53(3):421–36.

37. Dronina J, Samukaite-Bubniene U, Ramanavicius A. Advances and insights in the diagnosis of viral infections. J Nanobiotechnology. 2021 Oct 30;19(1):348.

38. Thaker SK, Ch'ng J, Christofk HR. Viral hijacking of cellular metabolism. BMC Biol. 2019 Jul 18;17(1):59.

39. Fontaine KA, Camarda R, Lagunoff M. Vaccinia Virus Requires Glutamine but Not Glucose for Efficient Replication. Frueh K, editor. J Virol. 2014 Apr 15;88(8):4366–74.

40. Thai M, Thaker SK, Feng J, Du Y, Hu H, Ting Wu T, et al. MYC-induced reprogramming of glutamine catabolism supports optimal virus replication. Nat Commun. 2015 Nov 12;6:8873.

41. Xiao X, Gaffar I, Guo P, Wiersch J, Fischbach S, Peirish L, et al. M2 macrophages promote beta-cell proliferation by up-regulation of SMAD7. Proc Natl Acad Sci [Internet]. 2014 Apr [cited 2025 Jan 31];111(13). Available from: https://pnas.org/doi/full/10.1073/pnas.1321347111

42. Nackiewicz D, Dan M, Speck M, Chow SZ, Chen YC, Pospisilik JA, et al. Islet Macrophages Shift to a Reparative State following Pancreatic Beta-Cell Death and Are a Major Source of Islet Insulin-like Growth Factor-1. iScience. 2020 Jan;23(1):100775.

43. Johnson AR, Justin Milner J, Makowski L. The inflammation highway: metabolism accelerates inflammatory traffic in obesity. Immunol Rev. 2012 Sep;249(1):218–38.

44. Fedorova NV, Ksenofontov AL, Serebryakova MV, Stadnichuk VI, Gaponova TV, Baratova LA, et al. Neutrophils Release Metalloproteinases during Adhesion in the Presence of Insulin, but Cathepsin G in the Presence of Glucagon. Mediators Inflamm. 2018;2018:1–9.

45. Kavazović I, Krapić M, Beumer-Chuwonpad A, Polić B, Turk Wensveen T, Lemmermann NA, et al. Hyperglycemia and Not Hyperinsulinemia Mediates Diabetes-Induced Memory CD8 T-Cell Dysfunction. Diabetes. 2022 Jan 19;71(4):706–21.

46. Hart BL. Biological Basis of the Behavior of Sick Animals.

47. Straub RH, Cutolo M, Buttgereit F, Pongratz G. Energy regulation and neuroendocrine–immune control in chronic inflammatory diseases. J Intern Med. 2010 Jun;267(6):543–60.

48. Fontaine KA, Sanchez EL, Camarda R, Lagunoff M. Dengue Virus Induces and Requires Glycolysis for Optimal Replication. J Virol. 2015 Jan 26;89(4):2358–66.

49. Passalacqua KD, Lu J, Goodfellow I, Kolawole AO, Arche JR, Maddox RJ, et al. Glycolysis Is an Intrinsic Factor for Optimal Replication of a Norovirus. mBio. 2019 Mar 12;10(2):10.1128/mbio.02175-18.

50. Muehlenbein MP, Hirschtick JL, Bonner JZ, Swartz AM. Toward quantifying the usage costs of human immunity: Altered metabolic rates and hormone levels during acute immune activation in men. Am J Hum Biol. 2010 Mar 22;22(4):546–56.

51. Munger J, Bennett BD, Parikh A, Feng XJ, McArdle J, Rabitz HA, et al. Systems-level metabolic flux profiling identifies fatty acid synthesis as a target for antiviral therapy. Nat Biotechnol. 2008 Oct;26(10):1179–86.

52. Toth L, Tolley EA, Krueger' J. SleeP as a Proanostic Indicator Durina Infectious Disease in Rabbits (43590).

53. Preston BT, Capellini I, McNamara P, Barton RA, Nunn CL. Parasite resistance and the adaptive significance of sleep. BMC Evol Biol. 2009;9(1):7.

54. Petersen MC, Shulman GI. Mechanisms of Insulin Action and Insulin Resistance. Physiol Rev. 2018 Oct 1;98(4):2133–223.

55. Šestan M, Marinović S, Kavazović I, Cekinović Đ, Wueest S, Turk Wensveen T, et al. Virus-Induced Interferon-γ Causes Insulin Resistance in Skeletal Muscle and Derails Glycemic Control in Obesity. Immunity. 2018 Jul;49(1):164-177.e6.

56. Wensveen FM, Šestan M, Turk Wensveen T, Polić B. 'Beauty and the beast' in infection: How immune–endocrine interactions regulate systemic metabolism in the context of infection. Eur J Immunol. 2019 Jul;49(7):982–95.

57. Plummer MP, Bellomo R, Cousins CE, Annink CE, Sundararajan K, Reddi BAJ, et al. Dysglycaemia in the critically ill and the interaction of chronic and acute glycaemia with mortality. Intensive Care Med. 2014 Jul 1;40(7):973–80.

58. Xiu F, Stanojcic M, Diao L, Jeschke MG. Stress Hyperglycemia, Insulin Treatment, and Innate Immune Cells. Int J Endocrinol. 2014;2014:1–9.

59. Halter JB, Beard JC, Porte D. Islet function and stress hyperglycemia: plasma glucose and epinephrine interaction. Am J Physiol-Endocrinol Metab. 1984 Jul 1;247(1):E47–52.

60. Hyperglycaemia protects the heart after myocardial infarction: aspects of programmed cell survival and cell death - Malfitano - 2010 - European Journal of Heart Failure - Wiley Online Library [Internet]. [cited 2025 Jan 30]. Available from: https://onlinelibrary.wiley.com/doi/10.1093/eurjhf/hfq053

61. Qiu D, Zhang L, Zhan J, Yang Q, Xiong H, Hu W, et al. Hyperglycemia Decreases Epithelial Cell Proliferation and Attenuates Neutrophil Activity by Reducing ICAM-1 and LFA-1 Expression Levels. Front Genet. 2020 Dec 18;11:616988.

62. Sleiman I, Morandi A, Sabatini T, Ranhoff A, Ricci A, Rozzini R, et al. Hyperglycemia as a Predictor of In-Hospital Mortality in Elderly Patients without Diabetes Mellitus Admitted to a Sub-Intensive Care Unit. J Am Geriatr Soc. 2008;56(6):1106–10.

63. Vigliano I, Fusco A, Palamaro L, Aloj G, Cirillo E, Salerno MC, et al. γ Chain transducing element: A shared pathway between endocrine and immune system. Cell Immunol. 2011 Jan 1;269(1):10–5.

64. Tian Z, Sun R, Wei H, Gao B. Impaired natural killer (NK) cell activity in leptin receptor deficient mice: leptin as a critical regulator in NK cell development and activation. Biochem Biophys Res Commun. 2002 Nov;298(3):297–302.

65. Lee FYJ, Li Y, Yang EK, Yang SQ, Lin HZ, Trush MA, et al. Phenotypic abnormalities in macrophages from leptin-deficient, obese mice. Am J Physiol-Cell Physiol. 1999 Feb 1;276(2):C386–94.

66. Drel VR, Mashtalir N, Ilnytska O, Shin J, Li F, Lyzogubov VV, et al. The Leptin-Deficient (*ob/ob*) Mouse. Diabetes. 2006 Dec 1;55(12):3335–43.

67. Taniguchi CM, Emanuelli B, Kahn CR. Critical nodes in signalling pathways: insights into insulin action. Nat Rev Mol Cell Biol. 2006 Feb;7(2):85–96.

68. Helderman JH, Reynolds TC, Strom TB. The insulin receptor as a universal marker of activated lymphocytes. Eur J Immunol. 1978 Aug;8(8):589–95.

69. Helderman JH, Strom TB. Emergence of insulin receptors upon alloimmune T cells in the rat. J Clin Invest. 1977 Feb 1;59(2):338–44.

70. Tsai S, Clemente-Casares X, Zhou AC, Lei H, Ahn JJ, Chan YT, et al. Insulin Receptor-Mediated Stimulation Boosts T Cell Immunity during Inflammation and Infection. Cell Metab. 2018 Dec;28(6):922-934.e4.

71. Šestan M, Mikašinović S, Benić A, Wueest S, Dimitropoulos C, Mladenić K, et al. An IFNγ-dependent immune–endocrine circuit lowers blood glucose to potentiate the innate antiviral immune response. Nat Immunol. 2024 Jun;25(6):981–93.

72. Yakar S, Adamo ML. Insulin-Like Growth Factor 1 Physiology. Endocrinol Metab Clin North Am. 2012 Jun;41(2):231–47.

73. Clemmons DR. Metabolic Actions of IGF-I in Normal Physiology and Diabetes. Endocrinol Metab Clin North Am. 2012 Jun;41(2):425–43.

74. Rubin JB, Shia MA, Pilch PF. Stimulation of tyrosine-specific phosphorylation in vitro by insulin-like growth factor I. Nature. 1983 Sep;305(5933):438–40.

75. Beschorner WE, Divic J, Pulido H, Yao XU, Kenworthy P, Bruce G. ENHANCEMENT OF THYMIC RECOVERY AFTER CYCLOSPORINE BY RECOMBINANT HUMAN GROWTH HORMONE AND INSULIN-LIKE GROWTH FACTOR I: Transplantation. 1991 Nov;52(5):879–84.

76. Wolters TLC, Netea MG, Hermus ARMM, Smit JWA, Netea-Maier RT. IGF1 potentiates the pro-inflammatory response in human peripheral blood mononuclear cells via MAPK. J Mol Endocrinol. 2017 Aug;59(2):129–39.

77. Baudler S, Baumgartl J, Hampel B, Buch T, Waisman A, Snapper CM, et al. Insulin-like growth factor-1 controls type 2 T cell-independent B cell response. J Immunol Baltim Md 1950. 2005 May 1;174(9):5516–25.

78. Walsh PT, Smith LM, O'Connor R. Insulin-like growth factor-1 activates Akt and Jun N-terminal kinases (JNKs) in promoting the survival of T lymphocytes. Immunology. 2002;107(4):461–71.

79. Bilbao D, Luciani L, Johannesson B, Piszczek A, Rosenthal N. Insulin-like growth factor-1 stimulates regulatory T cells and suppresses autoimmune disease. EMBO Mol Med. 2014 Nov;6(11):1423–35.

80. DiToro D, Harbour SN, Bando JK, Benavides G, Witte S, Laufer VA, et al. Insulin-Like Growth Factors Are Key Regulators of T Helper 17 Regulatory T Cell Balance in Autoimmunity. Immunity. 2020 Apr;52(4):650-667.e10.

81. Tan SY, Mei Wong JL, Sim YJ, Wong SS, Mohamed Elhassan SA, Tan SH, et al. Type 1 and 2 diabetes mellitus: A review on current treatment approach and gene therapy as potential intervention. Diabetes Metab Syndr Clin Res Rev. 2019 Jan;13(1):364–72.

82. Muller LMAJ, Gorter KJ, Hak E, Goudzwaard WL, Schellevis FG, Hoepelman AIM, et al. Increased Risk of Common Infections in Patients with Type 1 and Type 2 Diabetes Mellitus. Clin Infect Dis. 2005 Aug 1;41(3):281–8.

83. Yang J, Zheng Y, Gou X, Pu K, Chen Z, Guo Q, et al. Prevalence of comorbidities and its effects in patients infected with SARS-CoV-2: a systematic review and meta-analysis. Int J Infect Dis. 2020 May;94:91–5.

84. Hemalatha Rajkumar PB. The Impact of Obesity on Immune Response to Infection and Vaccine: An Insight into Plausible Mechanisms. Endocrinol Metab Syndr [Internet]. 2013 [cited 2025 Feb 4];02(02). Available from: https://www.omicsonline.org/the-impact-of-obesity-on-immune-response-to-infection-and-vaccine-an-insight-into-plausible-mechanisms-2161-1017.1000113.php?aid=18763

85. Karlsson EA, Sheridan PA, Beck MA. Diet-Induced Obesity Impairs the T Cell Memory Response to Influenza Virus Infection. J Immunol. 2010 Mar 15;184(6):3127–33.

86. Hulme KD, Yan L, Marshall RJ, Bloxham CJ, Upton KR, Hasnain SZ, et al. High glucose levels increase influenza-associated damage to the pulmonary epithelial-endothelial barrier. eLife. 2020 Jul 22;9:e56907.

87. Khodakhah F, Tahamtan A, Marzban M, Shadab A, Tavakoli-Yaraki M, Hashemi SM, et al. Hyperglycemia results in decreased immune cell infiltration and increased viral load in the lung in a mouse model of RSV infection. Cytokine. 2021 Jul;143:155539.

88. Yu B, Li C, Sun Y, Wang DW. Insulin Treatment Is Associated with Increased Mortality in Patients with COVID-19 and Type 2 Diabetes. Cell Metab. 2021 Jan;33(1):65-77.e2.

89. Falo LD, Kovacsovics-Bankowski M, Thompson K, Rock KL. Targeting antigen into the phagocytic pathway in vivo induces protective tumour immunity. Nat Med. 1995 Jul;1(7):649–53.

90. Wagner M, Jonjić S, Koszinowski UH, Messerle M. Systematic Excision of Vector Sequences from the BAC-Cloned Herpesvirus Genome during Virus Reconstitution. J Virol. 1999 Aug;73(8):7056–60.

91. Mathys S, Schroeder T, Ellwart J, Koszinowski UH, Messerle M, Just U. Dendritic Cells under Influence of Mouse Cytomegalovirus Have a Physiologic Dual Role: to Initiate and to Restrict T Cell Activation. J Infect Dis. 2003 Mar 15;187(6):988–99.

92. Bubić I, Wagner M, Krmpotić A, Saulig T, Kim S, Yokoyama WM, et al. Gain of Virulence Caused by Loss of a Gene in Murine Cytomegalovirus. J Virol. 2004 Jul 15;78(14):7536–44.

93. Brizić I, Lisnić B, Brune W, Hengel H, Jonjić S. Cytomegalovirus Infection: Mouse Model. Curr Protoc Immunol. 2018 Aug;122(1):e51.

94. Gebhardt T, Wakim LM, Eidsmo L, Reading PC, Heath WR, Carbone FR. Memory T cells in nonlymphoid tissue that provide enhanced local immunity during infection with herpes simplex virus. Nat Immunol. 2009 May;10(5):524–30.

95. Hammarlund E, Lewis MW, Hansen SG, Strelow LI, Nelson JA, Sexton GJ, et al. Duration of antiviral immunity after smallpox vaccination. Nat Med. 2003 Sep;9(9):1131–7.

96. Lim JF, Berger H, Su I hsin. Isolation and Activation of Murine Lymphocytes. J Vis Exp JoVE. 2016 Oct 30;(116):54596.

97. Postat J, Olekhnovitch R, Lemaître F, Bousso P. A Metabolism-Based Quorum Sensing Mechanism Contributes to Termination of Inflammatory Responses. Immunity. 2018 Oct;49(4):654-665.e5.

98. Wensveen FM, Jelenčić V, Valentić S, Šestan M, Wensveen TT, Theurich S, et al. NK cells link obesity-induced adipose stress to inflammation and insulin resistance. Nat Immunol. 2015 Apr;16(4):376–85.

99. Wueest S, Rapold RA, Schumann DM, Rytka JM, Schildknecht A, Nov O, et al. Deletion of Fas in adipocytes relieves adipose tissue inflammation and hepatic manifestations of obesity in mice. J Clin Invest. 2010 Jan 4;120(1):191–202.

100. Cardoso F, Klein Wolterink RGJ, Godinho-Silva C, Domingues RG, Ribeiro H, da Silva JA, et al. Neuro-mesenchymal units control ILC2 and obesity via a brain–adipose circuit. Nature. 2021 Sep;597(7876):410–4.

101. 'Beauty and the beast' in infection: How immune–endocrine interactions regulate systemic metabolism in the context of infection - Wensveen - 2019 - European Journal of Immunology - Wiley Online Library [Internet]. [cited 2024 Nov 23]. Available from: https://onlinelibrary.wiley.com/doi/10.1002/eji.201847895

102. Klein SL, Flanagan KL. Sex differences in immune responses. Nat Rev Immunol. 2016 Oct;16(10):626–38.

103. Carthew RW. Gene Regulation and Cellular Metabolism: An Essential Partnership. Trends Genet. 2021 Apr;37(4):389–400.

104. Desousa BR, Kim KK, Jones AE, Ball AB, Hsieh WY, Swain P, et al. Calculation of ATP production rates using the Seahorse XF Analyzer. EMBO Rep. 2023 Oct 9;24(10):e56380.

105. Šestan M, Marinović S, Kavazović I, Cekinović Đ, Wueest S, Turk Wensveen T, et al. Virus-Induced Interferon-γ Causes Insulin Resistance in Skeletal Muscle and Derails Glycemic Control in Obesity. Immunity. 2018 Jul 17;49(1):164-177.e6.

106. Murali-Krishna K, Altman JD, Suresh M, Sourdive DJD, Zajac AJ, Miller JD, et al. Counting Antigen-Specific CD8 T Cells: A Reevaluation of Bystander Activation during Viral Infection. Immunity. 1998 Feb;8(2):177–87.

107. Wu KK, Huan Y. Streptozotocin-Induced Diabetic Models in Mice and Rats. Curr Protoc Pharmacol [Internet]. 2008 Mar [cited 2025 Jan 17];40(1). Available from: https://currentprotocols.onlinelibrary.wiley.com/doi/10.1002/0471141755.ph0547s40

108. Quah BJC, Warren HS, Parish CR. Monitoring lymphocyte proliferation in vitro and in vivo with the intracellular fluorescent dye carboxyfluorescein diacetate succinimidyl ester. Nat Protoc. 2007 Sep;2(9):2049–56.

109. Seliger B, Wollscheid U, Momburg F, Blankenstein T, Huber C. Characterization of the major histocompatibility complex class I deficiencies in B16 melanoma cells. Cancer Res. 2001 Feb 1;61(3):1095–9.

110. Ramos S, Ademolue TW, Jentho E, Wu Q, Guerra J, Martins R, et al. A hypometabolic defense strategy against malaria. Cell Metab. 2022 Aug;34(8):1183-1200.e12.

111. Teng RJ, Wu TJ, Ho MM. Mumps infection complicated by transient hyperinsulinemic hypoglycemia. Pediatr Infect Dis J. 1997 Apr;16(4):416–7.

112. Wang A, Huen SC, Luan HH, Yu S, Zhang C, Gallezot JD, et al. Opposing Effects of Fasting Metabolism on Tissue Tolerance in Bacterial and Viral Inflammation. Cell. 2016 Sep;166(6):1512-1525.e12.

113. Damasceno DC, Netto AO, Iessi IL, Gallego FQ, Corvino SB, Dallaqua B, et al. Streptozotocin-Induced Diabetes Models: Pathophysiological Mechanisms and Fetal Outcomes. BioMed Res Int. 2014;2014(1):819065.

114. Yu Y, Clippinger AJ, Alwine JC. Viral effects on metabolism: changes in glucose and glutamine utilization during human cytomegalovirus infection. Trends Microbiol. 2011 Jul;19(7):360–7.

115. Gou H, Bian Z, Li Y, Cai R, Jiang Z, Song S, et al. Metabolomics Exploration of Pseudorabies Virus Reprogramming Metabolic Profiles of PK-15 Cells to Enhance Viral Replication. Front Cell Infect Microbiol. 2021 Jan 29;10:599087.

116. Brown TP, Ganapathy V. Lactate/GPR81 signaling and proton motive force in cancer: Role in angiogenesis, immune escape, nutrition, and Warburg phenomenon. Pharmacol Ther. 2020 Feb;206:107451.

117. Šestan M, Raposo B, Rendas M, Brea D, Pirzgalska R, Rasteiro A, et al. Neuronal-ILC2 interactions regulate pancreatic glucagon and glucose homeostasis. Science. 2025 Jan 17;387(6731):eadi3624.

118. Kotas ME, Medzhitov R. Homeostasis, Inflammation, and Disease Susceptibility. Cell. 2015 Feb;160(5):816–27.

119. MacIver NJ, Jacobs SR, Wieman HL, Wofford JA, Coloff JL, Rathmell JC. Glucose metabolism in lymphocytes is a regulated process with significant effects on immune cell function and survival. J Leukoc Biol. 2008 Oct 1;84(4):949–57.

120. Xu X, Mardell C, Xian CJ, Zola H. Expression of functional insulin-like growth factor-1 receptor on lymphoid cell subsets of rats.

121. Liu JL, Yakar S, Leroith D. Conditional Knockout of Mouse Insulin-Like Growth Factor-1 Gene Using The Cre/Loxp System (44500).

122. Renier G, Clément I, Desfaits AC, Lambert A. Direct stimulatory effect of insulin-like growth factor-I on monocyte and macrophage tumor necrosis factor-alpha production. Endocrinology. 1996 Nov;137(11):4611–8.

123. O'Neill LAJ, Kishton RJ, Rathmell J. A guide to immunometabolism for immunologists. Nat Rev Immunol. 2016 Sep;16(9):553–65.

124. Fukushima T, Nakamura Y, Yamanaka D, Shibano T, Chida K, Minami S, et al. Phosphatidylinositol 3-Kinase (PI3K) Activity Bound to Insulin-like Growth Factor-I (IGF-I) Receptor, which Is Continuously Sustained by IGF-I Stimulation, Is Required for IGF-I-induced Cell Proliferation. J Biol Chem. 2012 Aug;287(35):29713–21.

125. Araki K, Turner AP, Shaffer VO, Gangappa S, Keller SA, Bachmann MF, et al. mTOR regulates memory CD8 T-cell differentiation. Nature. 2009 Jul 2;460(7251):108–12.

126. Zheng X, Luo X, Chen J, Guo M, Li H, Wu Y, et al. Igf-1 Suppresses Hepatocellular Carcinogenesis and Development by Activating T Lymphocytes in Mice [Internet]. 2024 [cited 2025 Feb 13]. Available from: https://www.ssrn.com/abstract=4954827

8. LIST OF FIGURES AND TABLES

LIST OF FIGURES AND TABLES

List of figures

Figure 1. Insulin promotes the antiviral CD8 T cell response. 16
Figure 2. Strong viral infection induces transient relative hypoglycemia..... 46
Figure 3. Infection-induced relative hypoglycemia occurs independently of sex..... 48
Figure 4. Prevention of glucose restriction negatively impacts the antiviral response 49
Figure 5. Hypoglycemia impairs viral replication in vitro..... 50
Figure 6. Metabolic deficiency does not cause impaired viral infection 53
Figure 7. Limiting glucose affects viral replication by altering cellular metabolism 54
Figure 8. Glucose restriction impairs lactate-mediated inhibition of the antiviral response.. 57
Figure 9. Relative hypoglycemia is a result of increased insulin production by the pancreas 59
Figure 10. Infection-induced relative hypoglycemia depends on decreased hepatic glycogenolysis.. 61
Figure 11. Type 1 diabetes impairs viral control..... 62
Figure 12. Insulin does not influence the anti-viral CD8 T cell response via its receptor.. 65
Figure 13. Kinetics of serum IGF-1 concentrations following viral infection..... 67
Figure 14. The proliferation of effector and memory CD8 T cells in vitro is not affected by IGF-1 stimulation..... 68
Figure 15. The phenotype of effector and memory CD8 T cells in vitro is not affected by IGF-1 stimulation.....69
Figure 16. In vitro IGF-1 stimulation increased IFNγ production by memory, but not effector CD8 T cells.....71
Figure 17. IGF-1 promotes glycolytic metabolism, increasing overall ATP production and improving the functionality of memory CD8 T cells…… .72
Figure 18. IGF-1 signalling promotes CD8 memory T cell formation in vivo..... 75
Figure 19. Deficiency of the IGF-1 receptor has no significant impact on the functionality and recall capacity of CD8 T cells in vivo..... 76
Figure 20. IGF-1 has no significant impact on CD8 T cell biology in the absence of NK cells ... 78
Figure 21. IGF-1R deficiency impairs the ability of memory CD8 T cells to control B16 melanoma tumour growth 79

List of tables

Table 1. Experimental mouse strains..... 23
Table 2. Antibodies, peptides, chemicals, and kits used in experiments..... 28
Table 3. List of primers used for PCR..... 32
Table 4. Primers used for qPCR measurement of gene expression..... 32

9. ABBREVIATIONS LIST

ABBREVIATIONS LIST

AIM2 - Absent in melanoma-2

ALRs - Absent in melanoma-2 (AIM2)-like receptors

APC - Antigen-presenting cells

ATP - Adenosine triphosphate

BAC - Bacterial artificial chromosome

BM - Bone marrow

BMDM - Bone marrow-derived macrophages

CD62L - L-selectin

CFSE - Carboxyfluorescein succinimidyl ester

CLRs - C-type lectin receptors

CTLs - Cytotoxic lymphocytes

DAMPs - Damage-associated molecular patterns

DCs - Dendritic cells

DNA - Deoxyribonucleic acid

DT - Diphtheria toxin

E2 - Estradiol

ECs - Endothelial cells

ECAR - Extracellular acidification rate

FACS - Fluorescence-activated cell sorting

$FADH_2$ - Flavin adenine dinucleotide

FPG - Fasting plasma glucose

GAS - Gamma interferon activation site

GeoMean - Geometric mean

GFP - Green fluorescent protein

GH - Growth hormone

GLUTs - Glucose transporters

GHRH - Growth hormone-releasing hormone

hCMV - Human cytomegalovirus

HCV - Hepatitis C virus

HFD - High-fat diet

HSV-1 - Herpes simplex virus-1

IC50 - Inhibitory concentration 50%

IFNs - Interferons

IFNAR - Type I interferon receptor

IFNα/β - Interferon-α/β

IFNγ - Interferon-gamma

IFNγR - Interferon-gamma receptor

IFU - Inclusion forming units

IGF-1 - Insulin-like growth factor 1

IGF-1R - Insulin-like growth factor 1 receptor

ILs - Interleukins

ILCs - Innate lymphoid cells

INSR - Insulin receptor

i.p. - Intraperitoneal

IR - Insulin resistance

IRF - Interferon regulatory factor

IRS - Insulin receptor substrates

ISGs - Interferon-stimulated genes

ISRE - Interferon-stimulated response element

i.v. - Intravenous

JAK/STAT - Janus kinase/signal transducer and activator of transcription

LAMRI - Laboratory of mouse engineering and breeding facility of the UNIRI

LCMV - Lymphocytic choriomeningitis virus

LDH - Lactate dehydrogenase

LPS - Lipopolysaccharides

MACS - Magnetic-activated cell sorting

MAPK - Mitogen-activated protein kinase

MAVS - Mitochondrial antiviral-signalling protein

mCMV - Murine cytomegalovirus

MEF - Mouse embryonic fibroblasts

MHC I - Major histocompatibility complex class I

MOI - Multiplicity of infection

mTOR - Mammalian target of rapamycin

NADH - Nicotinamide adenine dinucleotide

NCD - Normal chow diet

NF-κB - Nuclear factor-κB

NLRs - Nucleotide oligomerization domain (NOD)-like receptors

NOD - Nucleotide oligomerization domain

N4 - SIINFEKL

NK - Natural killer

OCR - Oxygen consumption rate

OVA - Ovalbumin

OXPHOS - Oxidative phosphorylation

PAMPs - Pathogen-associated molecular patterns

PCR - Polymerase chain reaction

PFU - Plaque-forming units

PI3K - Phosphoinositide 3-kinase

PR8 - Influenza A strain PR/8/34

PRRs - Pattern recognition receptors

qPCR - Quantitative polymerase chain reaction

RHG - Relative hypoglycemia

RIG-I - Retinoic acid-inducible

RLRs - Retinoic acid-inducible gene I (RIG-I)-like receptors

RNA - Ribonucleic acid

RSV - Respiratory syncytial virus

RT - Room temperature

RU - Relative units

SARS-CoV-2 - Severe acute respiratory syndrome coronavirus 2

SEM - Standard error of the mean

SPF - Specific pathogen-free

STZ - Streptozotocin

SVEC - Stromal vascular endothelial cells

T1D - Type 1 diabetes

T2D - Type 2 diabetes

TCA	- The citric acid cycle
TCR	- T-cell receptor
TLRs	- Toll-like receptors
TNF	- Tumour necrosis factor
VSMCs	- Vascular smooth muscle cells
WT	- Wild type

10. CURRICULUM VITAE

CURRICULUM VITAE

PERSONAL INFORMATION

Name:	Sanja Mikašinović
Address:	Škurinjska cesta 8a, 51000 Rijeka, Croatia
Phone number:	+385 99 675 6648
Mail:	sanja.mikasinovic@uniri.hr
Date of birth:	08/03/1996

WORK EXPERIENCE

15/10/2020 –	Research assistant at the Department of Histology and Embryology, Faculty of Medicine, University of Rijeka
05/2024 – 07/2024	Visiting PhD researcher at the laboratory of Prof. Dr. D. Konrad, Universitäts-Kinderspital Zürich, Switzerland
10/2019 – 10/2020	Traineeship at the Laboratory for Cellular and Developmental Neurobiology, University of Trieste

EDUCATION AND TRAINING

2021 –	Doctoral program in *Biomedicine* at the Faculty of Medicine, University of Rijeka, Rijeka (Croatia)
2017 – 2019	Graduate university program of *Biotechnology in Medicine* (Academic degree: Master of Science in Biotechnology in Medicine, with highest honor - *summa cum laude*), Department of Biotechnology, University of Rijeka, Rijeka (Croatia)
2014 – 2017	Undergraduate university program *Biotechnology and drug research* (Academic degree: Bachelor of Science in Biotechnology and drug research, with great honor - *magna cum laude*), Department of Biotechnology University of Rijeka, Rijeka (Croatia)
2010 – 2014	High school "Gimnazija Andrije Mohorovičića Rijeka", Rijeka (Croatia)

CONGRESS AND MEETINGS

- Annual Meeting of the Croatian Immunological Society, October 2024, Sisak, Croatia (selected talk presentation)
- 2nd Biomedicine and Health Congres „Science and Us “, May 2024, Rijeka, Croatia (poster presentation)
- 12th EFIS-EJI South Eastern European Immunology School, October 2023, Čiovo–Trogir, Croatia (poster presentation)
- Annual Meeting of the Croatian Immunological Society, October 2023, Brijuni, Croatia (selected talk and poster presentation)
- 5th International Conference on ImmunoMetabolism: Molecular and Cellular Immunology of Metabolism, May 2023, Chania, Crete (poster presentation)
- Annual Meeting of the Croatian Immunological Society, October 2022, Sveti Martin na Muri, Croatia (poster presentation)
- First 5 years of the CerVirVac symposium, September 2022, Rijeka, Croatia (poster presentation)
- 7th Croatian Congress of Microbiology with International Participation, May 2022, Sveti Martin na Muri, Croatia (poster presentation)
- 15th ENII EFIS EJI Summer School on Advanced Immunology, May 2022, Alghero, Sardinia, Italy (poster presentation)
- Annual Meeting of the Croatian Immunological Society, October 2021, Čiovo–Trogir, Croatia (selected talk and poster presentation)
- 6th European Congress of Immunology ECI 2021, September 2021, online, Beograd, Srbija (poster presentation)
- Young Neuroscientists Meeting, June 2019, Trieste, Italy (selected talk presentation)
- 9th Student Congress of Neuroscience – NeuRi, April 2019, Rijeka – Rab, Croatia (poster presentation)
- 8th Student Congress of Neuroscience – NeuRi, April 2018, Rijeka – Rab, Croatia (selected talk presentation)

AWARDS AND ACKNOWLEDGEMENTS

- The Award for the Best Young Scientist, Faculty of Medicine, University of Rijeka, 2024
- 1st Award for Poster Presentation of Scientific Work in the Biomedicine section at the "Science and Us", 2nd Biomedicine and Health Congress, 2024, Rijeka, Croatia

- Winner of EFIS-IL Short-term fellowships, visiting PhD researcher at the laboratory of Prof. Dr. D. Konrad, Universitäts-Kinderspital Zürich, Switzerland, 2 months, 2024
- 1st Award for Presentation of Scientific Work, Annual Meeting of the Croatian Immunological Society, Sveti Martin na Muri 2022
- Winner of EFIS travel grant for participation in ENII EFIS/EJI Summer School 2022
- The Dean's Award for an outstanding academic achievement, 2020
- Winner of Erasmus+ fellowship, one-year internship at the Laboratory for Cellular and Developmental Neurobiology, University of Trieste, Italy, 2019 - 2020
- Scholarship for outstanding students from the City of Rijeka 2015 – 2019

ORGANISATIONAL / MANAGERIAL SKILLS

- Actively participating in the organization of the Annual Meeting of the Croatian Immunological Society, 2022, Sveti Martin na Muri, Croatia
- Actively participating in the organization of ''Open days at Department of Biotechnology''

MEMBERSHIPS

- Croatian Immunological Society (CIS); from 2020
- EFIS Young Immunologists Task Force; from 2020

PUBLICATIONS

1. Šestan, Marko*; **Mikašinović, Sanja***; Benić, Ante; Wueest, Stephan; Dimitropoulos, Christoforos; Mladenić, Karlo; Krapić, Mia; Hiršl, Lea; Glantzspiegel, Yossef; Rasteiro, Ana et al. **An IFNγ-dependent immune–endocrine circuit lowers blood glucose to potentiate the innate antiviral immune response** // Nature Immunology. 2024 (IF 27.8)

2. Benić, Ante; **Mikašinović, Sanja**; Wensveen, Felix M.; Polić, Bojan. **Activation of Granulocytes in Response to a High Protein Diet Leads to the Formation of Necrotic Lesions in the Liver** // Metabolites. 2023 (IF 3.5)

3. Petrović, Antonela; Ban, Jelena; Tomljanović, Ivana; Pongrac, Marta; Ivaničić, Matea; **Mikašinović, Sanja**; Mladinic, Miranda. **Establishment of Long-Term Primary Cortical Neuronal Cultures From Neonatal Opossum Monodelphis domestica** // Frontiers in Cellular Neuroscience. 2021 (IF 4.2)